Final Report

On

Field Demonstration of Durable Link Slabs for Jointless Bridge Decks Based on Strain-Hardening Cementitious Composites – Phase 3: Shrinkage Control

By

Victor C. Li (Principal Investigator), En-Hua Yang, and Mo Li

The Advanced Civil Engineering Materials Research Laboratory

Department of Civil and Environmental Engineering

University of Michigan, Ann Arbor, MI 48109-2125, USA

Submitted to

Michigan Department of Transportation

January 28, 2008

Research Sponsor: Michigan Department of Transportation

MDOT Project Manager: Roger Till

Award Reference Number: MDOT Contract No. 2003-0026

Work Authorization # 10

Contract Period: July 25, 2006 – Jan 31, 2008

Technical Report Documentation Page

1. Report No. Research Report RC-1506	2. Government Accession No.	3. MDOT Project Manager Roger Till
4. Title and Subtitle Field Demonstration of Durable Link Slabs for Jointless Bridge Decks Based on Strain-Hardening Cementitious Composites – Phase 3: Shrinkage Control		5. Report Date March 17, 2008
7. Author(s) Victor C. Li (Principal Investigator) En-Hua Yang, and Mo Li		6. Performing Organization Code
9. Performing Organization Name and Address The Advanced Civil Engineering Material Research Laboratory Department of Civil and Environmental Engineering University of Michigan, Ann Arbor, MI 48109-2125, U.S.A.		8. Performing Org Report No.
12. Sponsoring Agency Name and Address Michigan Department of Transportation Construction and Technology Division P.O. Box 30049 Lansing, MI 48909		10. Work Unit No. (TRAIS) 11. Contract Number: Master Contract #03-0026 11(a). Authorization Number: Work Auth #10
15. Supplementary Notes		13. Type of Report & Period Covered July 25, 2006 – Jan 31, 2008 14. Sponsoring Agency Code

16. Abstract

The research is on the development of durable link slabs for jointless bridge decks based on strain-hardening cementitious composite - engineered cementitious composite (ECC). Specifically the superior ductility of ECC was utilized to accommodate bridge deck deformations imposed by girder deflection, concrete shrinkage, and temperature variations, providing a cost-effective solution to a number of deterioration problems associated with bridge deck joints.

In this phase 3, research was initiated at developing a solution for early age cracking observed on the Grove Street Bridge ECC link-slab. Although these cracks are small, about half the size allowable by ASSHTO, and they are bridged by fibers, with load carrying capability, it is desirable to as much as possible eliminate such early age cracking.

Systematic investigations (both numerical and experimental) have been conducted on identifying factors which cause early age cracking, replicating early age cracking behavior observed in the field, developing new ECC materials solution to prevent early age cracking, documenting new ECC fresh and hardened properties, verifying new ECC performance by means of the large frame restrained shrinkage test, and revising special provision of ECC link slab. Grove Street Bridge was monitored constantly over the whole project period.

It was concluded that material properties, construction quality, and structural geometry are all important factors causing early cracking. The invention of a low shrinkage ECC crates a larger buffer to prevent the same type of early age cracking in future ECC link slabs. The revised special provision of ECC link slab further regulates the skew angle limit and emphasizes the importance of casting and curing of ECC link slab. A large frame restrained shrinkage test, adopting the new ECC material and following the revised special provision, shows no early age cracking and verify the performance of future ECC link slab. The crack pattern and crack width in Grove Street bridge ECC link slab were found to remain after being open to traffic for 27 months (3 winters).

17. Key Words ECC link slab, Jointless bridge deck, Strain-hardening, Durability, shrinkage control, Crack width control, Implementation, Demonstration	18. Distribution Statement No restrictions. This document is available to the public through the Michigan Department of Transportation.		
19. Security Classification (report) Unclassified	20. Security Classification (Page) Unclassified	21. No of Pages	22. Price

DISCLAIMER

The contents of this report reflect the views of the authors, who are responsible for the facts and accuracy of the information presented herein. This document is disseminated under the sponsorship of the Michigan Department of Transportation, in the interest of information exchange. The Michigan Department of Transportation assumes no liability for the contents or use thereof.

ACKNOWLEDGEMENTS

The presented research has been sponsored by the Michigan Department of Transportation, which is gratefully acknowledged. The authors thank the Michigan DOT project manager Roger Till and the other members of the MDOT research Advisory Panel for their useful comments, discussions and support.

Table of Contents

1. Introduction

1.1 Background

This research is an extension of the Michigan Department of Transportation (MDOT) sponsored project titled "Field Demonstration of Durable Link Slabs for Jointless Bridge Decks Based on Strain-Hardening Cementitious Composites" (Li et al, 2005).

Figure 1.1: ECC link slab on Grove Street bridge over I-94 (S02 of 81063) (completed November 1st, 2005)

The "Field Demonstration of Durable Link Slabs for Jointless Bridge Decks" project was based on the incorporation of Engineered Cementitious Composites (ECC), a strain-hardening cementitious composite, into multi-span bridge decks. These highly ductile materials are used to replace the expansion joints within simple span bridges, forming a continuous deck protecting both the bridge girders and substructure from corrosive agents, and eliminating costly and repeated maintenance of joints. This project was completed in December, 2005 and an ECC link slab on the Grove Street Bridge over I-94 was built through the collaboration between MDOT, Advanced Civil Engineering Materials Research Laboratory (ACE-MRL), and contractors. In that project, 40 cubic yards of ECC were cast in place by conventional ready mix trucks to build the first ECC link slab in the United States (**Figure 1.1**). With a strain capacity exceeding 2% (Li et al, 2005), these composites can be used to replace traditional steel expansion devices and can fully accommodate the thermal deformations of adjacent bridge spans. A length of 7.5% of each adjacent bridge span was replaced with ECC material to accommodate the imposed

thermal, shrinkage, and live load deformation typical within expansion joints. The link slab measured 16'-11" in the bridge longitudinal direction and 66'-5" in the transverse direction. The bridge has a high skew angle of 45 degrees.

The ECC mixture design used in the link slab was Mix 45 (ECC M45). Consistent with the first ECC special provision (**Appendix A**), substitute raw materials were allowed for use in the link slab provided that they showed similar composite properties in both the fresh and hardened states. Two substitute materials were submitted by Clawson Concrete for evaluation. These were a different high range water reducer, and fly ash from a different material supplier. High range water reducer from Euclid© Company with the trade name Plastol® 5000 was submitted as a replacement for the W.R. Grace product specified within the special provision. This product is a polycarboxylate-based water reducer similar in chemical composition to both the W.R. Grace and Degaussa products previously approved. Additionally, Type F fly ash produced by Headwaters Companies in Eastlake, Ohio was submitted as an alternative to the Type F fly ash specified by Boral Materials Technologies in Rockdale, Texas. Material samples of each of these materials were provided by the manufacturer and tested as a direct replacement (i.e. identical mix design) for the specified material. Flow, compressive strength, and uniaxial tension tests were performed on ECC materials using both of these replacements. Based on these test results, both substitutes were approved and adopted in the actual construction.

Placement of the ECC link slab for Phase 1 and Phase 2 took place on September 10, 2005 and on October 18, 2005, respectively. Research team personnel were placed at both the concrete batching plant and onsite at the Grove Street Bridge to observe, monitor, and document all aspects of the material mixing, placing, and finishing. Research team members at the Clawson Concrete batching plant assisted by answering questions and performing flowability and general rheology inspections before concrete trucks left the plant. This helped assure that the material would be acceptable upon arrival at Grove Street. Research personnel at the Grove Street site were responsible for answering onsite questions, conducting fresh material testing (i.e. flowability tests, matrix consistency and

fiber dispersion inspections, temperature, air content, etc.), approval of the fresh material, and oversight of the ECC material placement, finishing, and curing.

For the approximate 20 cubic yards of ECC material needed for each phase of the construction, three trucks with 7 cubic yards of ECC material were batched and sent to the site. Fresh material tests were conducted for each truck on site, along with preparing specimens for testing hardened mechanical properties. Test results of both fresh and hardened properties met the requirements within the ECC special provision (**Appendix A**).

Although the placement and quality control reveals nothing out of ordinary, early age cracking was found in the link slab 3 days after placement for both Phase 1 and Phase 2. In Phase 2, stricter monitoring of ready truck washing water was conducted, resulting in a stiffer fresh mix. Early age cracking remains albeit with larger crack spacing. **Figures 1.2(a)** and **(b)** show the cracking pattern and associated crack widths within the link slab from Phase 1. **Figure 1.3(a)** shows the cracking pattern from Phase 2 and **Figure 1.3(b)** reveals steel reinforcing bars apparently acting as stress concentrators for crack initiation within the link slab. The structural functionality of ECC link slab is expected not to be affected by this early age cracking due to the tensile strain hardening properties of ECC. However, the observed crack widths, approximately 0.006” to 0.01”, while smaller than the allowable limit by AASHTO of 0.013”, is substantially larger than the design crack width in ECC of 0.004”. The long-term durability of the link slab could be a concern since crack widths are and large enough for aggressive corrosion agents to penetrate to the steel reinforcement. This motivated the desire to understand the origin and to develop methods to control such cracks in ECC structures.

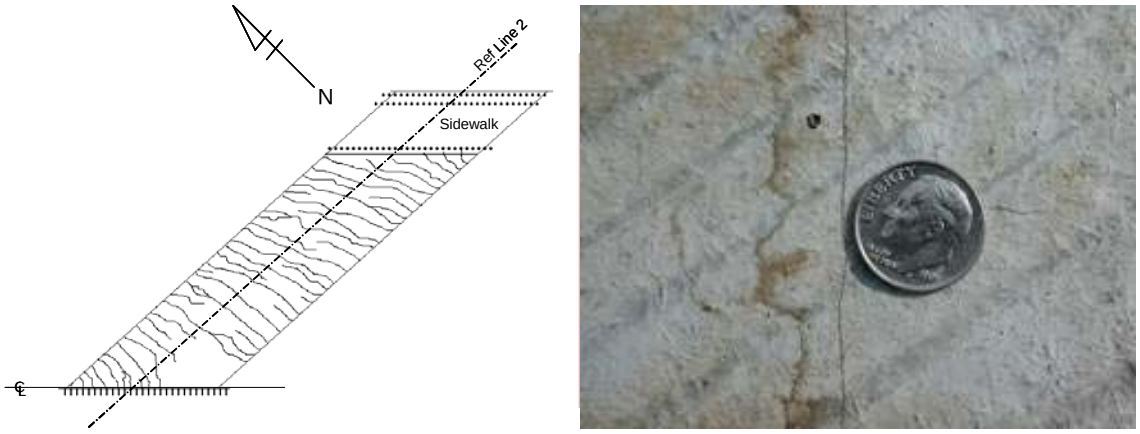

(a) (b)

Figure 1.2: (a) Diagram of crack pattern in ECC link slab – phase one and (b) early age cracking within ECC link slab with crack width approximately 0.006” to 0.01” (after 3 Days, September 13th, 2005).

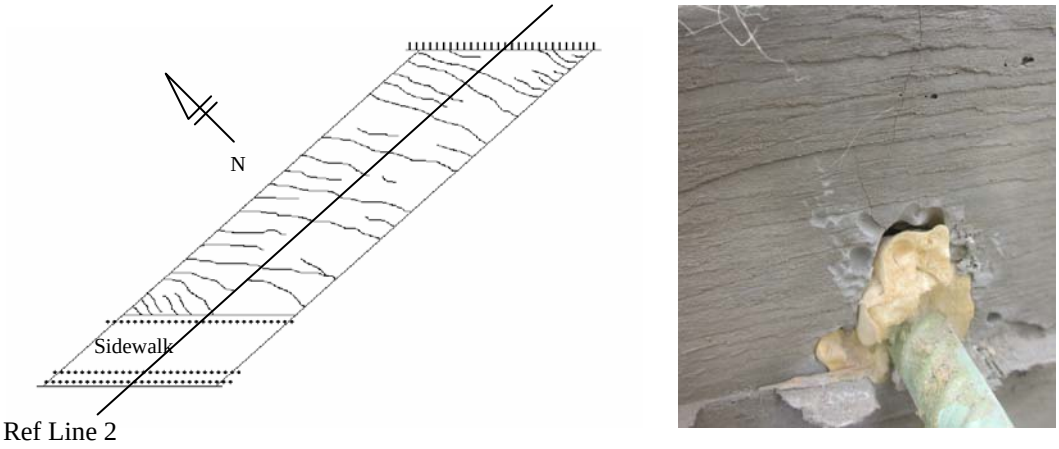

(a) (b)

Figure 1.3: (a) Diagram of crack pattern in ECC link slab – Phase 2 and (b) epoxy-coated steel reinforcing bars as stress concentrator for crack initiation.

1.2 First Large Frame Restrained Shrinkage Test

In order to replicate the early age cracking, a restrained shrinkage test on ECC M45 using a large steel frame was conducted. The schematic of large frame restrained shrinkage testing setup is shown in **Figure 1.4**.

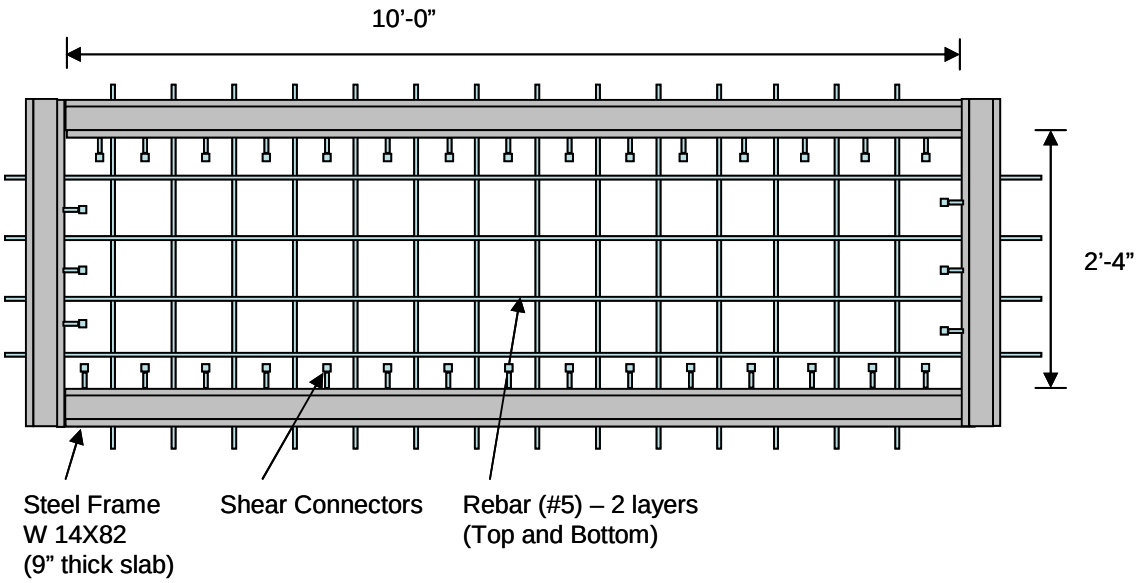

Figure 1.4: Schematic of large frame restrained shrinkage testing setup

This frame was constructed of four W14 X 82 steel I-beams and was connected by welding (**Figure 1.5(a)**) to adequately resist the shrinkage forces within the ECC slab and promote cracking. The interior area of the frame measured 10' by 2'-4" and could accommodate a 9" thick slab (full depth of the Grove Street ECC link slab). To transfer restraint from the frame to the slab, a series of 0.75" diameter shear connectors were placed on the frame every 8" along the sides at mid depth as depicted in **Figure 1.5(b)**. A debonding paper was placed on the bottom of the frame (**Figure 1.5(c)**). Two layers epoxy coated reinforcing bars (#5) were placed in the frame. The reinforcing steel was installed at 8" spacing in each layer and each direction (longitudinal and transverse) and with 2" clear cover (**Figure 1.5(d)**). Five thermocouples were installed in the center of the frame (**Figure 1.5(e)**) in order to monitor the thermal gradients along the depth of the slab. **Figure 1.5(f)** shows the final configuration of the large scale restrained shrinkage frame.

(a) (b)

(c) (d)

(e) (f)

Figure 1.5: Large frame restrained shrinkage test construction

The large frame restrained shrinkage test of ECC slab was poured on November 2, 2006. A gravity-based mixer (**Figure 1.6**) was used to simulate the processing of ECC by the

ready mix truck in field and to produce a total of 18 cubic feet of ECC Mix 45 material to fill the frame. The mixture proportion of Mix 45 used in the large frame shrinkage test was identical with those used in the actual ECC link slab and can be found in **Table 1.1**. The raw materials (Type I cement and F-110 silica sand) and chemical additives (Euclid Plastol® 5000 high rate water reducer and Euclid Eucon Retarder 75) used were also identical with those used in the actual ECC link slab except that the source of the Type F fly ash is different. In the Grove Street bridge ECC link slab, a Type F fly ash from East Lake, Ohio, supplied by the Headwater Company was adopted. Here, we use a Type F fly ash from Rockdale, Texas, supplied by the Boral Material Technologies. The East Lake power plant do not package and sell their fly ash in the form of pail, drum, or supersack. The fly ash is usually shipped by the pneumatic truck to the concrete batching plant and discharged to the storage bin directly. Therefore, acquisition of the East Lake fly ash for producing large frame restrained shrinkage test is difficult. In fact, the quality of fly ash varies from batch to batch. In other words, use of fly ash from the same power plant does not guarantee that the same ash properties can be obtained if the fly ash comes from a different batch. In processing the ECC material by using the gravity-based mixer, the batching sequence of the ingredients was the same as that used in the ready mix truck and can be found in **Table 1.2**.

Figure 1.6: The gravity-based mixer used for producing large frame restrained shrinkage test of ECC slab

Table 1.1: Mixing proportions of ECC (M 45) for large frame slab

Material	Amount (lbs/cyd)
Cement	974
Fly Ash	1168
Water	563
Sand	778
HRWR	13.6
Fiber (vol%)	44
Stabilizer	2 oz per 100 lb cement

Table 1.2: Batching sequence of ECC for large frame slab

Activity	Elapsed Time (min)
1. Charge all sand	2
2. Charge portion of mixing water, all HRWR, and all hydration stabilizer	2
3. Charge all fly ash	2
4. Charge all cement	2
5. Charge remaining mixing water to wash drum fins	4
6. Mix at high speed RPM until material is homogenous	5
7. Charge fibers and mix until material is homogenous	5
Total	22

The slab was cured outdoor under plastic for 7 days. Following this curing regime, the slab was exposed to outdoor environment and monitored for crack formation (**Figure 1.7 (a)**). The maximum, minimum, and average outdoor temperature and relative humidity of Ann Arbor from November 2 to December 7 are listed in **Table 1.3**. The hydration peak of ECC Mix 45 occurred at the 14^{th} hour after pouring and the internal temperature profile along the depth of the slab at the peak of hydration is shown in **Figure 1.8**. As can be seen, the thermal gradient generated within the ECC slab is about 10^{o}F, which is not significant. It is therefore concluded the thermal gradient in a 9" think ECC link slab is not a cause for the early age cracking in the field. While this restrained shrinkage frame does more fully represent the field conditions in the ECC link slab, the same type of cracking observed in the link slab could not be replicated. After 7 days of curing, no early age shrinkage cracks could be found and after 21 days (7 curing and 14 outdoor environment exposure) a couple of small microcracks (0.0005") could be seen as shown

in **Figure 1.7 (b)**. Those cracks were likely introduced by the drying shrinkage at a later age.

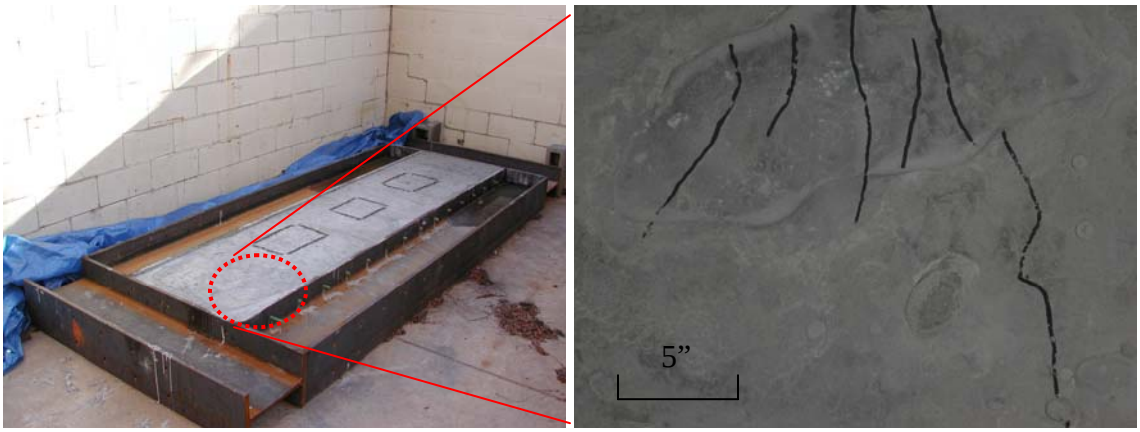

(a) (b)

Figure 1.7: (a) Large frame restrained shrinkage test of ECC slab and (b) microcracks observed after 21 days. Cracks were traced by a black marker.

Table 1.3: Recorded Ann Arbor temperature and relative humidity from Nov. 2 to Dec. 7

	Maximum	Minimum	Average
Temperature (^{o}F)	66	16	38
Relative Humidity (%)	100	32	80

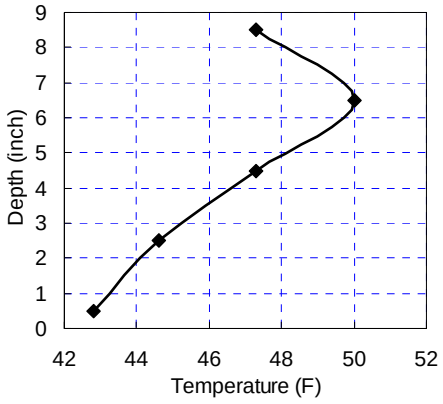

Figure 1.8: Temperature profile along the depth of ECC slab at peak of hydration (14th hour after pouring)

The result from the large frame restrained shrinkage test indicates that large size, full depth, high restraint, and epoxy reinforcement as stress concentrator are not the only sources responsible for the early age cracking observed in the field. The large scale frame restrained shrinkage test is expensive and time consuming to carry out. Therefore, to reveal the underlying causes of the early age cracking phenomenon in ECC link slab, systematic studies on early age cracking mechanisms were conducted.

1.3 Objectives of Research

The ultimate goal of the research is the reduction and possibly elimination of the early age cracking observed in the demonstration ECC link slab on Grove Street Bridge over I-94 (S02 of 81063). To achieve this goal, a number of objectives must be met. These include systematic identification of sources of early age cracking observed in ECC link slab, developing materials solutions to minimize the early age cracking while ensuring that the fresh and mechanical properties specified by MDOT for ECC material are met, and development of design/construction execution recommendations for future ECC bridge link slab applications.

This research looks to build upon the significant theoretical, experimental, and field findings from the previous research (Li et al, 2005), ultimately improving design and construction of a durable ECC link slab in Michigan. This will be accomplished by directly relating the deliverables from previous MDOT supported research to the objectives within this extended project. This close relation between the completed and extended continuation research looks to optimize the output of both research projects.

In addition to building upon previous MDOT research, this project extension looks to incorporate the work of other ECC researchers beneficial to ECC link slab construction. In particular, work already performed in Japan (Kanda et al., 2006) may lead to very practical methods to prevent the type of cracking observed within the demonstration ECC link slab. This project extension also looks to work closely with MDOT designers, consultants, material suppliers, and approved contactors to guarantee the success and

practicality of the proposed modifications. Additionally, the experience gained in reducing shrinkage within the ECC link slab should prove invaluable in future MDOT work.

2. Literature Review (Task 1)

2.1 Potential Causes of Early Age Cracking on Grove Street Bridge ECC Link Slab

Several potential causes of those early age cracks are identified and itemized below. The early age cracking observed in the link slab is likely a combined result of these potential sources.

Excessive shrinkage

The ECC material version used in the Grove Street link slab has a larger shrinkage compared to that of normal concrete due to high cement content and low water-cementitious material ratio in ECC (Wang and Li, 2006). This material property has been known about ECC for some time, yet in all other circumstances shrinkage deformation resulted in the formation of tightly spaced microcracking, rather than larger macrocracks. ECC material shrinkage can also be affected by the curing period and method, time of casting, weather condition, use of different ingredients (e.g. fly ash, HRWR, etc.), use of retarder, and excessive water (especially in Phase I). Shrinkage reducing admixture and shrinkage compensation component (Kanda et al., 2006) can be incorporated into ECC mix design to reduce shrinkage of ECC.

High restraint

Strain alone, caused by shrinkage, creep, or thermal loading, does not induce stresses nor cracks. The forces and pressures provided by restraint cause tensile stress. Steel reinforcement connecting the link slab to the adjacent hardened concrete deck, cold jointing to the adjacent concrete, and shear studs within the link slab transition zone provide restraint within the ECC link slab. These mechanical interlocking mechanisms restrain any change of volume in the slab due to early age shrinkage.

Epoxy reinforcement as stress concentrator

Nearly all cracks within the Grove Street link slab seem to initiate from steel reinforcement (**Figure 1.3(b)**). Those "holes" created by the epoxy coated rebars within the ECC link slab may serve as stress concentrators and crack initiators due to change of geometry and weak bonding between ECC and epoxy coated reinforcements, when combined with ECC shrinkage.

Early age shrinkage before σ-δ curve development

The tight crack width in hardened ECC is a result of effective fiber bridging provided by the presence of micro polymer fibers and optimized fiber/matrix interface properties. This fiber bridging is quantified through the stress versus crack opening relation (i.e. σ-δ relation) within the ECC material. Typically, this fiber bridging associated with interfacial bond development is built up with time. In most cases, once mechanical loads are applied to the material, the σ–δ relation has already developed enough to resist any localized cracking. At early age however, the σ-δ curve has not been fully developed, and therefore a larger crack width can appear due to early age shrinkage.

High skew angle

Fu et al (2007) conduced a survey of state transportation agencies in the U.S. and found that deck corner cracking in skew bridges was commonly observed. Cracking was observed in the ECC link slab as well as on the adjacent concrete deck placed in 2005 on Grove Street Bridge. The crack pattern found on concrete deck and in the ECC link slab on the Grove Street bridge bears similarity as those reported by Fu et al. The crack widths found in the ECC link slab on Grove Street were 0.005" to 0.007", while those found in the adjacent concrete deck were in the range of 0.13" to 0.17". Fu et al did not report crack width.

Of importance is the early age cracking revealed in the deck on I-94 Wbd over Gratiot (MDOT, 2006). This deck has a skew angle of $28^{o}50'30"$. The cracks appear on the 4th day and the crack geometric pattern in general matches those on the ECC link slab, even

though the crack widths appear significantly larger from the available photos, and wider spaced. The similarity in geometric pattern of the cracks and their early age development suggested that the skew angle may contribute to the tendency of early age cracking in the ECC link slab, even though the mechanism behind this phenomenon is not at present fully understood. Recommendations made by early developers of concrete link slab suggested that link slabs should not be used in bridges with skew angle above 25 degrees (Gilani and Jansson, 2004). Within the ECC link slab, cracking at the acute angle corners was also observed. The presence of a 45º skew angle within the link slab may be a source for crack formation.

Improper curing

The first few days after concrete material placement are critical to its strength, durability, permeability, and volume stability. Although curing compound was applied on ECC link slab right after surface finishing and texturing, wet burlap and plastics were not applied until several hours later. Since the ambient condition of bridge site is windy and dry, it is expected that water evaporation rate could be high which may introduce higher shrinkage. In addition, no water hose was placed on ECC link slab and no continuous wet curing for the first several days. This violates the curing requirement specified in ECC link slab special provision and can also introduce higher shrinkage at early age.

2.2 Engineered Cementitious Composites (ECC) Design Theory

2.2.1 ECC Design Framework

ECC tensile strain hardening is a result of realizing and tailoring the synergistic interaction between fiber, matrix, and interface. Micromechanics has been used as a tool to link material microstructures to ECC tensile strain hardening behavior. Desirable tensile strain capacity several hundred times that of normal concrete can be achieved by tailoring material microstructures once the established linkages are utilized in material component tailoring. Therefore, scale linking (**Figure 2.1**) represents the design

philosophy behind the development of ECC in which investigation of microscale phenomena and tailoring material microstructure are the keys to understanding and designing desirable composite macroscale behavior.

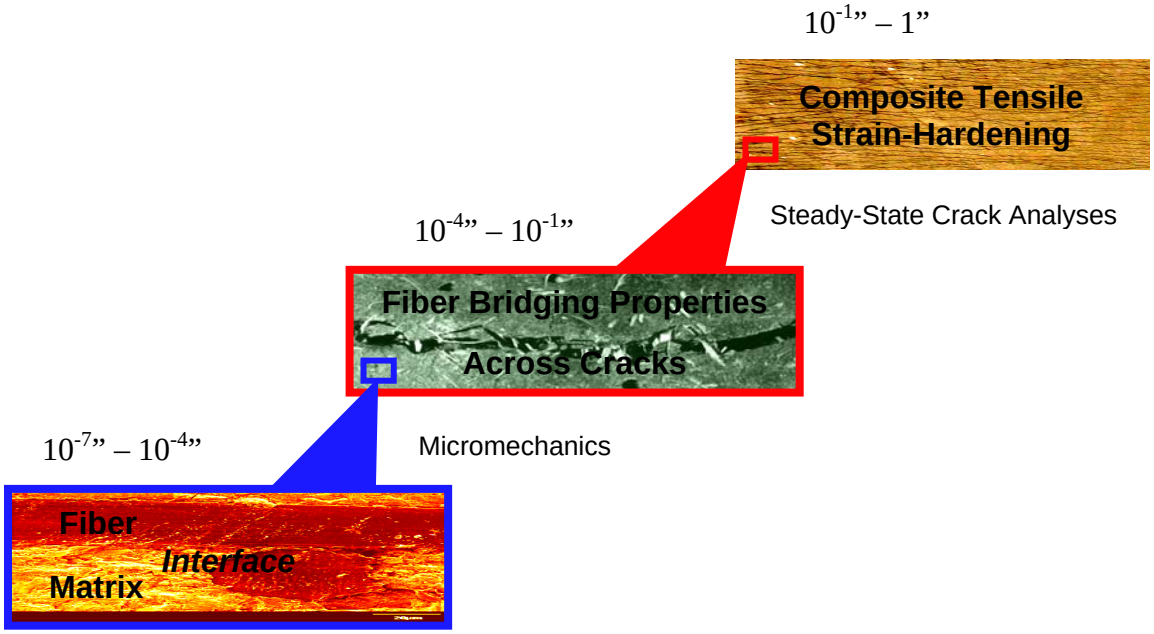

Figure 2.1: Scale linking in ECC

As shown in **Figure 2.1**, ECC shows multiple cracking and tensile strain hardening in composite macroscale (10^{-1}" – 1"). One scale below is the mesoscale (10^{-4}" – 10^{-1}"). In this scale, fibers bridge across the crack and fiber bridging spring law governs the bridging behavior. Still one scale down is the material microstructure (10^{-7}" – 10^{-4}"), which consists of fiber, matrix, and interface. Micromechanics model links microscale constituent parameters to fiber bridging constitutive behavior in the mesoscale. Steady state crack analysis connects fiber bridging property to tensile strain hardening in composite macroscale. Once established, the model-based linking provides a backward path for material microstructure/ingredient tailoring, which allows systematic composite optimization for maximum tensile ductility with the minimum amount of fibers. Microstructure tailoring includes deliberate selection or modification of fiber, matrix, and interface properties, including the addition of nano-size particles (e.g. carbon and nano-fibers) and fiber surface coating. This conceptual framework represents a holistic approach in composite design accounting for the interaction between the fiber, matrix, and interface.

2.2.2 ECC Tensile Strain-hardening Criteria

ECC is a fiber reinforced brittle mortar matrix composite and the pseudo strain-hardening behavior in ECC is achieved by sequential development of matrix multiple cracking (**Figure 2.2**). The fundamental requirement for multiple cracking is that steady state crack propagation prevails under tension, which requires the crack tip toughness J_{tip} to be less than the complementary energy J'_b calculated from the bridging stress σ versus crack opening δ curve, as illustrated in **Figure 2.3** (Marshall and Cox, 1988; Li and Leung, 1992).

$$J_{tip} \le \sigma_0 \delta_0 - \int_0^{\delta_0} \sigma(\delta) d\delta \equiv J_b^{'} \tag{2.1}$$

$$J_{tip} = \frac{K_m^2}{E_m} \tag{2.2}$$

where σ_0 is the maximum bridging stress corresponding to the opening δ_0, K_m is the matrix fracture toughness, and E_m is the matrix Young's modulus. **Equation 2.1** employs the concept of energy balance during flat crack extension between external work, crack tip energy absorption through matrix breakdown (matrix toughness), and crack flank energy absorption through fiber/matrix interface debonding and sliding. This energy-based criterion determines the crack propagation mode (steady state flat crack or Griffith crack).

The stress-crack opening relationship $\sigma(\delta)$, which can be viewed as the constitutive law of fiber bridging behavior, is derived by using analytic tools of fracture mechanics, micromechanics, and probabilistics. In particular, the energetics of tunnel crack propagation along fiber/matrix is used to quantify the debonding process and the bridging force of a fiber with given embedment length (Lin et al, 1999). Probabilistics is introduced to describe the randomness of fiber location and orientation with respect to a crack plane. The random orientation of fiber also necessitates the accounting of the mechanics of interaction between an inclined fiber and the matrix crack. As a result, the $\sigma(\delta)$ curve is expressible as a function of micromechanics parameters, including interface chemical bond G_d, interface frictional bond τ_0, and slip-hardening coefficient β

accounting for the slip-hardening behavior during fiber pullout. In addition, snubbing coefficient f and strength reduction factor f' are introduced to account for the interaction between fiber and matrix as well as the reduction of fiber strength when pulled at an inclined angle. Besides interfacial properties, the σ(δ) curve is also governed by the matrix Young's modulus E_m, fiber content V_f, and fiber diameter d_f, length L_f , and Young's modulus E_f.

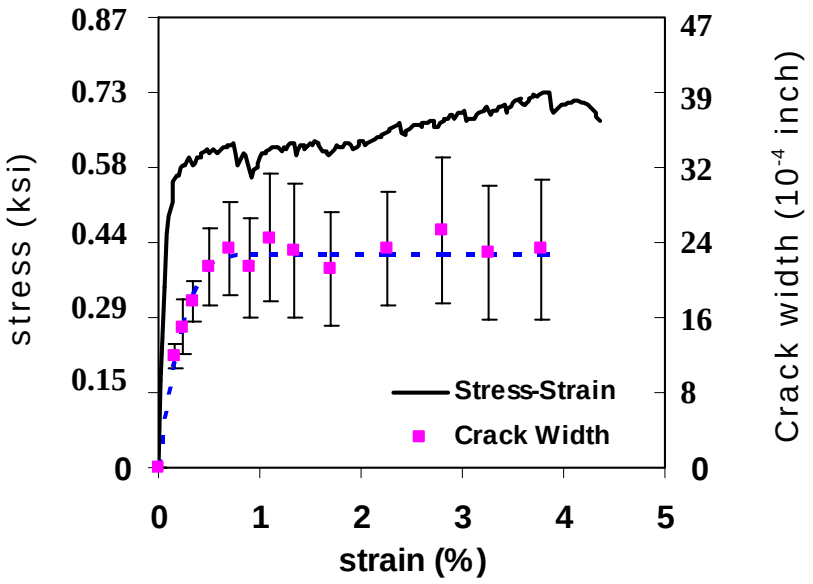

Figure 2.2: Typical tensile stress-strain-crack width relationship of PVA-ECC M45

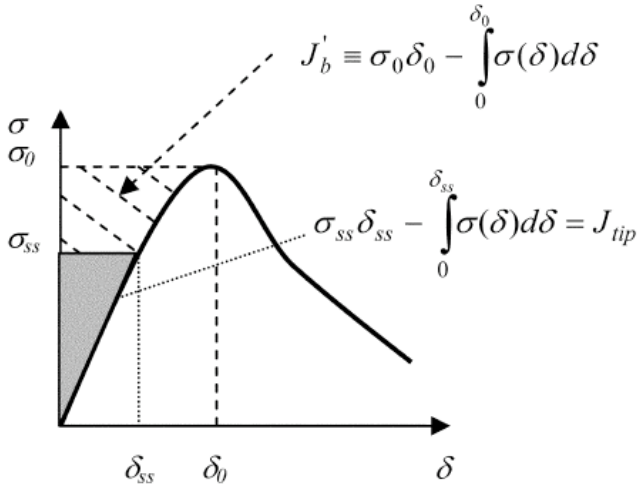

Figure 2.3: Typical σ(δ) curve for tensile strain-hardening composite. Hatched area represents complimentary energy J'_b. Shaded area represents crack tip toughness J_{tip}.

Another condition for the pseudo strain-hardening is that the matrix tensile cracking strength σ_c must not exceed the maximum fiber bridging strength σ_0.

$$\sigma_c < \sigma_0 \tag{2.3}$$

where σ_c is determined by the matrix fracture toughness K_m and pre-existing internal flaw size a_0. While the energy criterion (**Equation 2.1**) governs the crack propagation mode, the strength-based criterion represented by **Equation 2.3** controls the initiation of cracks. Satisfaction of both **Equations 2.1** and 2.**3** is necessary to achieve ECC behavior; otherwise, normal tension-softening FRC behavior results. Details of these micromechanical analyses can be found in previous works (Lin et al, 1999; Li, 1992).

Due to the randomness nature of preexisting flaw size and fiber distribution in ECC, a large margin between J'_b and J_{tip} is preferred. The pseudo strain-hardening (PSH) performance index has been used to quantitatively evaluate the margin and is defined as follows (Kanda, 1998).

$$\begin{aligned} PSH\ energy &= \frac{J'_b}{J_{tip}} \\ PSH\ strength &= \frac{\sigma_o}{\sigma_c} \end{aligned} \tag{2.4}$$

Materials with larger PSH index should have better chance of saturated multiple cracking. The saturation of multiple cracking is achieved when microcracks are more or less uniformly and closely spaced (at around 0.04”-0.08”), and cannot be further reduced under additional tensile loading of a uniaxial tensile specimen. Robustness of tensile ductility refers to the consistency of tensile capacity from one specimen to another. To measure the extent of saturation of multiple cracking, PSH intensity has been used and is defined as crack spacing ratio (Kanda, 1998).

$$PSH\ \ Intensity = \frac{x_d^{test}}{x_d} \tag{2.5}$$

where x_d is the theoretical crack spacing calculated from mechanics (Li and Wu, 1992; Wu and Li, 1992) and x_d^{test} is the crack spacing measured experimentally. Crack spacing here is defined as the distance between two adjacent cracks. The minimum value of PSH

intensity is 1 which indicates a fully saturated multiple cracking state. According to Aveston et al (1971), the PSH intensity should fall between 1 and 2 for saturated PSH behavior.

3. Identification and Replication of Early Age Cracking (Task 2)

3.1. Identification of Factors Influencing Early Age Cracking

Based on the discussion with the research advisory panel on December 14, 2006, systematic studies were conducted on potential factors that may contribute to the early age cracking behavior observed in the Grove Street bridge ECC link slab. These factors were categorized into four groups, namely Material, Processing, Curing, and Structure, and were given priority ratings. Some adjustments of these ratings were made subsequently after reviewing additional documents, especially those related to cracking in concrete decks with a high skew angle. The final ratings are shown in **Table 3.1**. In the end, however, we conducted studies on all these influencing factors, as described below.

Table 3.1: List of factors which may contribute to early age cracking, and proposed priority rating of investigation (5: highest, 1: lowest)

Factors		Priority
Material	Fly ash source/Alkali content	3
	Excessive water	4
	Excessive retarder	4
Processing	Mixing time	2
	Mixing equipment	2
Curing	Ambient temperature	4
	Ambient relative humidity	5
	Wind	4
	Curing compound	2
Structure	Skew angle	5
	Boundary conditions/Restraint	5
	Rebar as stress concentrator	5

This research task examined each potential factor one-by-one by using a small scale restrained ring test and restrained prism test where appropriate. The small scale restrained tests were chosen for more rapid assessment of early age cracking, and are suiTable for all factors except for the skew angle effect. For the investigation of skew angle, a finite element analysis was performed to evaluate skew angle effect on the stress field of ECC link slab.

3.1.1 Restrained Shrinkage Ring Test

Eleven potential factors were separated into four groups and investigated by means of the restrained shrinkage ring test. Testing procedure followed ASTM C1581 "Standard Test Method for Determining Age at Cracking and Induced Tensile Stress Characteristics of Mortar and Concrete Under Restrained Shrinkage" and AASHTO PP-34 "Standard Practice for Estimating the Crack Tendency of Concrete". The test set-up and specimen dimensions are shown in **Figure 3.1**. For each specimen, a layer of ECC material was cast around a rigid steel ring. A plastic covered construction carton tube was used as an outer mold during casting. The outer mold was removed 24 hours after casting. The specimen was subsequently exposed to predetermined environmental exposure. Shrinkage deformation of the ECC layer was restrained by the steel ring, resulting in an internal radial pressure and a circumferential tensile stress state that may cause cracking. The crack number and crack width were measured using a portable microscope. Measurements were taken at three different locations along each crack and the average value was reported.

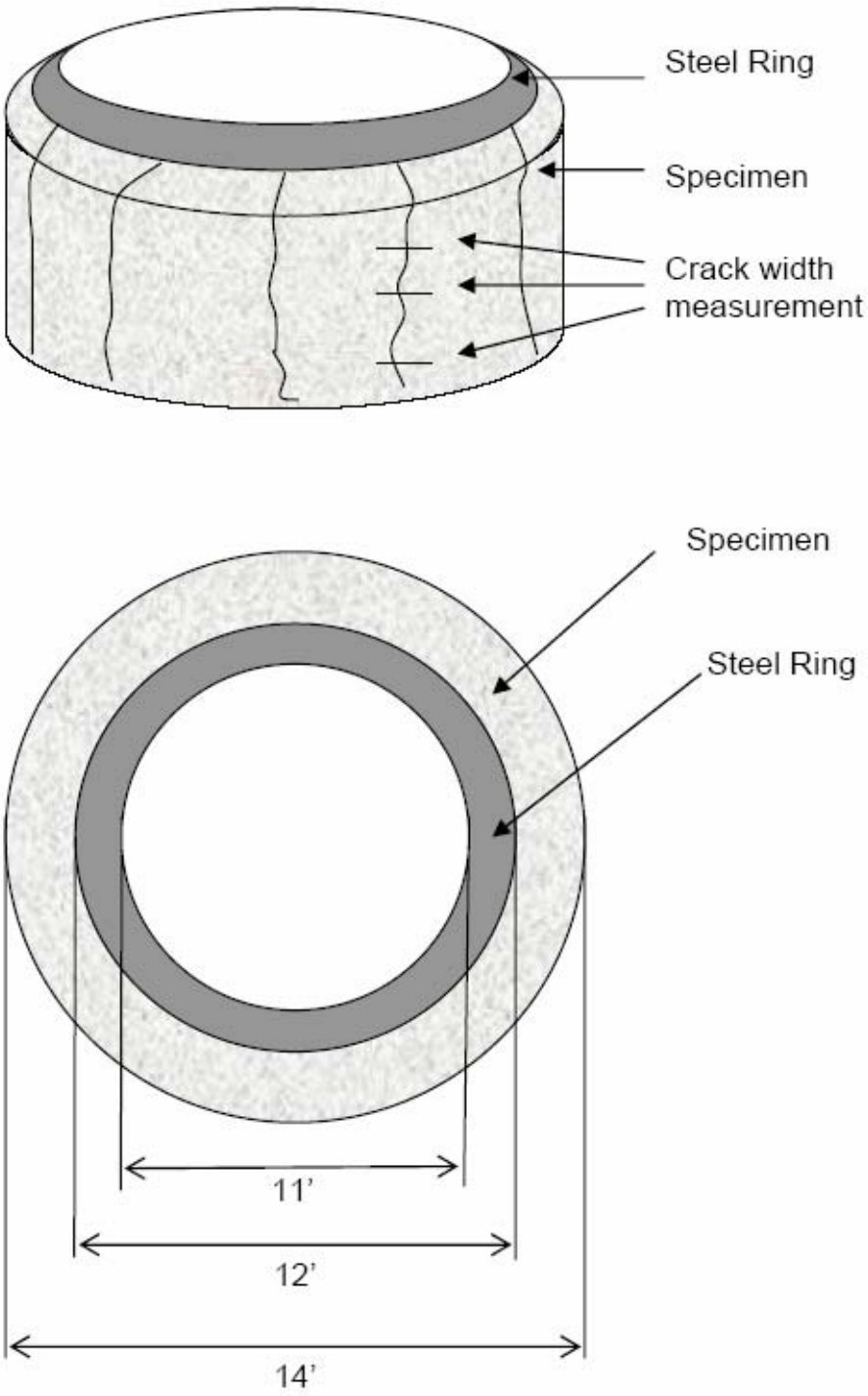

Figure 3.1: Scheme of the restrained shrinkage ring test setup and dimensions

3.1.2 Material Related Factors

Experimental Program

Three factors related to ECC material composition were investigated by means of the restrained shrinkage ring test. They are fly ash source, excessive water represented by the water to cement ratio, and excessive retarder represented by the retarder to cement ratio. In this test series, we also included another potential material related factor, excessive high range water reducer represented by the superplasticizer to cement ratio, to get a more complete picture of early age cracking causes. M45 (Mix 1) was tested as control and the mix proportion of M45 are listed in **Table 3.2**. This mix proportion is identical with the ECC material used in phase I link slab construction, except that no retarder was used in M45. In all mixes, 0.315" PVA fiber was adopted. 0.315" PVA fiber was also used in ECC link slab. Mix 2 to Mix 6 were tested to investigate the effect of the four material composition related factors. Table 2 shows the mix design of Mix 2 to Mix 6. The studied factor is highlighted in yellow (shaded in black & white print).

Table 3.2: Mixing proportions of ECC M45

Cement	Fly Ash	Sand	Water	HRWR	Fiber (vol. %)
1	1.2	0.8	0.59	0.014	2

Table 3.3: Mix design for investigation of material related factors

	w/c	FA source	Retarder/C	SP/C
Mix1-Control	0.59	Boral	0	0.014
Mix2	0.64	Boral	0	0.014
Mix3	0.54	Boral	0	0.014
Mix4	0.59	Headwaters	0	0.014
Mix5	0.59	Boral	0.003	0.014
Mix6	0.59	Boral	0	0.016

Mix 1 to 3 were used to identify the effect of water variation (w/c = 0.54 to 0.64). Mix 4 used fly ash from a different source to investigate the influence of fly ash origin. For M45 (mix 1), class F fly ash from Boral Material Technologies Inc. Rockdale power

plant, Texas was used. For Mix 4, class F fly ash from Headwaters East Lake power plant, Ohio was adopted. Fly ash from this power plant was also used in the construction of ECC link slab at Grove Street bridge in 2005. The physical and chemical properties of these two fly ashes provided by Headwaters Company and Boral Material Technologies Inc. can be found in **Tables 3.4** and **3.5**, respectively. From **Tables 3.4** and **3.5**, the major differences of the two fly ashes are the alkali content, which could be a source of early age cracking. It was found from the literatures that the alkali content has an influence on the early-age cracking properties of cement-based materials. The cracking initiation time of mortars with higher alkali content is advanced (He et al, 2004). From **Tables 3.4** and **3.5**, East Lake fly ash has a higher alkali content than the Rockdale fly ash, which implies a shorter cracking initiation time by using East Lake fly ash. If the cracking initiates before the full development of fiber bridging, wide crack width can result. Mix 5 incorporated excessive retarder (Euclid Eucon Retarder 75) and Mix 6 used excessive high range water reducer to examine the effect of excessive chemical additives. In all mixes, Euclid Plastol® 5000 was used as the high range water reducer. Those two chemical additives (retarder and HRWR) from Euclid Chemical Company were also used in the construction of Grove Street ECC link slab.

Table 3.4: Class F fly ash from Rockdale, TX

SiO_2, %	55.71	Moisture Content, %	0.16
Al_2O_3, %	22.56	Loss on Ignition, %	0.41
Fe_2O_3, %	5.61	Amount Retained on #325 Sieve, %	23.63
Sum, %	83.88	Specific Gravity	2.29
CaO, %	10.44	Autoclave Soundness, %	0.02
MgO, %	1.78	Strength Activity Index w/ Portland Cement at 7 days, % of Control	77.1
SO_3, %	0.54		
Na_2O, %	0.24	Strength Activity Index w/ Portland Cement at 28 days, % of Control	85.5
K_2O, %	0.79		
Total Alkalis, %	0.76	Water Required, % of Control	94.6
Available Alkalis, %	0.26		

Table 3.5: Class F fly ash from East Lake, OH

SiO_2, %	42.31	Moisture Content, %	0.06
Al_2O_3, %	25.47	Loss on Ignition, %	1.37
Fe_2O_3, %	15.73	Amount Retained on #325 Sieve, %	20.4
Sum, %	83.51	Specific Gravity	2.56
CaO, %	8.72	Autoclave Soundness, %	-0.02
MgO, %	2.32	Strength Activity Index w/ Portland Cement at 7 days, % of Control	78.1
SO_3, %	0.73		
Na_2O, %	N/A	Strength Activity Index w/ Portland Cement at 28 days, % of Control	86.85
K_2O, %	N/A		
Total Alkalis, %	N/A	Water Required, % of Control	93
Available Alkalis, %	0.67		

A Hobart mixer was used to produce all ECC materials and the mixing procedure and mixing time followed **Table 3.8**. No curing compound was applied on the upper surface of the ring. The outer mold was removed 24 hours after casting. The specimen was then exposed to laboratory room condition with ambient temperature of 70±5^{o}F and ambient relative humidity of 45±10% and there was no wind effect (**Figure 3.2**).

Figure 3.2: Restrained shrinkage ring test demolded after 24 hours and cured in the laboratory air condition. A portable microscope used to monitor crack width.

Results and Discussion

The results of the restrained shrinkage ring tests are shown in **Table 3.6** with a summary of the average crack widths in ring specimen at the 7th day. Within **Table 3.6** the shrinkage strain of the material was computed by dividing the total shrinkage measured within the specimen (through summation of all crack widths) by the ring circumference (40.84").

Table 3.6: Summary of restrained shrinkage ring test results on material related factors

Mix	Average crack width (10^{-4} in)	Maximum crack width (10^{-4} in)	Number of cracks	Total shrinkage (10^{-4} in)	Shrinkage strain (%)
1 – Control	22±8	43	14	308	0.0754
2 – High W/C	12±3	28	15	180	0.0441
3 – Low W/C	30±19	79	13	390	0.0955
4 – Fly ash	21±14	51	16	336	0.0823
5 – High Re/C	18±7	31	11	198	0.0485
6 – High SP/C	19±8	35	11	209	0.0512

* Each data point is an average of 2 tests
** Ranges shown are standard deviation

As can be seen from the various mix designs tested, use of fly ash from East Lake, Ohio power plant (mix 4) did not result in a large change in shrinkage strain or crack width. However, a change in mixing water from 0.64 to 0.54 w/c ratio (mix 1 to 3) did increase the shrinkage strain and also the average crack width. Excessive retarder (mix 5) and superplasticizer (mix 6) have a more significant effect in reducing total shrinkage than crack width.

3.1.3 Processing Related Factors

Experimental Program

Mixing equipment and mixing time are the two factors related to the processing of ECC materials and were investigated by the restrained shrinkage ring test. In this test series, M45 was used as the test material. The mix proportion of M45 can be found in **Table 3.2**.

Class F fly ash from Boral Material Technologies Inc. and Euclid Plastol® 5000 high range water reducer from Euclid Chemical Company were used. No retarder was used and no curing compound was applied on the upper surface of the ring. In all mixes, 0.315" PVA fiber was adopted.

Table 3.7 gives different processing related parameters in producing three mixes (Mix 7 to 9). Mix 7 was the control test. The Hobart mixer was used to produce Mix 7 and the mixing time after charging fiber was 5 minutes. A gravity-based mixer (**Figure 3.3**) was used to produce Mix 8 in order to investigate the effect of mixer type on early age shrinkage. Gravity-based mixer (conventional ready-mix truck) was used in the construction of ECC link slab. For Mix 9, the Hobart mixer was also used. However, the mixing time after charging fiber was extended to 10 minutes. This was used to examine the possible effect of mixing time on early age shrinkage. The batching sequences for the Hobart mixer and the gravity-based mixer can be found in **Tables 3.8** and **3.9**, respectively.

The outer mold of the ring was removed 24 hours after casting. The specimen was subsequently exposed the laboratory room condition with ambient temperature of 70±5^{o}F and ambient relative humidity of 45±10% and there was no wind effect.

Table 3.7: Mix 7 to 9 for investigation of processing related factors

	Mixer	Mixing time after charging fiber
Mix 7 – Control	Hobart	5
Mix 8	Gravity	5
Mix 9	Hobart	10

Table 3.8: Batching sequence for producing ECC by the Hobart mixer (Li et al., 2005)

Activity	Elapsed Time (min)
1. Charge all dry materials (cement, fly ash, sand)	2
2. Charge water, HRWR	3
3. Charge fibers	5
Total	10

Table 3.9: Batching sequence for producing ECC by the gravity-based mixer

Activity	Elapsed Time (min)
1. Charge all sand	2
2. Charge portion of mixing water, all HRWR, and all hydration stabilizer	2
3. Charge all fly ash	2
4. Charge all cement	2
5. Charge remaining mixing water to wash drum fins	4
6. Charge fibers and mix until material is homogenous	5
Total	17

Figure 3.3: A 1 cubic foot capacity gravity mixer

Results and Discussion

Table 3.10 shows the 7th day results of the restrained shrinkage ring tests considering processing related factors. As can be seen, the mix produced by the gravity mixer (mix 8) has larger crack width when compared with the control. This may be attributed to poor fiber dispersion of mix 8, and therefore the efficiency of fiber bridging diminished. In fact, fiber clump was visually observed in producing mix 8. Prolonged mixing time (mix 9) did not have much influence on crack width and overall shrinkage. Two ring specimens were tested for each mix.

Table 3.10: Summary of restrained shrinkage ring test results on processing related factors

Mix	Average crack width (10^{-4} in)	Maximum crack width (10^{-4} in)	Number of cracks	Total shrinkage (10^{-4} in)	Shrinkage strain (%)
7 – Control	20±7	35	16	320	0.0784
8 – Mixer	25±15	71	12	300	0.0735
9 – Time	22±8	39	15	330	0.0808

* Each data point is an average of 2 tests
** Ranges shown are standard deviation

3.1.4 Curing Related Factors

Experimental Program

Curing represents another important category in determining early age cracking behavior. Four curing related factors, curing ambient temperature, curing ambient relative humidity, wind effect, and applying of curing compound, were investigated by means of the restrained shrinkage ring test. **Table 3.11** shows different curing related parameters in producing five mixes (ranges shown are standard deviation). M45 was the testing material and Mix 10 was the control test. The mix proportion of M45 can be found in **Table 3.1**. Class F fly ash from Boral Material Technologies Inc. and Euclid Plastol® 5000 high range water reducer from Euclid Chemical Company were used. No retarder was used. In all mixes, 0.315" PVA fiber was adopted. A Hobart mixer was used to produce all ECC materials and the mixing procedure followed **Table 3.8**.

Table 3.11: Mix 10 to 14 for investigation of curing related factors

	Ambient curing temperature (^{o}F)	Ambient curing relative humidity (%)	Wind effect	Applying curing compound
Mix 10 - Control	70±5	45±10	No	No
Mix 11	95±5	45±10	No	No
Mix 12	70±5	95±5	No	No
Mix 13	70±5	45±10	Yes	No
Mix 14	70±5	45±10	No	Yes

* Ranges shown are minimum and maximum values

Upon removing the outer mold 24 hours after casting, Mix 10 was cured in the laboratory air with ambient temperature of 70±5^{o}F and relative humidity of 45±10%. To examine the effect of curing temperature, Mix 11 was cured in an oven at 95±5^{o}F right after casting and until the 7th day (the outer mold was removed 24 hours after casting). To investigate the effect of curing humidity, Mix 12 was cured in a sealed plastic bag until the 7th day (the outer mold was removed 24 hours after casting). Mix 13 considered the wind effect by providing a constant wind blow through a 14" fan (**Figure 3.4**) in the first seven days (the outer mold was removed 24 hours after casting). Curing compound, Kurez VOX White Pigmented, from Euclid Chemical Company was applied on the top surface of Mix 14 right after casting to investigate the effect of applying curing compound.

Figure 3.4: Use of 14" fan to provide constant wind effect at early age

Results and Discussion

Table 3.12 summarizes the curing related restrained shrinkage ring test results at the 7th day. It shows that higher curing temperature (mix 11) tends to increase the crack width and overall shrinkage. It is likely that high curing temperature promotes hydration degree and autogenous shrinkage before the fully development of fiber bridging at early age. For mix 13, larger crack width and lower shrinkage strain were observed when applying a

constant wind blow at early age. It may be concluded that wind effect could promote water evaporation and drying shrinkage before the fully development of fiber bridging at early age. However, water evaporation at early age can also cause termination of hydration and autogenous shrinkage, and therefore this may contribute to the lower total shrinkage of mix 13. No crack was found in mix 12 at the 7th day when cured in a sealed plastic bag. This may be attributed to that high humidity prevents water evaporation and drying shrinkage at early ages. This suggested the importance of keeping ECC from excessive drying at early age. Appling of curing compound in the ring test did not seem to have any significant effect.

Table 3.12: Summary of restrained shrinkage ring test results on curing related factors

Mix	Average crack width (10^{-4} in)	Maximum crack width (10^{-4} in)	Number of cracks	Total shrinkage (10^{-4} in)	Shrinkage strain (%)
10 – Control	21±4	35	13	273	0.0668
11 – Temp	31±9	59	11	341	0.0835
12 – Humidity	-	-	0	-	-
13 – Wind	26±12	47	8	208	0.0509
14 – Compound	19±5	35	14	266	0.0651

* Each data point is an average of 2 tests
** Ranges shown are standard deviation

3.1.5 Structural Related Factors

Effect of rebar as stress concentrator

The presence of steel reinforcing bars in ECC link slab may cause local stress concentration which promotes the occurrence of crack at early age. To investigate the effect of rebar as stress concentrator, a prism specimen reinforced with #5 rebar along the longitudinal and transverse direction was used (**Figure 3.5**). The longitudinal rebar is meant to provide restrain and the transverse rebar served as stress concentrator.

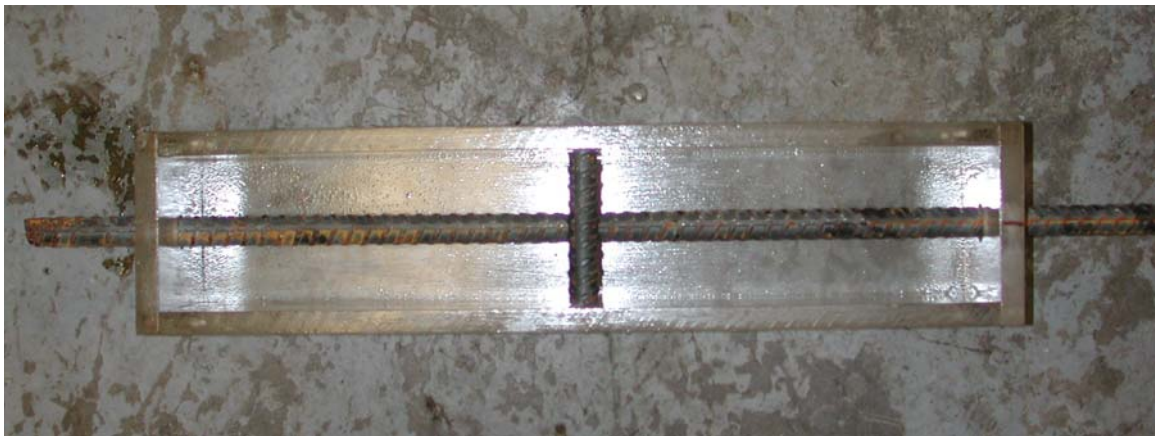

Figure 3.5: Mold of reinforced prism specimen

ECC material used was M45 and the mix proportion can be found in **Table 3.2**. Class F fly ash from Boral Material Technologies Inc. and Euclid Plastol® 5000 high range water reducer from Euclid Chemical Company were used. No retarder was used and no curing compound was applied on the surface of the prism. 0.315" PVA fiber was used in this test. A Hobart mixer was used and the mixing procedure and mixing time followed **Table 3.8**. The prism was demolded after 24 hours and cured in sealed plastic bags for 7 days. The prism specimen was then exposed to the laboratory room condition with ambient temperature of 70±5^{o}F and ambient relative humidity of 45±10% and there was no wind effect.

Figure 3.6: A single crack initiated from the transverse rebar

A single crack with 0.001” in crack width appeared at the 14th day and initiated from the transverse rebar as shown in **Figure 3.6**. This observation confirms the effect of reinforcing bar as stress concentrator. The presence of rebar introduces geometry irregularity and therefore disturbs the stress field and causes stress concentration in surrounding ECC material.

Effects of skew angle - finite element analysis

A simplified 2-D numerical model was used to simulate the performance of skewed link slab under shrinkage by using a finite element program MLS (Multi-Layer Systems) of FEMMASSE (Finite Element Modules for Materials Science and Structural Engineering). The module MLS is capable of computing physical and mechanical behavior of structure, taking varying environmental conditions into account.

In this numerical study, we consider a skewed ECC link slab, with the same dimension as the link slab constructed on Grove Street. The geometry and mechanical boundary conditions of this model are shown in **Figure 3.7**. Reinforcing bars were not considered in this numerical model. It is recognized that complicated mechanical boundaries are present in the field, including girder support and restraints, resulting in a three dimensional problem. In this study, we treated the problem only in 2-D as a first approximation, with a highly simplified boundary condition as depicted in **Figure 3.7**. The supports are fixed line supports, which are imposed to the sides of the link slab macro. In this boundary condition, the two short edges are fixed in the y-direction and the two long edges are fixed in the 45 degree direction. The choice of this boundary condition is meant to provide a stronger restraint along the y direction which reflects the field condition. (Note: The restraint of Grove Street bridge ECC link slab in the y direction, transverse direction, should be much stronger than that in the x direction, traffic direction. The restraints of the link-slab in the transverse direction resulted from substructures, girders, shear studs, friction from the adjacent concrete slabs, and transverse reinforcing bars. The restraint in the traffic direction; however, was provided only by the longitudinal reinforcing bars and shear studs)

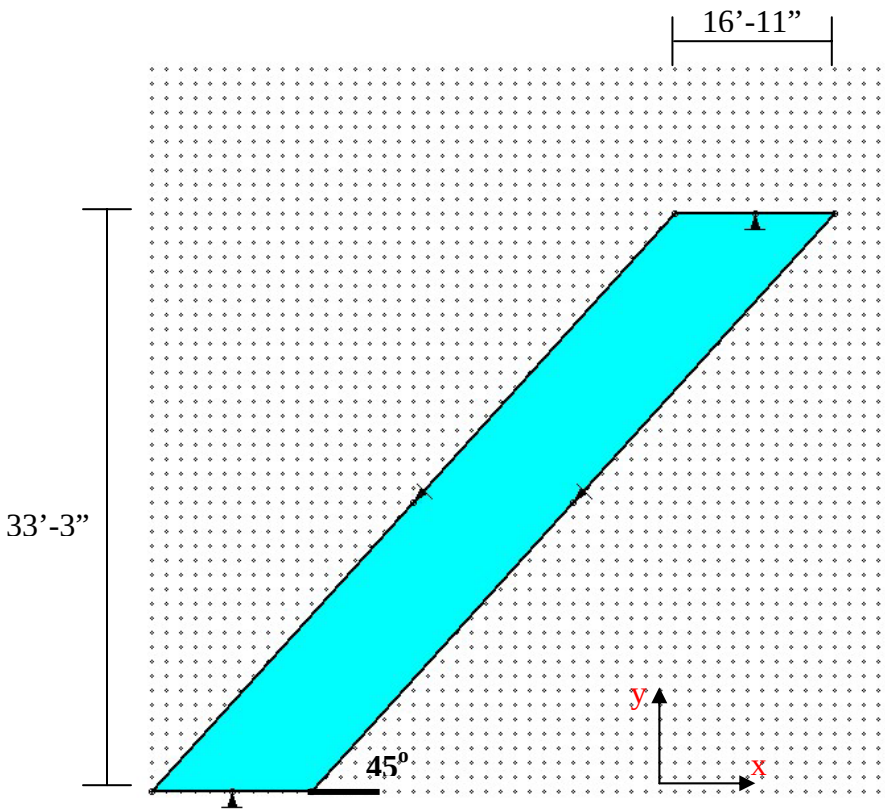

Figure 3.7: Geometry and boundary condition of ECC link slab FEM model

Material strain hardening model was applied to simulate ECC material, as shown in **Figure 3.8**. It should be noted that the parameters of the material models are age-dependent, and were fitted as curves according to experimentally measured results from material age of 24 hour to 28 day. For example, the initial slope of the three curves – the material Young’s modulus E changed with material ages according to experimental results as in **Figure 3.9**. The tensile strength of ECC from material age of 24 hour to 28day used the testing results in **Figure 3.10**. The first cracking strength of ECC was assumed to be 70 percent of the ultimate tensile strength. The tensile strain capacity of ECC was assumed to be 3% at all ages. Compressive strength of ECC material adopted the experimental data in **Figure 3.11**. Poisson’s ratio of ECC was assumed to be 0.2.

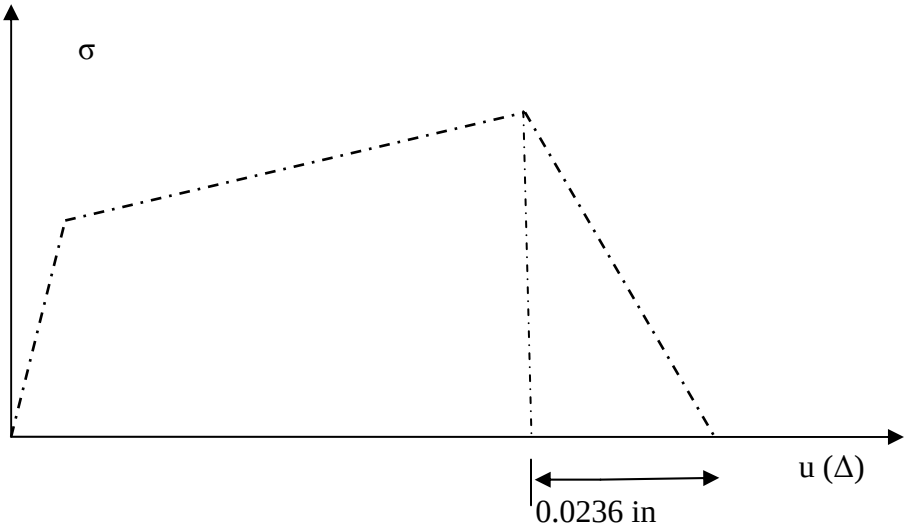

Figure 3.8: Theoretical tensile curves of ECC material

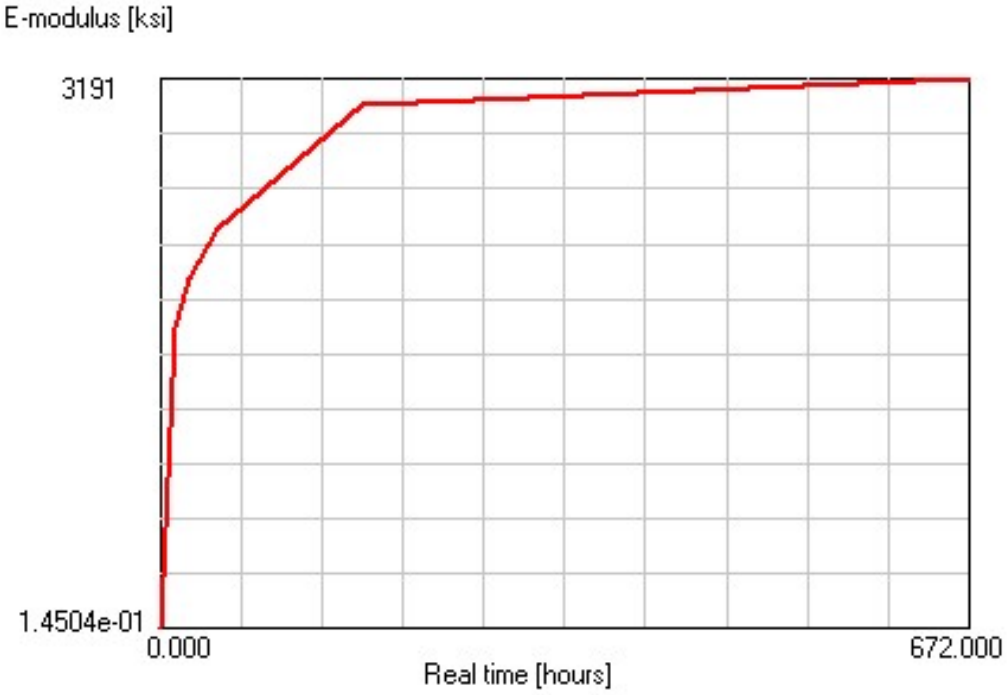

Figure 3.9: Age-dependent E-modulus of ECC

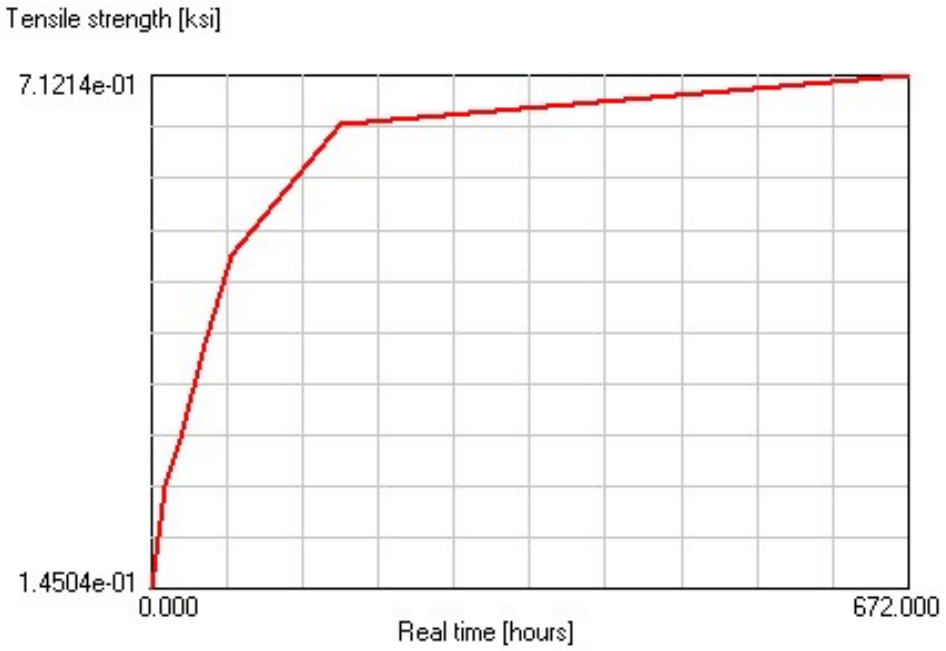

Figure 3.10: Age-dependent tensile strength of ECC

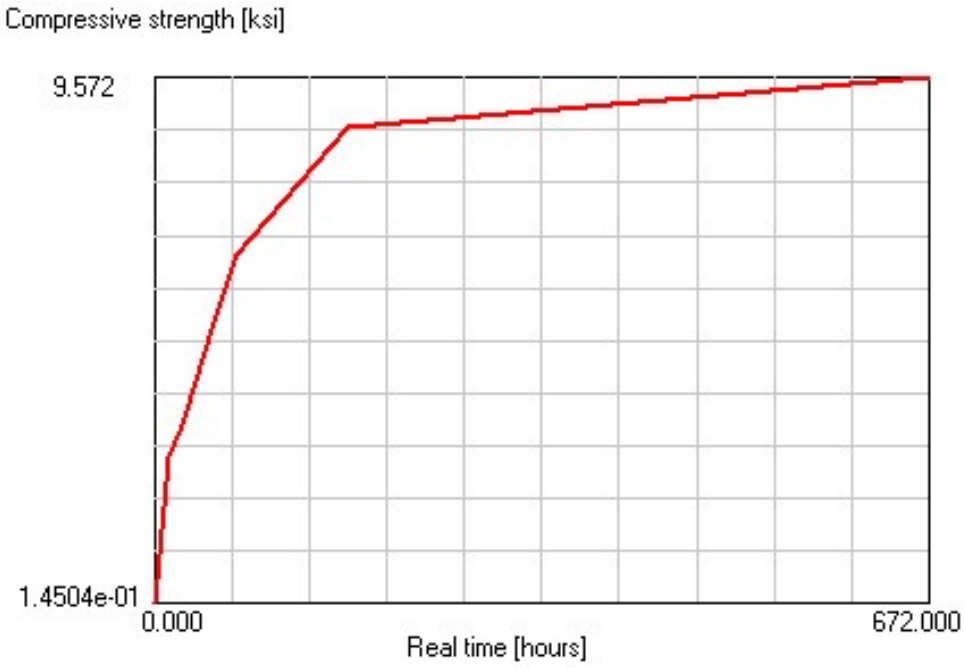

Figure 3.11: Age-dependent compressive strength of ECC

Shrinkage deformation of the ECC link slab was the "load" imposed to this model. It changed with material age too. The measured shrinkage strain of ECC in **Figure 3.12** was used as the input loading for this FEA model. For experimental measures of the

autogenous shrinkage (negative dilatation), please see **Section 5.3**.

Figure 3.12: Shrinkage strain of ECC as a function of material age

The principal tensile stress distribution of the skewed slab under restrained shrinkage at the age of 148 hours is illustrated in **Figure 3.13**. It can be seen that the principal tensile stress reaches the maximum value at the corner area of the skewed slab. To evaluate the effect of skew angle, another link slab model with 0 skew angle was analyzed and the results are shown in **Figure 3.14**. In this case, the principal stress distribution is uniform. This may explain why skewed decks tend to crack in the corner. **Figures 3.15(a)** to **(c)** show the σ_{xx}, σ_{yy}, and σ_{xy} distribution. From this information, one can calculate principle stress direction by using the following Eqn (3.1)

$$\tan 2\theta_p = \frac{2\sigma_{xy}}{\sigma_x - \sigma_y} \tag{3.1}$$

As shown in **Figure 15(d)**, the principal stress direction matches the crack pattern observed in Grove Street bridge ECC link slab (**Figure 3.16**).

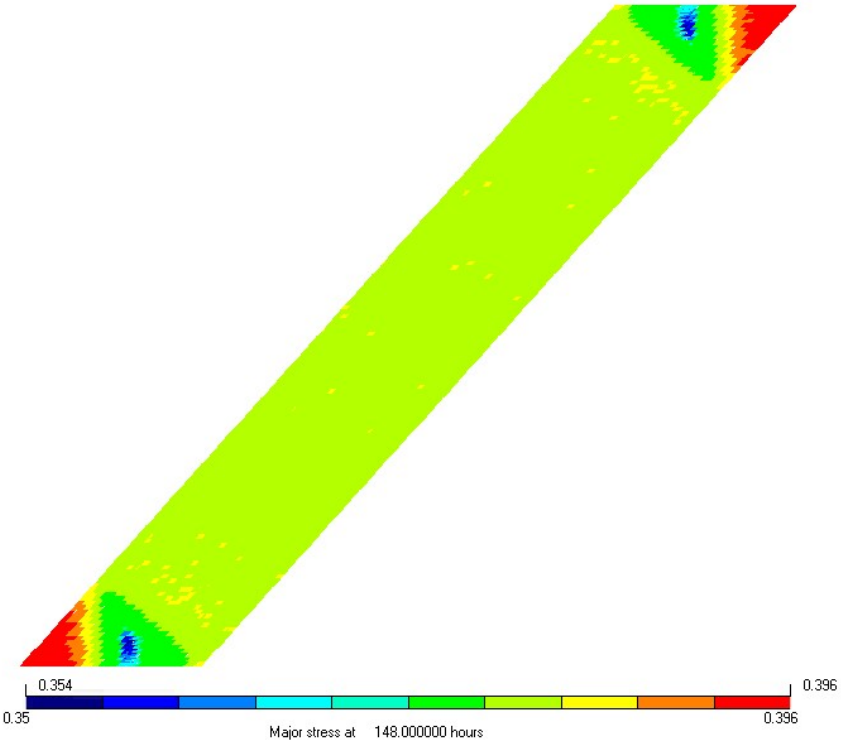

Figure 3.13: Principal tensile stress [ksi] distribution of skewed slab with skew angle of 45º and at the age of 148 hours

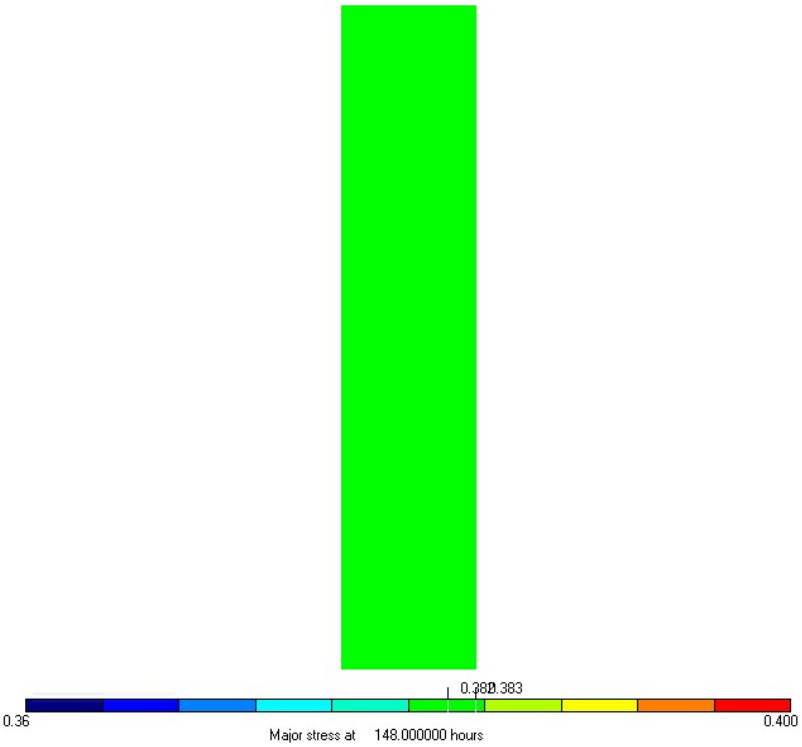

Figure 3.14: Principal tensile stress distribution of ECC Link slab with no skew angle at the age of 148 hours

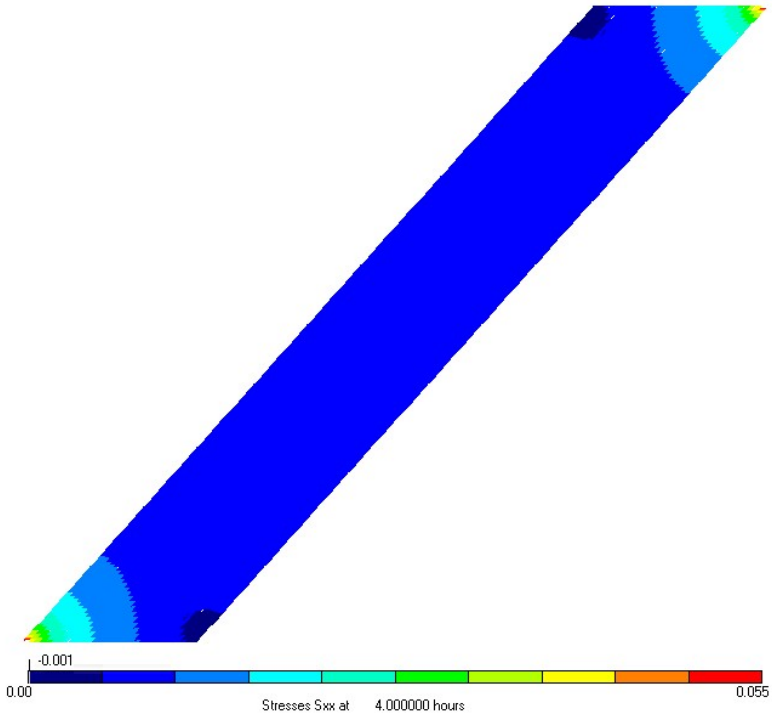

(a)

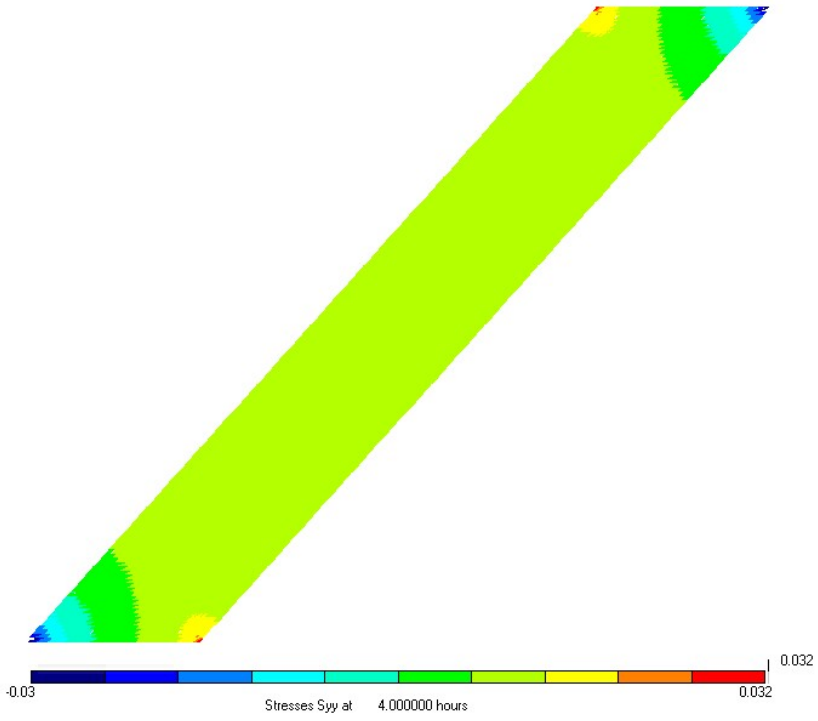

(b)

Figure 3.15: (a) σ_{xx}, and (b) σ_{yy} in the skew slab at the age of 4 hours

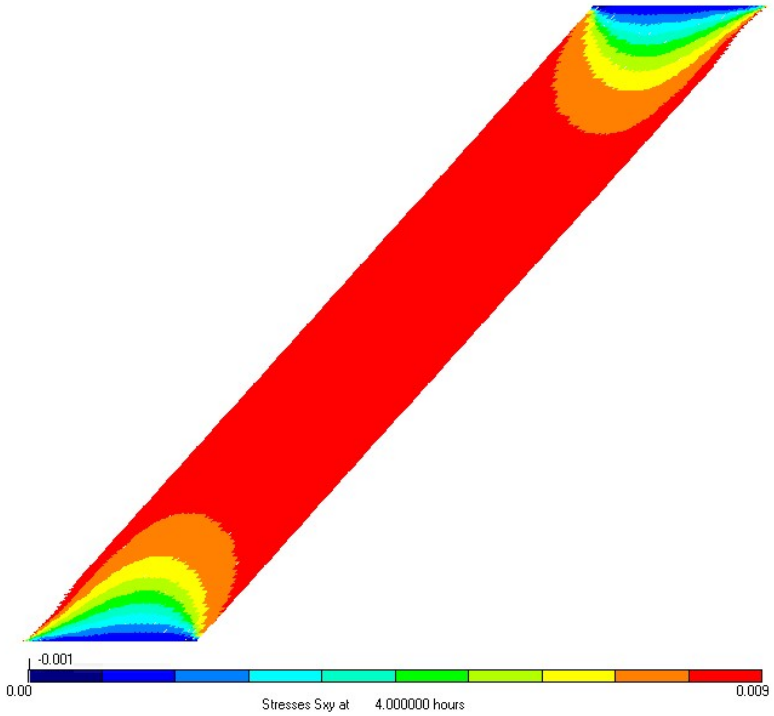

(c)

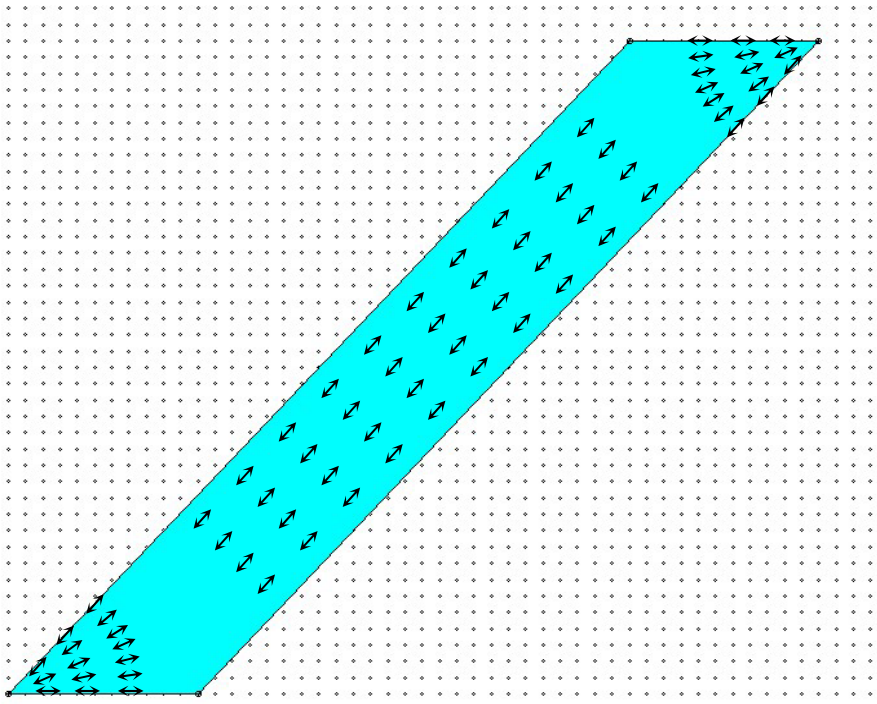

(d)

Figure 3.15: (c) σ_{xy} distribution and (d) calculated principal stress direction distribution in the skew slab at the age of 4 hours

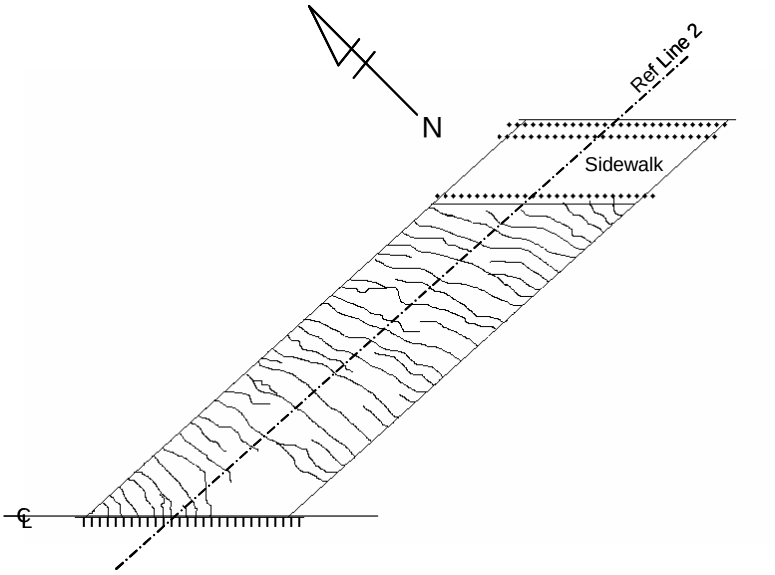

Figure 3.16: Crack pattern in Grove street bridge ECC link slab – phase I (Sept. 17, 2005, the 7th day)

Figure 3.17 shows the calculated principle stress versus time curve at two different points (point 1 at acute corner of link slab [black line], point 2 at center of link slab [green line]) along with the time dependent ECC M45 material tensile cracking strength development curve (pink line). As the principle stress surpasses the ECC material tensile cracking strength, it indicates the formation of crack. Therefore, **Figure 3.17** may be used to predict the time of crack formation. As we discuss above, it is not surprising that the principle stress at the acute corner is always higher than that at center due to higher restraint in the acute area. As shown in this plot, the principle stress at point 1 and 2 (load/demand) surpass ECC material tensile cracking strength (resistance/supply) at the age of 38-hour and 63-hour, respectively. The result indicates that the formation of crack should start from the acute corner and gradually spread to the center. The time of cracking should be within the second to the third day, which matches the field observations.

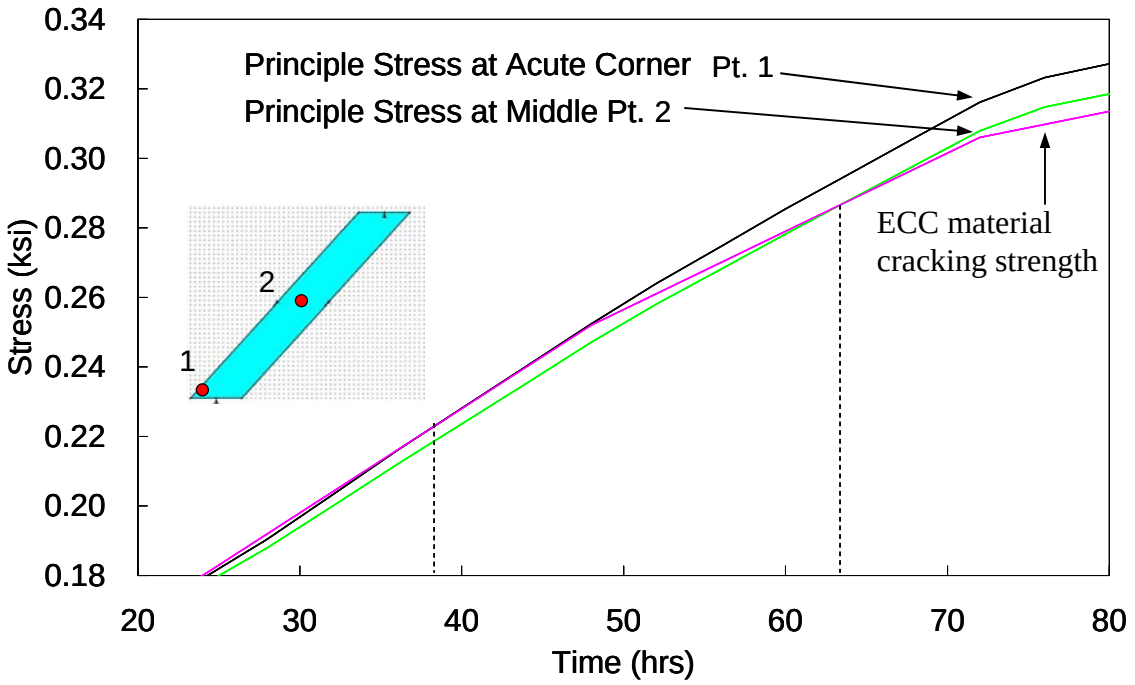

Figure 3.17: Predicted time of crack formation in ECC link slab

The above finite element analysis, although highly simplified, provides convincing evidences that skew angle not only alters the principle stress distribution but also the principle stress direction, which causes crack curving in the acute corner, in the link slab. As discussed above, the actual boundary conditions are more complicated than assumed in this study. However, from the small scale restraint ring tests and prism test, and skew angle analysis, we have gained enough insights for identifying and replicating the early age cracking observed in the Grove Street bridge ECC link slab.

3.2 Replication of Early Age Cracking

3.2.1 Experimental Program

Results from the small scale restrained shrinkage tests and finite element analysis suggest that low water to cement ratio, low retarder to cement ratio, low SP to cement ratio, use

of gravity-based mixer, higher curing temperature, lower curing relative humidity, wind effect, rebar as stress concentrator, and skew angle all contribute to the early age cracking behavior. After identifying the most influential factors, an attempt was made to replicate the early age cracking in ECC link slab by means of a small frame restrained shrinkage test.

Figure 3.18(a) shows the small frame restrained shrinkage test setup schematically. The frame measured 40" by 20" and could accommodate a 4.5" thick slab. Epoxy coated reinforcing bars (#5) were placed in the frame at either 8" or 6" spacing. The reinforcing steel was installed at mid depth, or as close as possible due to fabrication considerations. To transfer restraint from the frame to the slab, six 0.5" diameter shear connectors were placed on the frame along the sides at mid depth. A 3" thick concrete was poured along the perimeter of the frame to stiffen the whole structure and to prevent any movement of the steel reinforcing bars. To incorporate skew angle effect, a skew of 45^{o} was produced by casting concrete skew blocks on two sides. The resulting frame (**Figure 3.18(b)**) can accommodate a skewed ECC slab measured 20" by 14".

M45 was chosen to be the testing material and the mix proportion can be found in **Table 3.2**. Class F fly ash from Boral Material Technologies Inc. and Euclid Plastol® 5000 high range water reducer from Euclid Chemical Company were used. This mix proportion was identical to the Grove street Phase I ECC link slab except that no retarder was used and no curing compound was applied on the surface of the small frame ECC slab. 0.315" PVA fibers were adopted in the small frame test which is identical with the ECC link slab mix. A gravity mixer (**Figure 3.3**) was used to produce the ECC material. The batching sequence and mixing time followed **Table 3.9**.

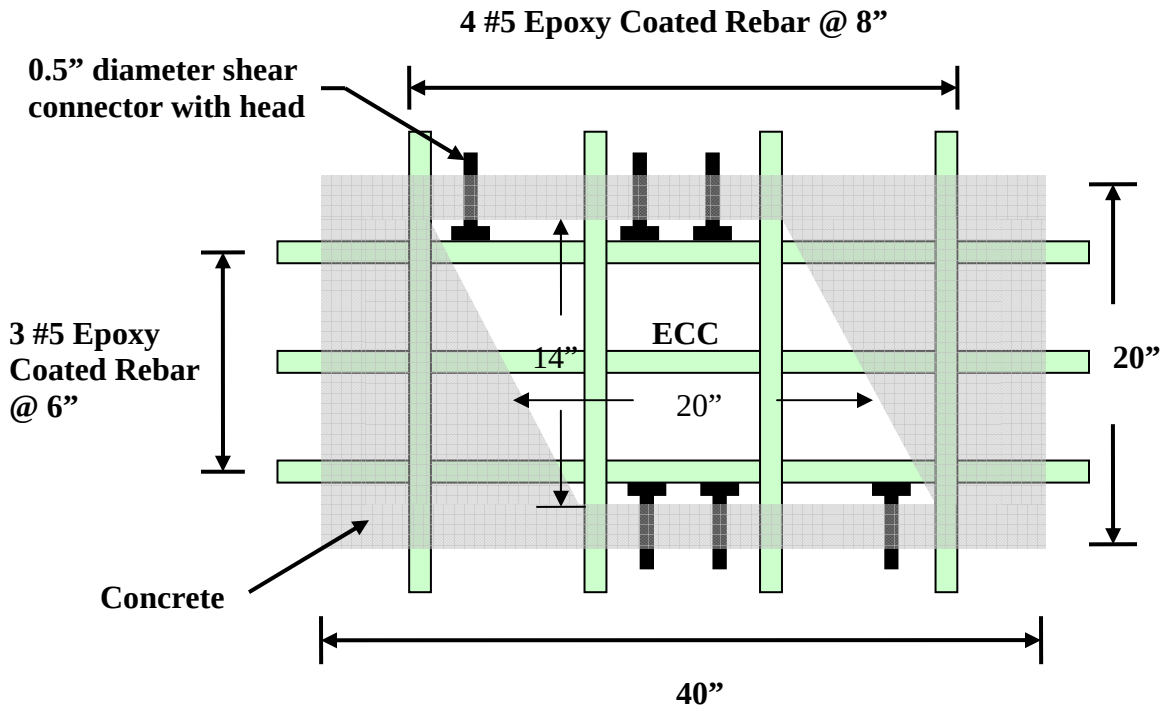

(a)

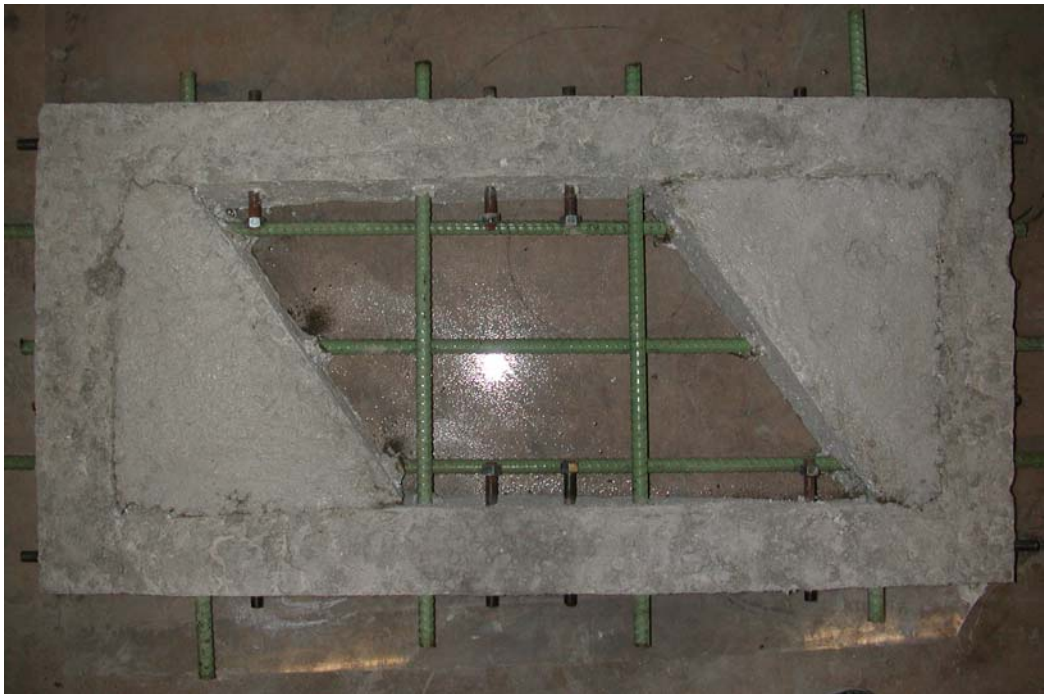

(b)

Figure 3.18: Restrained small frame test setup with consideration of skew angle

The slab was cast on a plastic glass plate to simulate the debonding paper on the bottom side of the link slab. Skewed ECC M45 slab was cast on June 22, 2007. The slab was placed in an open outdoor space and exposed to outdoor environment. The outdoor temperature for the first seven days ranges from 43^{o}F to 90^{o}F, the outdoor relative humidity ranges from 34% to 100%, and the wind speed ranges from 0 to 21 mph. Generally speaking, it was sunny, windy and dry during the first seven days. There was no rain during this time period. It was observed that the slab can be heated to as high as 120^{o}F in the middle of the day due to direct sun exposures. The frame was moved to the laboratory for crack monitoring on the 8th day.

3.2.2 Results and Discussion

The crack pattern and crack width (**Figures 3.19** and **3.20**) in the slab in the small frame restrained shrinkage test recorded on the 8th day appear very similar to those observed for the Grove Street link slab (**Figure 3.16**). The crack first developed on the 4th day. **Figure 3.19** shows the crack pattern of the backside of the ECC slab. Cracks were highlighted by a thick marker. Because the slab was cast against a plastic glass panel, the backside of the slab is fairly smooth and therefore it is much easier to observe the cracks from this side. In this test and in the field, it was found that cracks are perpendicular to the interface, and tend to form a curve shape in the two corners with acute angles. The crack observed in ECC link slab is about 0.005" to 0.007" in width. Similar crack width was also observed in the small frame ECC slab (**Figure 3.20**).

Based on the small frame restrained shrinkage test results, we can conclude that the formation of early age cracking in Grove street ECC link slab was a combination of several factors. Those factors include low water to cement ratio of M45 mix, use of gravity mixer, wind effect, high ambient temperature, low ambient humidity, presence of steel reinforcing bars, excessive restraint, and skew angle. We can now explain the different cracking behavior in phase I and phase II ECC link slab, large frame restrained shrinkage test, and small frame restrained shrinkage test.

Figure 3.19: Crack pattern in restrained small frame ECC slab (June 30, 2007, the 8th day)

(a) (b)

Figure 3.20: Cracks in restrained small frame ECC slab with crack width of (a) 0.006” and (b) 0.005”

Fewer cracks were observed in phase II ECC link slab when compared with that in phase I. Although a lower water to cement ratio mix was used in the construction of phase II as shown in **Table 3.13**, which according to the current test results should result in larger crack width, a couple of counteracting factors were also present in phase II construction, which may cause the reduction of early age cracking. These include the use of higher amount of high range water reducer, much lower ambient temperature, and higher ambient relative humidity. The environmental conditions for constructing ECC link slab, large frame, and small frame are listed in **Table 3.14**.

Table 3.13: Mix proportion of ECC materials used in Grove Street bridge and two restrained frame tests

	Cement	Sand	Fly ash	Water	SP	Retarder	PVA (vol.%)
Phase I	1	0.8	1.2	0.59	0.014	0.0015	2
Phase II	1	0.8	1.2	0.57	0.015	0.0015	2
Large frame	1	0.8	1.2	0.59	0.014	0.0015	2
Small frame	1	0.8	1.2	0.59	0.014	0	2

Table 3.14: Environmental conditions of Grove Street bridge and two restrained frame tests during the first seven days (data from The Weather Underground)

	Temperature (^{o}F)	Humidity (%RH)	Wind speed (mph)
Phase I (Sept. 10 – 17, 2005)	46 – 91 (Ave 66)	23 – 100 (ave 70) (covered with plastics/wet burlap after 6 hours)	0 – 16
Phase II (Oct. 18 – 25, 2005)	32 – 69 (Ave 47)	32 – 97 (ave 72) (covered with plastics/wet burlap after 6 hours)	0 – 25
Large frame (Nov. 2 – 9, 2006)	16 – 66 (Ave 40)	32 – 100 (ave 77) (snow and rain, covered with plastics right after casting)	No wind effect (Against two walls)
Small frame (June 22 – 29, 2007)	43 – 90 (Ave 68)	34 – 100 (ave 70) (No cover)	0 – 21

In the case of large frame slab test, very little cracking was found and the crack width found was extremely tight. This may be a result of the fact that there was no wind effect

(the specimen shielded by two walls), very low ambient temperature and no sunshine exposures, better curing (covered with plastics right after casting, rain in the first several days), 0 skew, and less restraint provided from the frame. Except for the size, the small frame test; however, has the most similar conditions as those of phase I ECC link slab and therefore similar early age cracking behavior can be replicated and observed.

4. Development and Verification of New ECC Materials Solution (Task 3)

This section summarizes the development of a new version of ECC, which may be used in future ECC link slab. Focus has been placed on ECC material redesign to create a buffer against the tendency of cracking on bridge decks with high skewed angles. Two approaches have been used in the material development investigation in this study. The first approach is to reduce the cracking tendency of the ECC material. This can be done by lowering early age shrinkage deformations within ECC. The second approach is to increase the resistance to crack opening when cracks do form. In addition, the newly developed ECC material must retain required properties for the durable link slab application (i.e. fresh and hardened properties).

4.1 Effect of Fly Ash on ECC Shrinkage and Crack Width Control

Previous research (Atis, 2004) shows that fly ash can help reduce shrinkage of concrete. Eight ECCs with various fly ash contents (fly ash to cement ratio, FA/C, ranges from 1.2 to 5.6 by weight) were examined in this research. The mix design of ECCs can be found in **Table 4.1**. Type I ordinary Portland cement (OPC) was used in all mixtures. The fly ash used was an ASTM class F fly ash from Boral, Texas and the physical properties and chemical compositions of the fly ash are listed in **Table 3.4**. In this fly ash, 75% of the particles are smaller than 0.0018". A fine silica sand with a maximum grain size of 0.01" and a mean size of 0.004" was adopted in ECC mixtures. The size distribution of this silica sand is listed in **Table 4.2**. In all mixtures, the water to cement (w/c) ratio was controlled at 0.25 ± 0.01. Slight adjustment in the amount of superplasticizer and w/c in

each mixture was performed to achieve consistent rheological properties for better fiber distribution and workability. All ECCs; therefore, have similar fresh properties with self-consolidating performance. Polyvinyl Alcohol (PVA) fiber was used at a moderate volume fraction of 2% in this study. The dimensions of the PVA fiber are 0.315" in length and 0.0015" in diameter on average. The nominal tensile strength of the fiber is 235 ksi and the density of the fiber is 2192 lb/yd^3.

Table 4.1: Mix proportion of ECCs

Mix	FA/C	Cement lb/yd^3	Fly Ash lb/yd^3	Sand lb/yd^3	Water lb/yd^3	SP lb/yd^3	PVA Fiber lb/yd^3	Total lb/yd^3
1	1.2	962	1154	768	559	11.46	43.8	3500
2	1.6	804	1286	768	556	10.19	43.8	3471
3	2.0	694	1388	768	549	9.30	43.8	3456
4	2.4	610	1466	768	544	8.59	43.8	3441
5	2.8	546	1527	768	539	8.91	43.8	3432
6	3.2	492	1575	768	526	9.30	43.8	3415
7	3.6	448	1616	768	521	9.77	43.8	3407
8	5.6	320	1791	768	506	10.87	43.8	3424

Table 4.2: Size distribution of silica sand

< 0.0059" %	< 0.0039" %	< 0.0030" %	< 0.0021" %
93	77	33	8

4.1.1 Mixing and Curing

A Hobart mixer with 0.46 ft^3 capacity was used in preparing all ECC mixtures. Solid ingredients, including cement, fly ash, and sand, were first mixed for a couple of minutes. Water and superplasticizer were then added into the dry mixture and mixed for another three minutes. The liquefied fresh mortar matrix should reach a consistent and uniform state before adding fibers. After examining the mortar matrix and making sure there is no clump in the bottom of the mixer, PVA fibers were slowly added into the mortar matrix and mixed until all fibers are evenly distributed. The mixture was then cast into molds.

Specimens were demolded after 24 hours. After demolding, specimens were first cured in sealed bags at room temperature for 6 days and then cured in air at room temperature before testing. The relative humidity of the laboratory air is 45% ± 5%. This curing regime is meant to reflect the field curing condition.

4.1.2 Specimens

Free drying shrinkage measurements were made for all eight ECCs as a function of drying time. Tests were conducted according to ASTM C157/C157M-99 and C596-01 standards, except that the storing of the specimens before test was modified. The specimens were cured in sealed bags for 7 days before they were moved to laboratory air and the measurement was started. Free drying shrinkage deformation was monitored until hygral equilibrium was reached.

Compressive test was carried out for each mix at the age of 3, 28, and 90 days. Cylinders measuring 3” in diameter and 6” in length were used in this study. The ends of cylinders were capped with a sulfur compound to ensure a flat and parallel surface and a better contact with the loading device.

Coupon specimens measuring 6” by 3” by 0.5” were used to conduct uniaxial tensile test for each mix at the age of 3, 28, and 90 days. Uniaxial tensile test gives material tensile stress-strain behavior. In addition, crack width, another important tensile characterization of ECC material in relation to durability, was also examined. A servohydraulic testing system was used in displacement control mode to conduct the tensile test. The loading rate used was 0.0001 in/s to simulate a quasi-static loading condition. Aluminum plates were glued both sides at the ends of coupon specimens to facilitate gripping. Two external linear variable displacement transducers were attached to the specimen with a gauge length of approximately 2” to measure the specimen deformation.

4.1.3 Results and Discussion

Figure 4.1 shows the free drying shrinkage deformation measurement of ECCs. Because of the absence of coarse aggregate, drying shrinkage deformation of ECC (FA/C = 1.2, the far left point in **Figure 4.1**) is higher than normal structural concrete. The general trend in **Figure 4.1** shows that fly ash can effectively reduce free drying shrinkage deformation in ECC material. Similar result has been reported for fly ash concrete (Atis, 2004). In the present study, 50% reduction of free drying shrinkage of ECC was found when fly ash to cement ratio was increased from 1.2 to 5.6. A possible mechanism is that unhydrated fly ash particles serve as fine aggregates (**Figure 4.8(b)**) to restrain the shrinkage deformation (Bisallion et al, 1994). This observation suggests that incorporating high volumes of fly ash can reduce the cracking tendency in ECC by reducing the drying shrinkage.

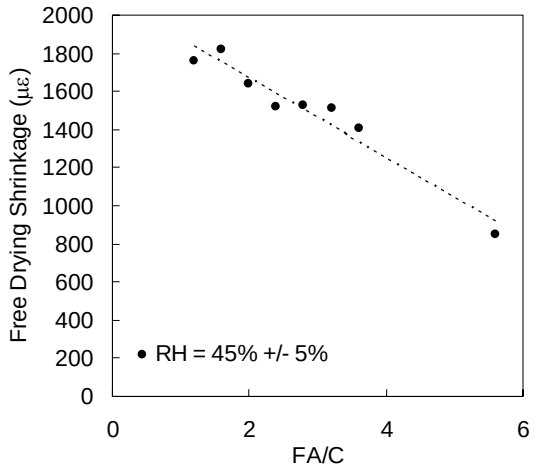

Figure 4.1: Free drying shrinkage of ECCs as a function of fly ash content. Each data point is an average of 2 tests.

The compressive strength of eight ECCs with different fly ash contents at the age of 3, 28, and 90 days are summarized in **Figure 4.2** and **Table 3.3**. As can be seen from the curve, the replacement of cement by class F fly ash generally reduces the compressive strength of ECC. However, even at 75% replacement of cement (FA/C = 2.8), the compressive strength of ECC at 28 days can still reach 5075 psi which exceeds the compressive

strength requirement for ECC link slab application (4500 psi). No significant strength gain is found in ECCs between 28 to 90 days due to the lack of continuous water supply (i.e. wet curing). Related research indicated that hydration of cement will stop completely when the internal humidity in hardened cement paste falls below 80 percent (Mindness et al, 2002). Therefore, gradual loss of internal humidity in ECCs after sealed cure for 7 days arrests further hydration.

Table 4.3: Compressive strength (ksi) of ECCs at different ages

FA/C / Age (days)	1.2	1.6	2.0	2.4	2.8	3.2	3.6	5.6
3	4.4±0.3	3.8±0.2	2.4±0.1	2.5±0.1	2.1±0.5	2.5±0.1	2.2±0.0	1.2±0.0
28	7.6±0.0	6.9±0.1	5.0±0.2	5.6±0.2	5.1±0.2	3.9±0.6	3.5±0.1	3.1±0.1
90	7.8±0.2	7.1±0.7	5.2±0.1	6.3±0.1	5.6±0.2	4.1±0.2	3.8±0.0	3.2±0.2

* Each data point is an average of 3 tests
** Ranges shown are standard deviation

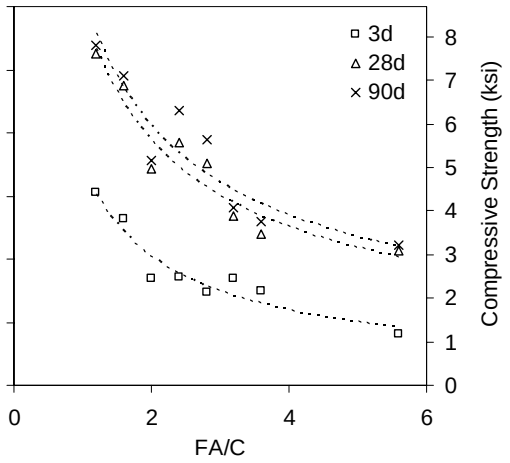

Figure 4.2: Compressive strength of ECCs as a function of fly ash content at different ages

Figure 4.3 shows the representative 28 days tensile stress-strain curves of ECCs. Tensile ductility at different ages is summarized in **Table 4.4** and is plotted against FA/C illustrated in **Figure 4.4**. Each data point in **Figure 4.4** is an average of 4 uniaxial tensile

tests. From the uniaxial tensile test, all ECCs exhibit tensile strain hardening behavior at different ages and the tensile strain capacity reaches 1.8-3.4% at the age of 90 days. The strain capacity of mix 1 (FA/C = 1.2) is slightly lower than 2% at the age of 90 days. This may be attributed to a stronger age dependence of mix 1. At later age, matrix toughness of mix 1 is higher, prevents initiation and propagation of crack, and results in lower strain capacity. This indicates that the most unique property of ECC, tensile ductility, is retained and is not sacrificed by replacing cement with large amount of class F fly ash. However, there is a general tendency of tensile strength reduction with increasing amount of fly ash.

Table 4.4: Tensile strain capacity (%) of ECCs at different ages

FA/C / Age (days)	1.2	1.6	2.0	2.4	2.8	3.2	3.6	5.6
3	4.6±1.3	4.2±0.8	4.1±0.2	4.3±1.0	4.4±0.3	4.3±1.1	4.0±0.3	3.8±0.4
28	2.7±1.1	3.7±0.6	3.0±1.1	2.9±0.8	3.0±0.7	2.7±0.7	2.5±0.3	3.3±0.2
90	1.8±0.9	3.0±1.4	3.1±1.5	2.3±0.7	3.3±1.4	2.9±0.9	2.6±1.2	3.4±0.6

* Each data point is an average of 4 tests
** Ranges shown are standard deviation

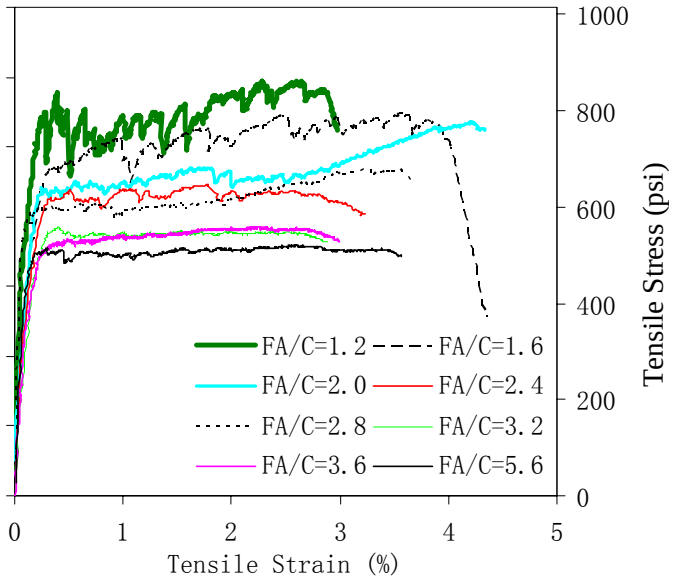

Figure 4.3: Tensile stress-strain curve of ECCs at the age of 28 days.

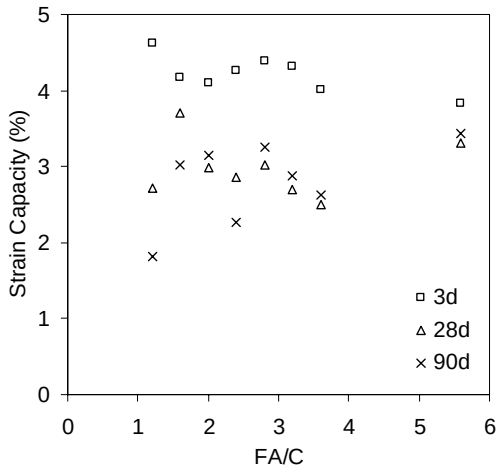

Figure 4.4: Tensile ductility of ECCs as a function of fly ash content at different ages.

Crack width of ECC at material hardening stage does not depend on structural geometry or size, or on steel reinforcement ratio, and has been recognized as an important material property of ECC. The imposed deformation is accommodated by ECC multiple cracks with constant crack width during the strain-hardening stage. The magnitude of crack width controls many transport properties in cracked concrete materials and has a direct impact on durability. **Table 4.5** and **Figure 4.5** give the effect of fly ash content on the residual crack width at different ages. The term residual crack width indicates that crack width is measured from the unloaded specimen after the uniaxial tensile test. It was observed in this study that the width of a loaded crack is approximate two times the width of the unloaded one. Each data point in **Figure 4.5** is an average of 4 coupon specimens and 20+ crack widths were measured from each specimen. *It was found that the crack width reduces as fly ash content increases at all ages.* The drop is significant especially in early ages (3 days, **Figure 4.6**). The larger crack width at early age is likely a result of lower bridging stiffness prior to full development of interfacial bond properties when load is applied to the specimen. At the age of 28 days, the residual crack width of some ECCs can be lower than 0.0004". This observation suggests that incorporating high volumes of fly ash can increase the resistance to shrinkage cracking in ECC by tight crack width control at early ages. In addition, crack width was identified a key factor in self-healing of ECC (Li and Yang, 2007). Tight crack width in ECC is likely to promote self-healing behavior.

Table 4.5: Residual crack width (10^{-4} inch) after tensile test of ECCs at different ages

FA/C / Age (days)	1.2	1.6	2.0	2.4	2.8	3.2	3.6	5.6
3	33±12	24±3	13±2.4	11±2	6±2	5±2	5±1	5±1
28	12±3	14±5	6±1	9±2	6±3	3±1	3±0	6±1
90	7±2	10±4	6±2	6±3	4±1	3±1	3±0	4±0

* Each data point is an average of 4 tests
** Ranges shown are standard deviation

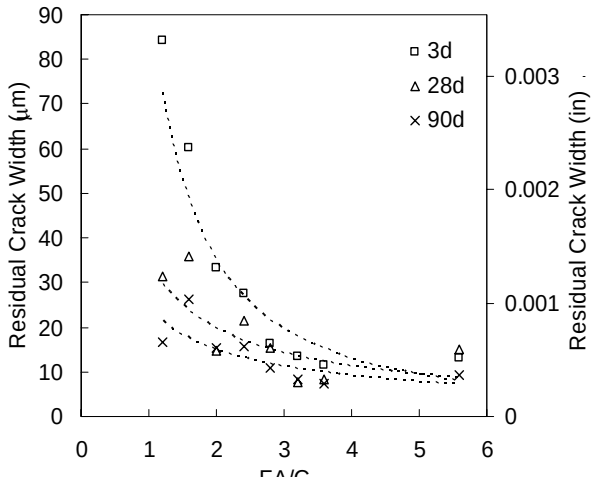

Figure 4.5: Residual crack width of ECC as a function of fly ash content at different ages.

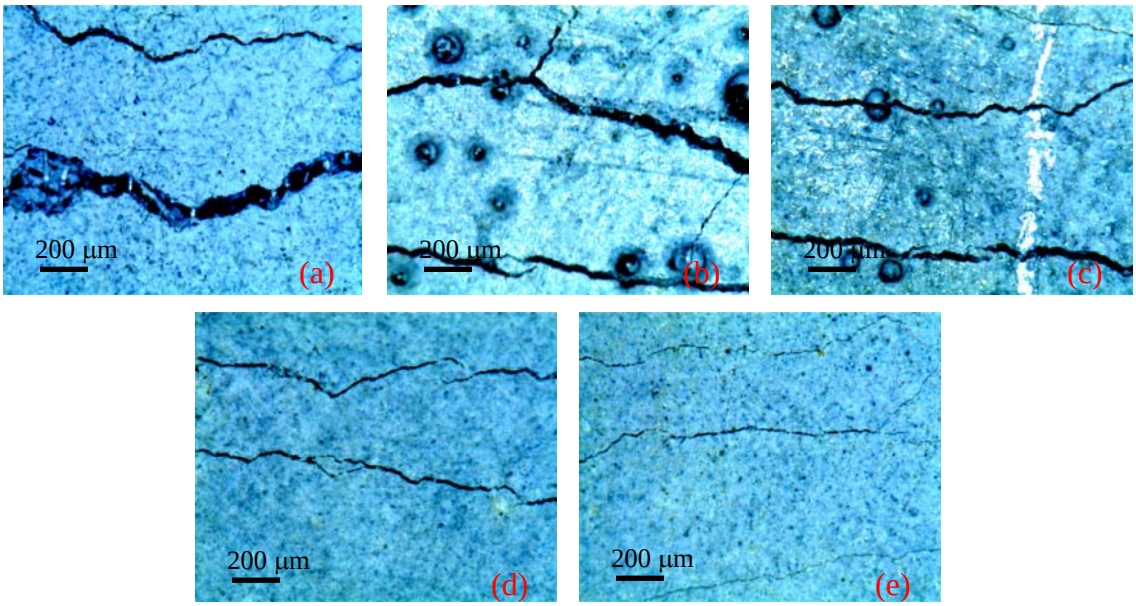

Figure 4.6: Microscopic photos of residual crack width of ECCs at the age of 3 days where FA/C are (a) 1.2, (b) 1.6, (c) 2.0, (d) 2.8, and (e) 3.6, respectively.

Single fiber pullout test (Redon, 2001) was carried out in order to reveal the effect of fly ash content on fiber/matrix interfacial properties and on crack width control of ECCs. Single fiber pullout specimen were cast from selected mixtures (mix 1, 2, 3, 5, and 7) and tested after curing for 28 days. Results are presented in **Figure 4.7**. As can be seen, the chemical bond G_d drops with increase of fly ash content. Lower G_d indicates easier interface debonding without fiber breaking. This is a result of lower hydration degree in fiber/matrix interface as more cement is replaced by fly ash.

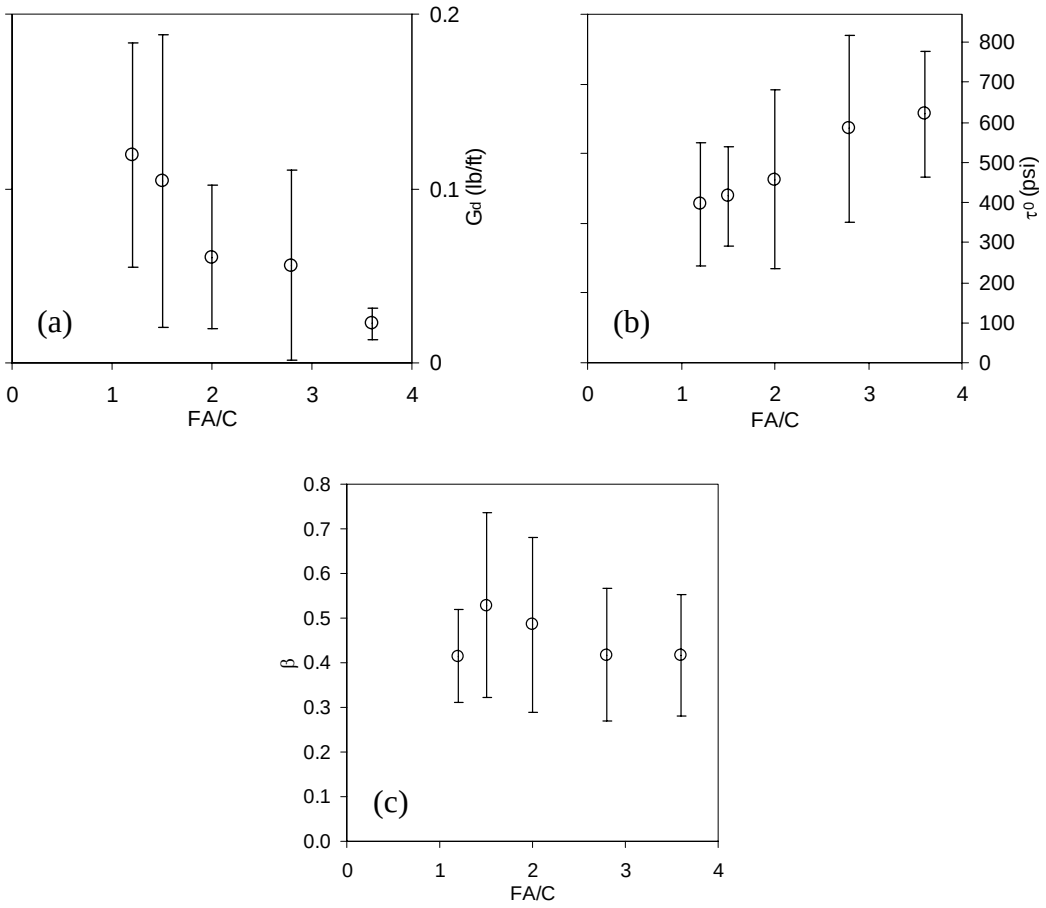

Figure 4.7: (a) Chemical bond strength, (b) frictional bond strength, and (c) slip-hardening coefficient of ECC as a function of fly ash content at the age of 28 days. Each data point is an average of 10 tests.

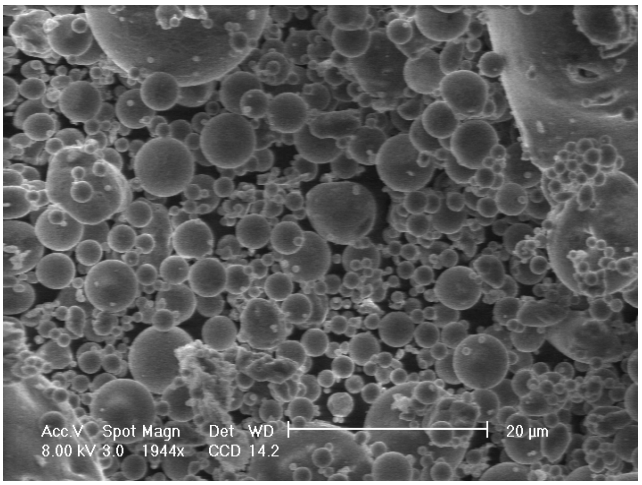

(a)

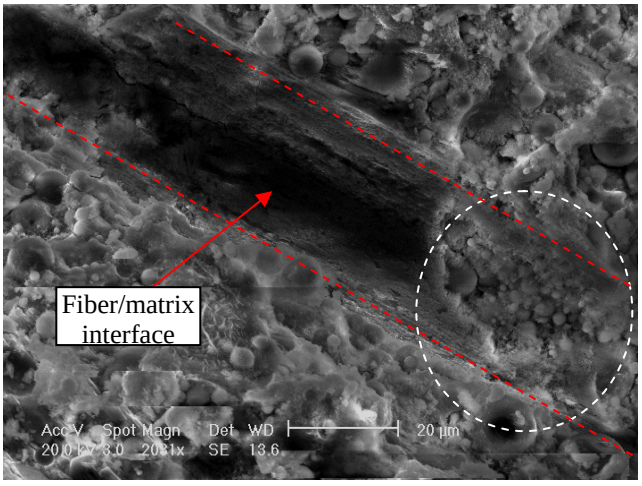

(b)

Figure 4.8: SEM photos of (a) Class F fly ash and (b) ITZ of ECC with 85% replacement of cement at the age of 90 days.

Interestingly, the frictional bond τ_0 shows a reverse trend. High τ_0 indicates a strong holding force in the interface and resistance to fiber sliding. As a result, crack width reduction is attained at higher fly ash content. A possible mechanism that contributes to higher τ_0 may be that unhydrated fly ash with smooth spherical shape (**Figure 4.8(a)**) and small particle size (76.37% < 0.0018") increases the compactness of interface transition zone (ITZ) (Kayali, 2004), and therefore increases interface frictional bond. **Figure 4.8(b)** illustrates the densely packed fiber/matrix interface in ECC with high volumes of fly ash. This picture was taken from an ECC with 85% replacement of cement (FA/C = 5.6) by a

scanning electron microscope (SEM) at an age of 90 days. The dark grove shows the impression left by a fiber (removed before taking this image) on the fiber/matrix interface (marked by the dash line). The circled area shows the morphology right beneath the fiber/matrix interface. To a certain degree, it reflects the structure of ITZ. It is clear that many unhydrated fly ash particles serving as inner fillers are distributed in the matrix and densely pack the interface zone. In addition, unlike chemical bond which relies on chemical reaction, this physical packing mechanism should be less dependent on age, and therefore crack width in high volume fly ash ECC remains tight at early ages. This is particularly valuable in the event that tensile stress build up occurs due to restrained autogenous shrinkage in the first few days after ECC placement. The slip-hardening coefficient was found to be independent of fly ash content as shown in **Figure 4.7(c)**.

4.2 Development of Low Shrinkage ECC for Link Slab Application

4.2.1 Restrained Shrinkage Ring Test

To screen the possible solutions of preventing early age cracking, restrained shrinkage ring tests were conducted first. Four potential measures, including adopting expansive cement (EC), doping shrinkage reducing admixtures (SRA), incorporating internal curing (IC) media, and using high volumes of fly ash (FA) were studied to evaluate their effectiveness in the reduction of early age cracking. M45 (mix 1) was tested as control. Mix proportion of each measure can be found in **Table 4.6**. The studied factor is highlighted in yellow. In all mix, Type I ordinary Portland cement (OPC) was used. The fly ash used was an ASTM class F fly ash from Boral, Texas and the physical properties and chemical compositions of the fly ash are listed in **Table 3.4**. F-110 fine silica sand supplied by US Silica and superplasticizer, ADVA Cast 530, from W.R. Grace were used in all mixtures. PVA fibers supplied by Kuraray were used. In all mixes, 0.315" PVA fiber was adopted. Expansive cement (EC), Komponent, used in mix 2 was provided by CTS cement manufacturing corporation. It is recommended by the supplier to replace 15% of cement by Komponent and mix 2 follows this recommendation. Shrinkage

reducing admixture (SRA), Eclipse plus, from W.R. Grace was used in mix 3. The doping amount, 1.5 gal/yd^3, follows the recommendation provided by the supplier for standard concrete mix. Porous recycled glass lightweight aggregates were used as internal curing (IC) media in mix 4. The porous aggregates, Poraver, were provided by Dennert and have diameters ranging from 0.079" to 0.157".

Table 4.6: Mixing proportions of potential measures to reduce early age cracking

	OPC	Sand	FA	Water	SP	PVA (vol.)	SRA	EC	IC (vol.)
Mix 1	1	0.8	1.2	0.59	0.014	0.02	0	0	0
Mix 2	1	0.94	1.4	0.68	0.014	0.02	0	0.176	0
Mix 3	1	0.8	1.2	0.59	0.014	0.02	0.012	0	0
Mix 4	1	0.8	1.2	0.63	0.014	0.02	0	0	0.07
Mix 5	1	1.41	2.8	1	0.013	0.02	0	0	0

The results of the restrained shrinkage ring tests are shown in **Table 4.7** with a summary of the average crack widths and number of cracks in each ring specimen at the 7th day.

Table 4.7: Summary of restrained shrinkage ring test results of potential shrinkage reduction measures

	Average Crack Width (10^{-4} inch)	Maximum Crack Width (10^{-4} inch)	Number of Crack	Total Shrinkage (10^{-4} inch)	Shrinkage Strain (%)
Mix 1 – Control	22±8	43	14	308	0.064
Mix 2 – EC	13±2	16	5	65	0.014
Mix 3 – SRA	-	-	0	-	-
Mix 4 – IC	19±7	31	12	228	0.047
Mix 5 – FA	-	-	0	-	-

* Each data point is an average of 2 tests
** Ranges shown are standard deviation

As can be seen from the various mix tested, use of shrinkage reducing admixture and high volumes of fly ash are effective and no crack was found after 7-day exposure. Use of expansive cement also has a positive effect in reducing early age cracking. However,

it is less effective when compared with SRA and FA in the present study. This is probably due to the fact that the outer mold was removed and the ring was exposed in air after one day. It is required in the specification of Komponent to have a 7-day wet curing regime in order to compensate the shrinkage deformation effectively. More reduction of early age cracking can be expected by using Komponent when prolonged wet curing is carried out. Use of porous aggregates as internal curing media has limit effect in reducing early age cracking, and therefore it was concluded that the porous aggregates are not an ideal internal curing media.

Table 4.8: Mix proportion of low shrinkage ECC (LS-ECC)

ECC Mix Design Parameter	**Value (lb/cyd)**
Mix Water (net)	531
Portland Cement, Type I	595
Fly Ash, Type F	1399
Fine Aggregate, Dry	770
Polycarboxylate Superplasticizer	9.1
Expansive Cement	105
Shrinkage Reducing Admixture	8.4
Poly-vinyl-alcohol Fibers	43.7

Based on the studies shown in the previous sections, a low shrinkage ECC (LS-ECC) was developed. The mix proportion of LS-ECC can be found in **Table 4.8**. In this mix design, three measures including high volumes of fly ash, shrinkage reducing admixture, and expansive cement were adopted in order to prevent early age cracking. These three different measures have different shrinkage control mechanisms. Shrinkage reducing admixture reduces water surface tension, and therefore it can reduce the drying shrinkage effectively. Expansive cement was adopted to prevent any hydration induced shrinkage (autogenous shrinkage). The use of high volumes of fly ash is meant to lower shrinkage and provide tight crack width control even if cracks appear at early ages. A lower dosage of shrinkage reducing admixture, expansive cement, and fly ash were chosen when compared with previous ring test (SRA: 1.07 gal/yd^3, EC: 10% replacement, FA to Cement (OPC + EC) ratio: 2.0). This decision was made due to the economic consideration and recognizing the simultaneous presence of multiple shrinkage relieving

measures adopted in this mix design. In addition, the choice of 2.0 FA to Cement (OPC + EC) ratio guarantees the satisfaction of compressive strength requirement for ECC link slab application at different ages.

Restraint shrinkage ring tests were conducted to evaluate the performance of LS-ECC. In previous study (**Section 3**), it was concluded higher curing temperature, lower curing humidity, and lower w/c are the most dominant factors responsible for early age crack formation. Therefore, three LS-ECC rings were tested out to verify the early age cracking resistance under three different conditions. Ring 1 was the standard LS-ECC mix with 0.8 in Water to Cement (OPC + EC) ratio (**Table 4.8**). Ring 1 was demolded after one day and exposed in laboratory air condition with ambient temperature of 68±2^{o}F and ambient relative humidity of 45±5%. Ring 2 was the same mix but was exposed to higher temperature (98±2^{o}F) condition. Ring 3 was a LS-ECC mix with lower Water to Cement (OPC + EC) ratio, 0.77. Ring 3 was exposed to the same condition as ring 1. **Table 4.9** summarizes the test results. As can be seen, no crack was found in ring 1 and ring 3 and only 1 crack was found in ring 2 at the 7th day. The restrained shrinkage ring tests indicate LS-ECC has a much better performance in terms of reducing early age cracking and control tight crack width when compared with ECC M45 used in the Grove Street Bridge link slab.

Table 4.9: Summary of restraint shrinkage ring test results on LS-ECC

	Ave Crack Width (x10^{-4} inch)	Max Crack Width (x10^{-4} inch)	Crack No.	Total Shrinkage (x10^{-4} inch)	Shrinkage Strain (%)
Ring 1 – Control	-	-	0	-	-
Ring 2 – Temp	6	6	1	6	0.0015
Ring 3 – W/C	-	-	0	-	-

4.2.2 Small Frame Restrained Shrinkage Test

To verify the performance of the resulting LS-ECC, the same small frame restrained shrinkage test as depicted in **Section 3** (**Figure 3.18 (a)**) was conducted. To have a

comparison with the last small frame restrained shrinkage test on ECC M45, a skew of 45^{o} was also used in this restrained shrinkage test on LS-ECC. The resulting frame is shown in **Figure 4.9**.

Figure 4.9: Restrained small frame test setup with consideration of skew angle and the presence of steel rebars as stress concentrators

Figure 4.10: Small frame restrained shrinkage test on LS-ECC

The concrete frame was cured for 28 days and the LS-ECC was then cast (**Figure 4.10**). Upon casting, no curing compound was applied on the surface. The small frame was exposed to the laboratory air condition (68±2^{o}F and 45±5%RH) right after pouring and no plastic was used to cover the surface. No crack was found at the 7th day. The small frame restrained shrinkage test indicates that LS-ECC can effectively reduce the formation of early age cracking even in the presence of high skew angle and steel rebars acting as stress concentrators.

The restrained shrinkage ring tests and the small frame restrained shrinkage test suggest LS-ECC could be a potential material solution for future ECC link slab application.

4.2.3 Large Frame Restrained Shrinkage Test

Large frame restrained shrinkage test setup

To further verify the performance of LS-ECC, a second large frame restrained shrinkage test on LS-ECC was conducted. The schematic of the second large frame restrained shrinkage testing setup is shown in **Figure 4.11**. The frame measured 13'-4" by 5'-8" and could accommodate a 9" thick slab. Two layers epoxy coated reinforcing bars (#5) were placed in the frame. The reinforcing steel was installed at 8" spacing in each layer and each direction (longitudinal and transverse) and with 2.5" clear cover. A 20" wide concrete frame was poured along the perimeter of the frame to stiffen the whole structure and to prevent any movement of the steel reinforcing bars. The width of the peripheral concrete frame (20") was decided based on calculation, so that a 20" wide concrete frame has the same stiffness as that of the first steel large frame. Steel reinforcing bars (#3) were added to both top and bottom layers across the corners to resist cracking in the corners, as shown in **Figure 4.11**. No debonding paper (roofing paper) was used on the bottom of the slab to provide a higher restraint. To incorporate skew angle effect, a skew of 25^{o} (maximum skew angle recommend by Gilani and Jansson, 2004) was produced by casting concrete skew blocks in two sides. The purpose of this large frame test is to demonstrate that early age cracking can be prevented. The large frame test also serves as basis for the revision of special provision in **Section 6.1**. From the finite element analysis in **Section 6.1**, it indicates that 45 degree skew angle slab has a higher potential of cracking. Therefore, the skew angle was modified from 45 degree to 25 degree in this study. The resulting frame can accommodate a skewed ECC slab measured 10' by 2'-4" by 9" (length x width x depth).

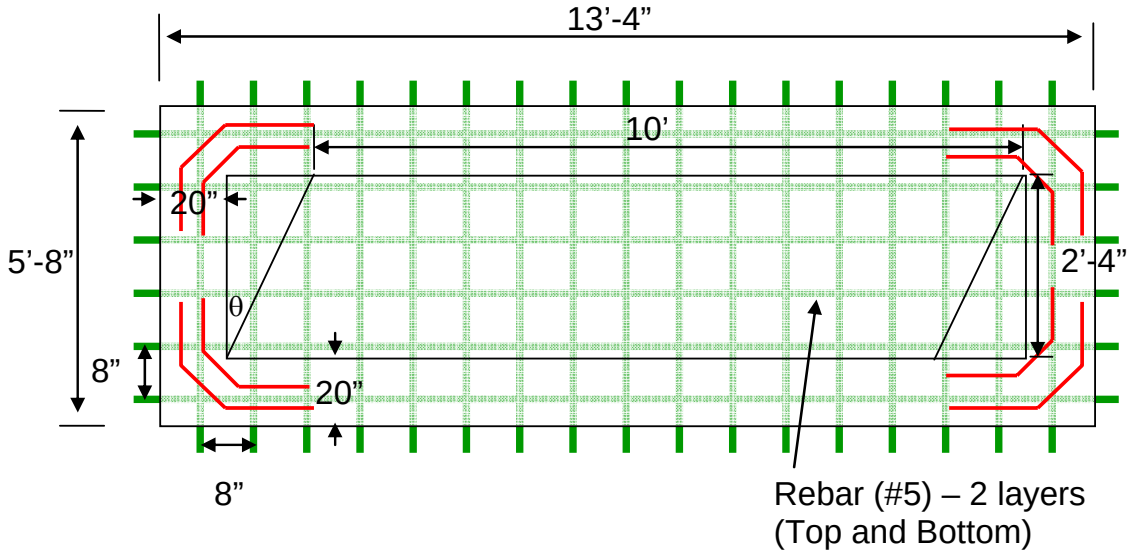

Figure 4.11: Schematic of second large frame restrained shrinkage testing setup ($\theta = 25^{o}$)

The design idea of this large frame is based on the small frame restrained shrinkage test setup but enlarging the size. It has been demonstrated that the small frame can provide sufficient restraint and reproduce early age cracking as described in **Section 3.2**. One criticism for the first large frame restrained shrinkage test is that the steel reinforcing bars were not welded onto the frame, and therefore provides less restraint. In the new design, any movement all the steel reinforcing bars was restrained by the concrete frame. This setup is also more close to the field condition in which the reinforcements were restrained by the adjacent concrete deck slabs.

Construction, mixing, pouring, and curing of large frame restrained shrinkage test

The construction of the wood formwork started on September 17, 2007 and completed on October 1, 2007 as shown in **Figure 4.12**. Cast of the peripheral concrete frame was on October 12 (temperature 48^{o}F, relative humidity 52%, wind speed 6.9 mph). A normal structural concrete mix design (f'_c = 5000 psi) was chosen and the concrete material was provided and delivered by Clawson Concrete. Upon finishing, the concrete frame was cured and covered by plastics for 21 days before casting the LS-ECC slab (**Figure 4.13**).

Figure 4.12: Large frame restrained shrinkage test – wood formwork construction

Figure 4.13: Large frame restrained shrinkage test – 20” peripheral concrete frame

The large frame restrained shrinkage test on LS-ECC was poured at noon on November 2, 2007 (air temperature 49^{o}F, relative humidity 56%, wind speed 8.1 mph, LS-ECC temperature 57^{o}F). Daytime casting was recommended by MDOT RAP in order to test out the LS-ECC material performance for day-time construction, to add value to the use of ECC. Surface evaporation of LS-ECC link slab was about 0.08 psf per hour based on **Figure 4.14**, which is below the maximum acceptable evaporation rate 0.2 psf per hour (Section 706. MDOT Standard Specification for Construction). A gravity-based mixer (**Figure 1.6**) was used to produce a total of 18 cubic feet of LS-ECC material to fill the frame. The mix proportion of LS-ECC can be found in **Table 4.8**. In processing the ECC material by using the gravity-based mixer, the batching sequence of the ingredients is summarized in **Table 4.10**.

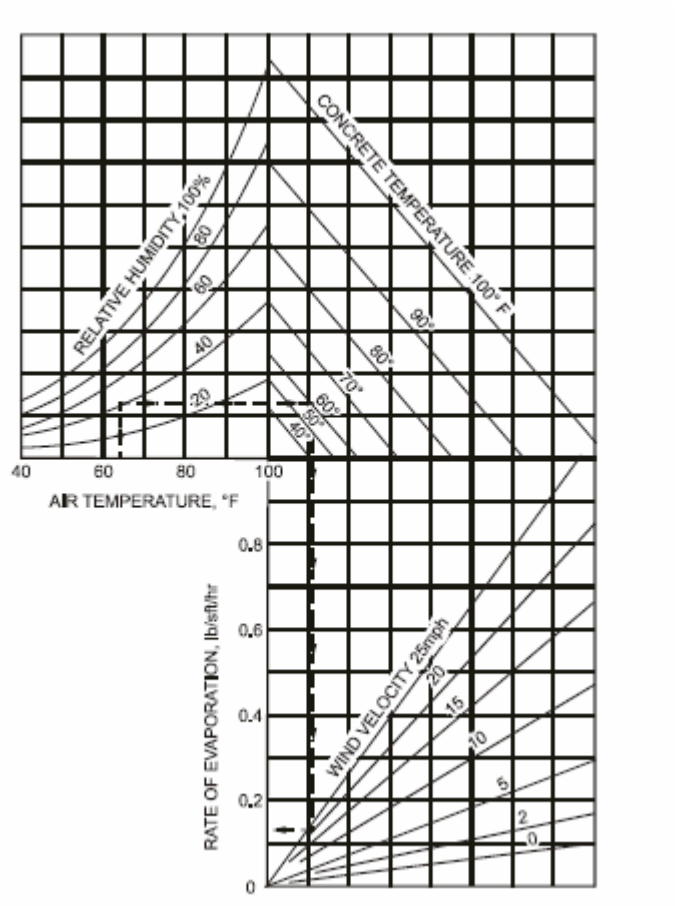

Figure 4.14: Surface evaporation from concrete material

Table 4.10: Batching sequence of LS-ECC for large frame slab

Activity	Elapsed Time (min)
1. Charge all sand	2
2. Charge all mixing water and all high range water reducer	2
3. Charge all fly ash	2
4. Charge all cement and expansive cement	2
5. Charge all shrinkage reducing admixtures	4
6. Mix at high speed RPM until material is homogenous	5
7. Charge fibers and mix until material is homogenous	5
Total	22

Upon finish, curing compound (Kurez VOX White Pigmented Curing Compound) from Euclid Chemical Company was applied on the surface as shown in **Figure 4.15**. The whole slab was then covered by wet burlap and plastic immediately to prevent excessive water evaporation (**Figure 4.16**). Soaker hoses were placed under the plastic as soon as the surface will support it without deformation. The slab was wet cured for 7 days. Following this curing regime, the slab was then exposed to outdoor environment and monitored for crack formation (**Figure 4.17**).

Figure 4.15: Large frame restrained shrinkage test – applying curing compound

Figure 4.16: Large frame restrained shrinkage test – curing

Figure 4.17: Large frame restrained shrinkage test

LS-ECC material quality assurance of large frame restrained shrinkage test

Fresh material tests were conducted on site, along with preparing specimens for testing hardened mechanical properties. The results of both fresh and hardened properties, i.e. slump flow, compressive, and uniaxial tensile, tests are shown below in **Figures 4.18** to **4.21** and **Tables 4.11** and **4.12**. It can be seen that all minimum values set within the revised ECC special provision (**Appendix B**) were met.

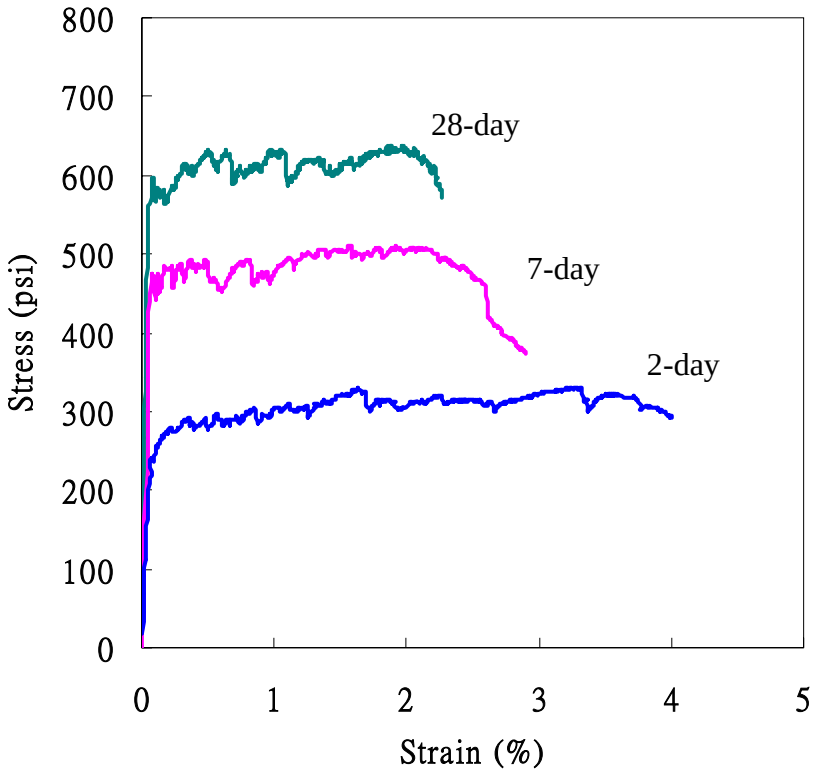

Figure 4.18: Representative tensile responses of LS-ECC from the large frame restrained shrinkage test

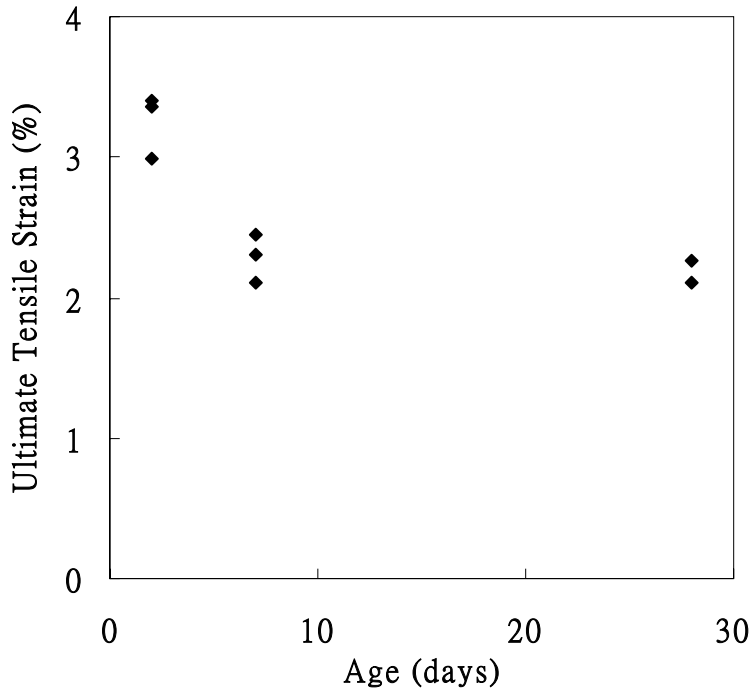

Figure 4.19: Ultimate tensile strain of LS-ECC from the large frame restrained shrinkage test at different age

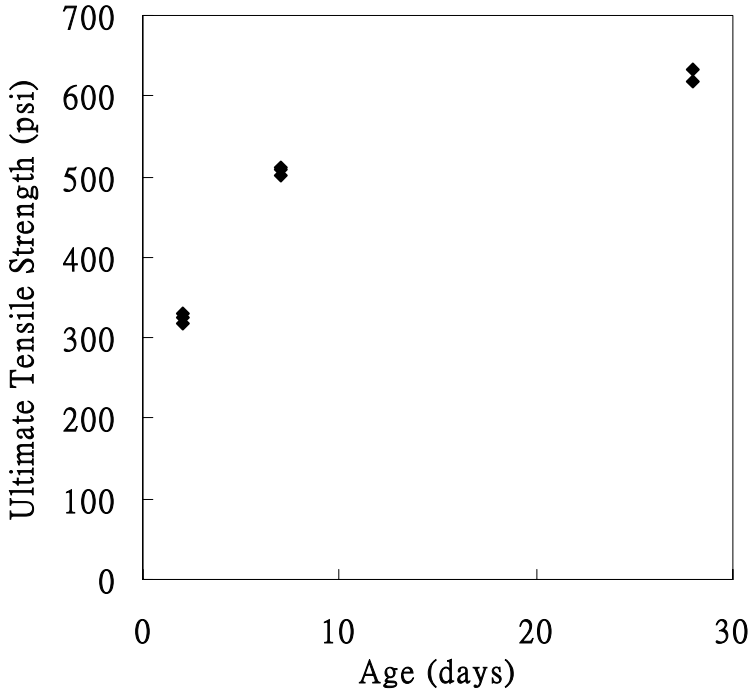

Figure 4.20: Ultimate tensile strength of LS-ECC from the large frame restrained shrinkage test at different age

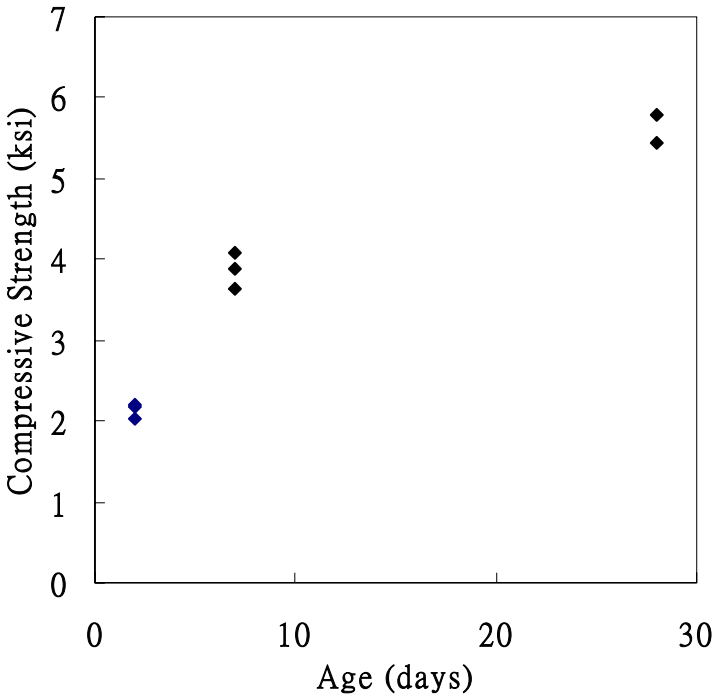

Figure 4.21: Compressive strength of LS-ECC from the large frame restrained shrinkage test at different age

Table 4.11: LS-ECC hardened properties at different age

age	Test									
	Compressive			Tensile						
	f'_c (ksi)	req'd (ksi)	#	σ_{ult} (psi)	req'd (psi)	ε_{ult} (%)	req'd (%)	crack width (10^{-4} inch)	req'd (10^{-4} inch)	#
2	2.13±0.09	-	3	324±7	-	3.3±0.2	2	32±5	40	3
7	3.87±0.23	3.2	3	507±5	500	2.3±0.2	2	22±7	40	3
28	5.62±0.24	4.5	2	626±9	500	2.2±0.1	2	18±11	40	2

* Ranges shown are standard deviation

Table 4.12: LS-ECC fresh properties

test	measured	req'd
temperature (^oF)	57	-
slump (inch)	32	30

Monitoring of crack

After 7 days of wet curing, no early age shrinkage cracks were found even at the acute corners as shown in **Figure 4.22**. The slab was continuously monitored for 2 month and still no cracks showed up. The restrained shrinkage ring tests, small frame restrained shrinkage test, and large frame restrained shrinkage test suggest LS-ECC could be a material solution for future ECC link slab application.

Figure 4.22: Large frame restrained shrinkage test construction

5. Documentation of LS-ECC Fresh, Shrinkage, and Mechanical Properties (Task 4)

5.1 Mixing and Fresh Properties

To prepare LS-ECC, a Hobart mixer with 0.46 ft^3 capacity was used. The mix proportion follows **Table 4.8**. Solid ingredients, including cement, fly ash, and sand, were first mixed for a couple of minutes. Water and shrinkage reducing admixture were added into

the dry mixture. After mixing for two minutes, superplasticizer was then added into the mixture and mixed for another two minutes. After the mortar matrix reached a consistent liquefied state, PVA fibers were slowly added into the mortar matrix and mixed until all fibers are evenly distributed. Slump flow test was performed and air content of LS-ECC was measured. The slump flow diameter was 30" which indicates a self-consolidating mix of LS-ECC. The air content of LS-ECC was 9.3%, which is in the same range as that of M45.

5.2 Free Drying Shrinkage of Low Shrinkage ECC

Free drying shrinkage tests were conducted according to ASTM C157/C157M-99 and C596-01 standards, except that the storing of the specimens before test was modified. The specimens were demolded after one day. Upon demolding, the specimens were moved to laboratory air and the measurement was started. Beside LS-ECC, M45 was also tested as control. Two specimens were tested for each material and the average drying shrinkage deformation versus time curved was plotted in **Figure 5.1**. As can be seen, drying shrinkage of LS-ECC was greatly reduced. At the 7^{th} day, shrinkage deformation of LS-ECC is 600 με which is about 40% less than that of ECC M45. The long term shrinkage deformation of LS-ECC is 1000 με, which is a little higher than that of normal structural concrete (600 – 800 με, Mindess et al. 2004). Compared with ECC M45, long term shrinkage deformation of LS-ECC can be reduced as much as 700 με. The reduction of drying shrinkage in LS-ECC is mainly attributed to the presence of high volumes of fly ash and shrinkage reducing agent in the new mix design. Expansive cement does not contribute much due to the lack of 7-day wet curing. Therefore, it is expected the reduction of shrinkage deformation of LS-ECC can be even more significant when proper curing (soaking with water hose) is executed in the field.

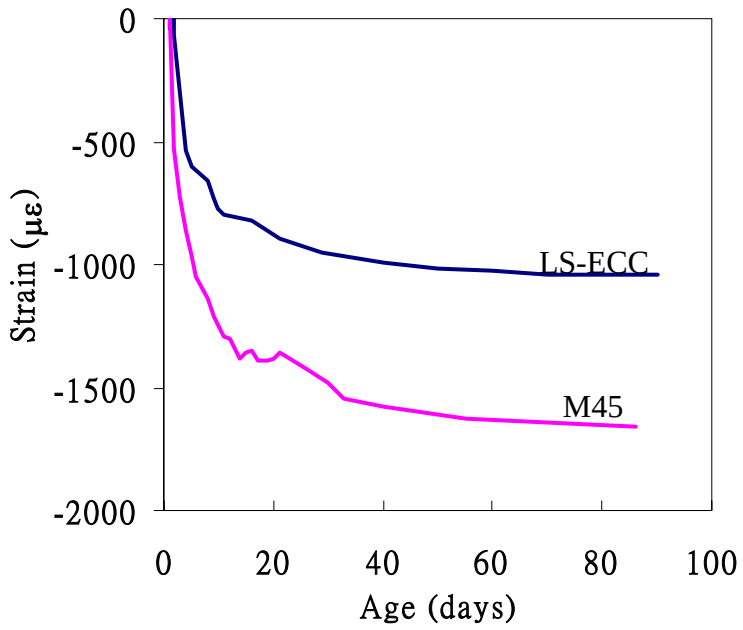

Figure 5.1: Free drying shrinkage development of ECC M45 and low shrinkage ECC

5.3 Autogenous Shrinkage of Low Shrinkage ECC

Membrane method was used to measure the autogenous shrinkage deformation of ECC material (Lura and Jensen, 2005). The measurement of autogenous shrinkage deformation was performed by monitoring the weight of ECC that was sealed in a membrane, submerged in paraffin oil, and suspended from a high-precision balance (resolution 0.000035 oz). The test setup is shown in **Figure 5.2**. For each test, 0.77 to 0.88 lbs of deaired, freshly mixed cement paste was cast in a membrane. The membranes consisted of polyurethane condoms with thickness 0.0016".

The membranes were cleaned and any lubricants were removed with a paper towel. After cleaning, the membranes were filled with ECC. The filled membrane was tightly closed with a knot (**Figure 5.3**). The excess part of the membrane was then cut off and a monofilament line was tied to the sample. The line, approximately 20" long, was tied to a stainless steel hook. The sample was then gently lowered into a steel container filled with paraffin oil that was placed in the water bath.

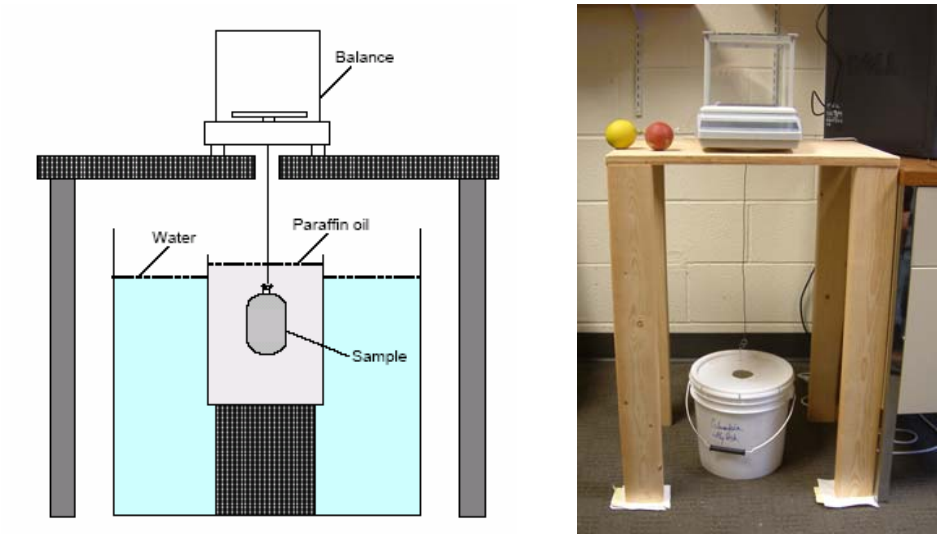

Figure 5.2: Test setup of autogenous shrinkage measurement of ECC

Figure 5.3: Polyurethane membranes with reservoir filled with ECC

The submerged weight of the sample was automatically recorded every 5 minutes from about 10 minutes after water addition up to 24 hours. Volumetric strain (ε_{vol}) of ECC can be calculated from the submerged weight change according to the following procedure:

$$\varepsilon_{vol} = \frac{\Delta V_{ECC}(t)}{V_{ECC}(10)} = \frac{W_{sub}(t) - W_{sub}(10)}{W_{air}(10) - W_{sub}(10)}$$

where $\Delta V_{ECC}(t)$ is the volume change of ECC at time t, $V_{ECC}(10)$ is the initial volume of

ECC, $W_{sub}(t)$ is the submerged weight of ECC at time t, $W_{sub}(10)$ is the initial submerged weight of ECC. The initial weight was taken 10 minutes after the addition of water to the mixer. Two specimens were tested for each material and the average shrinkage deformation versus time curved was plotted in **Figure 5.4.** Assuming isotropic deformation, linear strain equals to 1/3 of volumetric strain. Based on this assumption, the magnitude of autogenous shrinkage of LSECC and M45 at the age of 24 hours is 2.5 - 3 times larger than their free drying shrinkage at the age of 80 days. Also as can be seen, autogenous shrinkage (volumetric strain) of LS-ECC was about 40% less than that of ECC M45 at the age of 24 hours. This lower autogenous shrinkage of LS-ECC is attributed to the presence of expensive cement which compensates the shrinkage deformation due to cement hydration.

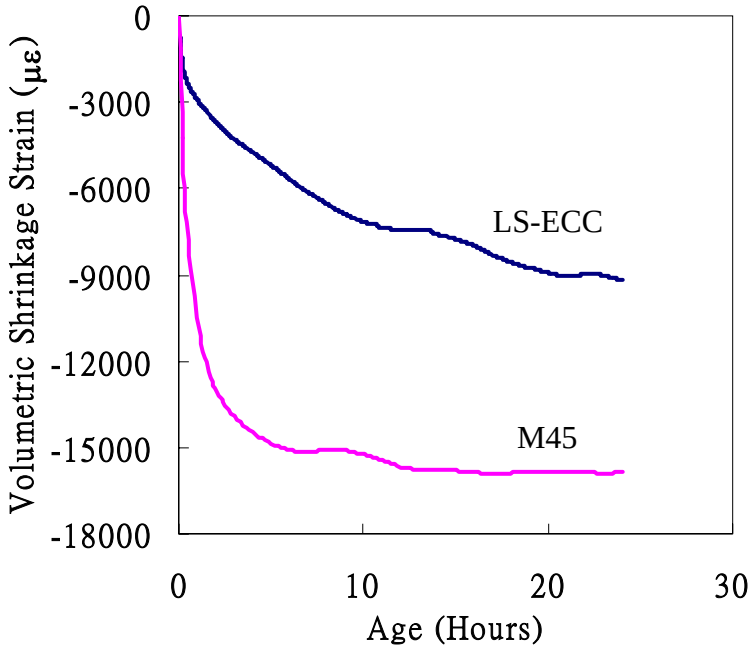

Figure 5.4: Autogenous shrinkage (volumetric strain) development of ECC M45 and low shrinkage ECC

5.4 Compressive Strength of Low Shrinkage ECC

Compressive test was carried out for LS-ECC mix at the age of 3, 7, 14 days and 28 days. Cylinders measuring 3” in diameter and 6” in length were used in this study. The ends of

cylinders were capped with a sulfur compound to ensure a flat and parallel surface and a better contact with the loading device. The cylinder specimens were cured in plastics for 7 days, which were then taken out and exposed to laboratory air until specified testing ages. **Figure 5.5** plots the compressive strength development of LS-ECC along with the required compressive strength for ECC link slab application based on the specific provision of ECC link slab. Each data point was the average result from three tests. As can be seen, LS-ECC can satisfy the compressive strength requirement for ECC link slab application at different ages.

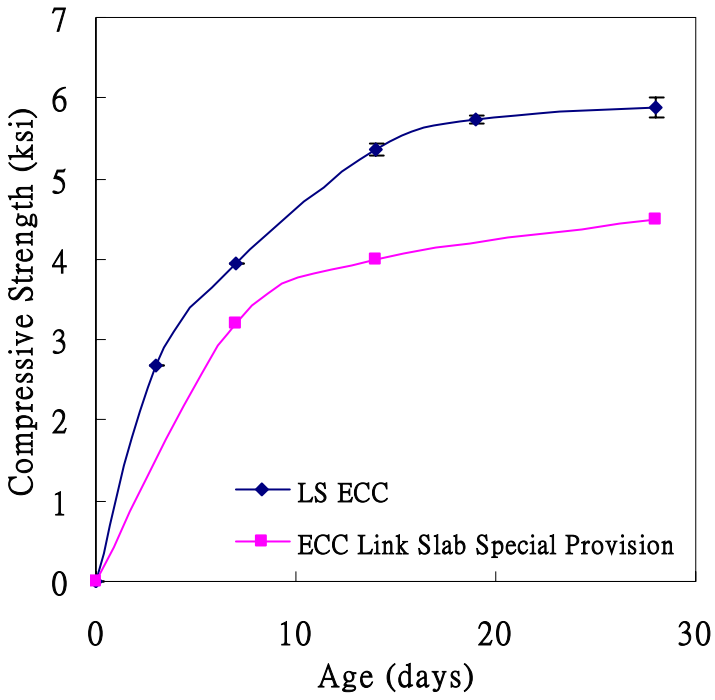

Figure 5.5: Compressive development of LS-ECC

Table 5.1: Summary of compressive strength of LS-ECC at different ages

age (days)	f'_c (ksi)	req'd (ksi)
3	2.681±0.008	-
7	3.953±0.002	3.2
14	5.362±0.066	4
28	5.873±0.125	4.5

* Each data point is an average of 3 tests
** Ranges shown are standard deviation

5.5 Tensile Properties of Low Shrinkage ECC

Uniaxial tensile tests were carried out on LS-ECC coupon specimens at the age of 2, 3, 7, 14 and 28 days. Coupon specimens measuring 8" by 3" by 0.5" were cured in sealed plastics for 7 days, which were then taken out and exposed to laboratory air until specified testing ages. A servohydraulic testing system was used in displacement control mode to conduct the tensile test. The loading rate used was 0.0001 in/s to simulate a quasi-static loading condition. Aluminum plates were glued both sides at the ends of coupon specimens to facilitate gripping. Two external linear variable displacement transducers were attached to the specimen with a gauge length of approximately 4" to measure the specimen deformation.

The results of uniaxial tensile tests are shown below in **Figures 5.6 to 5.8** and **Table 5.2** (ranges shown are standard deviation). Each data point was an average of three test results. As can be seen, LS-ECC shows tensile strain hardening behavior at all ages. Ultimate tensile strain capacity of LS-ECC gradually decreases at early age and stabilizes after the 7^{th} day with a stain capacity of 2.5%, which meets the required 2% strain capacity for the Grove Street ECC link slab application. Ultimate tensile strength increases with age and meets the required tensile strength at the age of 7 days (500 psi). Crack width of LS-ECC decreases with age and the magnitude of crack width in LS-ECC is smaller than M45 both at early ages and later ages.

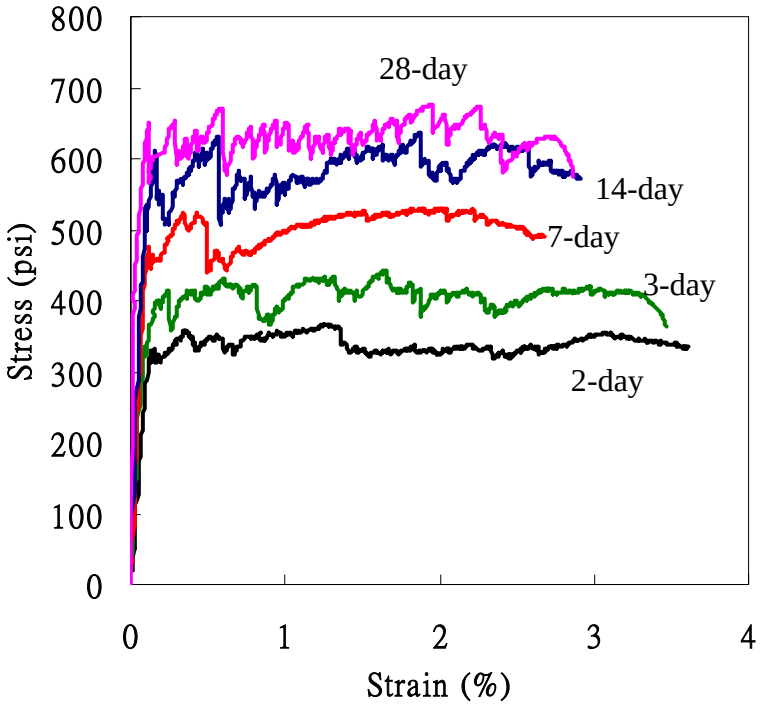

Figure 5.6: Representative uniaxial tensile stress-strain curves of LS-ECC at different ages

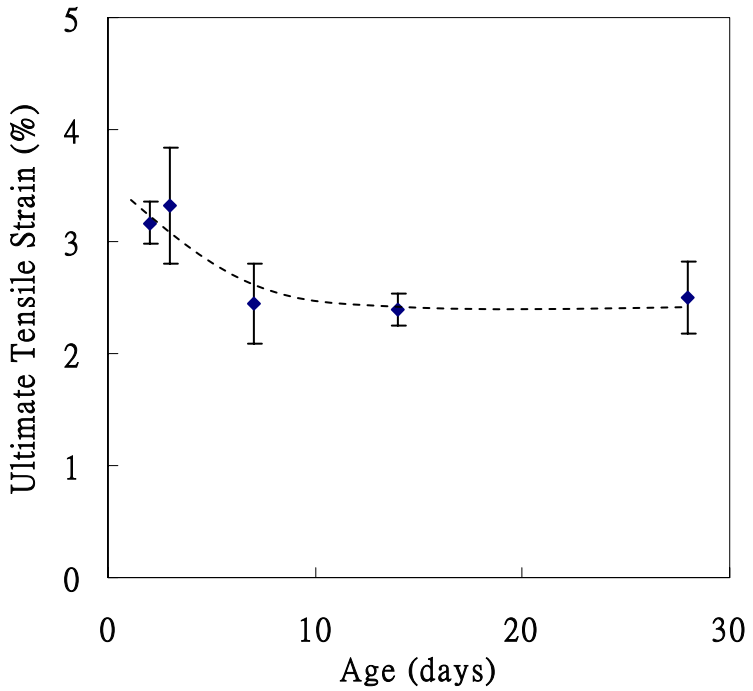

Figure 5.7: Ultimate tensile strain capacity of LS-ECC at different ages

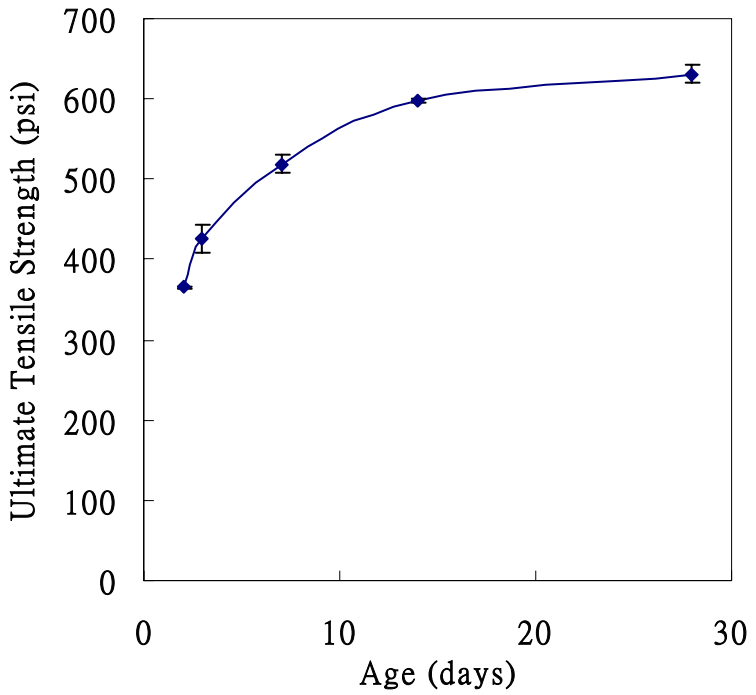

Figure 5.8: Ultimate tensile strength of LS-ECC at different ages

Table 5.2: Summary of tensile properties of LS-ECC at different ages

age (days)	ε_{ult} (%)	ε_{ult} req'd (%)	σ_{ult} (psi)	σ_{ult} req'd (psi)	crack width (10^{-4} inch)	allowable crack width (10^{-4} inch)
2	3.17±0.19	2	365±1	-	27±8	40
3	3.32±0.52	2	425±17	-	25±11	40
7	2.45±0.35	2	519±11	500	21±4	40
14	2.40±0.14	2	598±2	500	19±5	40
28	2.50±0.33	2	631±11	500	19±5	40

* Each data point is an average of 4 tests
** Ranges shown are standard deviation

5.6 Cost Analysis of Low Shrinkage ECC

Table 5.3 gives the cost comparison of ECC M45 and low shrinkage ECC. The cost of each ingredient is provided by supplier. It can be seen, low shrinkage ECC is $13 higher than M45 per cubic yard. Although expansive cement and shrinkage reducing

admixtures have been incorporated into LS-ECC mix design, which increase the price of LS-ECC, replacement of more ordinary Portland cement by fly ash in LS-ECC helps to lower the cost.

Table 5.3: Cost comparison of ECC M45 and LS-ECC (unit: dollar per cubic yard)

	OPC	EC	Sand	FA	Water	SP	SRA	PVA	Total
	$86/ton	$350/ton	$150/ton	$23/ton	$0/gal	$19/gal	$20/gal	$3/lb	
M45 ($/cyd)	41	0	57	13	0	25	0	131	267
LS-ECC ($/cyd)	27	12	57	16	0	17	20	131	280

6. Revision of ECC Link Slab Special Provision (Task 5)

Revised ECC link slab special provision can be found in **Appendix B**. This section summarizes and discusses the major revision within this new version of ECC link slab special provision.

6.1 Skewed Bridge

As discussed in the previous section, high skew angle introduces high stresses in the acute corner which contributes to link slab early age cracking. Therefore, it is necessary to set an allowable skew angle for the future ECC link slab application. Finite element method was used to evaluate the performance of LS-ECC when applied to link slabs with different skew angles, ranging from 0 to 45^{o}. The geometry and mechanical boundary conditions of the model are the same as shown in **Section 3.1.5**. **Figures 6.1** to **6.3** show the development of LS-ECC material cracking strength (from experimental data) and the development of principle tensile stress (computed) at the acute corner of LS-ECC link slab with 3 different skewed angles. Again, cracks form when the principle stress in link slab exceeds the material cracking strength. As can be seen, LS-ECC cracking strength is higher than the principle stress in the acute corner in all cases. However, the margin between them reduces as the skew angle increase which indicates the potential of

cracking increases. Base on the field observation, Gilani and Jansson (2004) proposed a skew angle limit of 25 degree. The large frame restrained shrinkage test (Section 4.2.3) with a 25 degree skew angle also shows no sign of cracking. Therefore, a skew angle upper limit of 25 degree is adopted in the revised ECC link slab special provision. It is recommended that the next ECC link slab should perform on a bridge with skew angle no larger than 25 degree. This restraint may be removed or relaxed as engineers build up more experience and confidence in the future link slab projects.

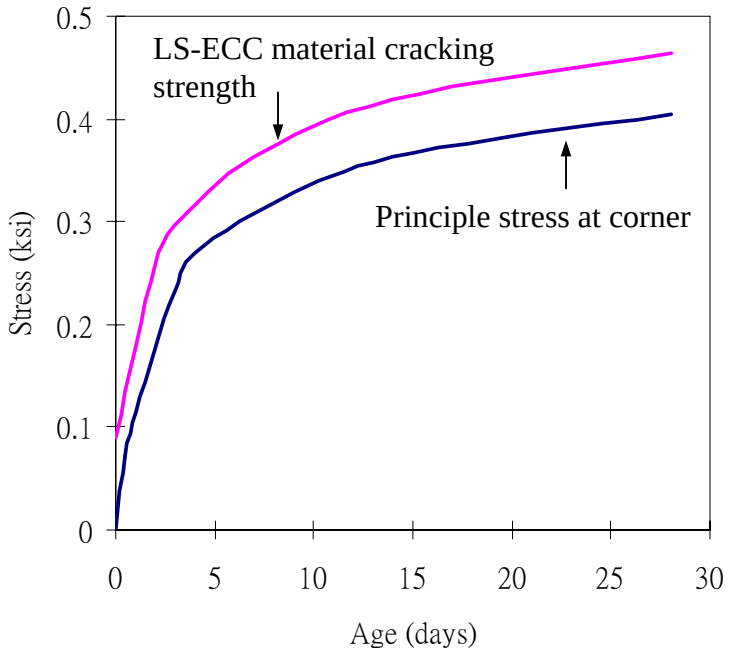

Figure 6.1: Tensile stress and strength development at the corner of a 0 degree skewed LS-ECC link slab

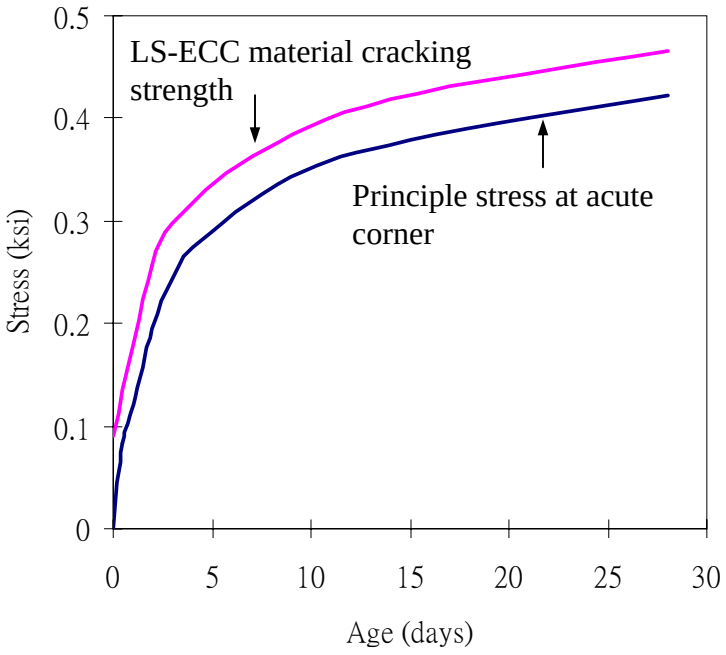

Figure 6.2: Tensile stress and strength development at the acute corner of a 30 degree skewed LS-ECC link slab

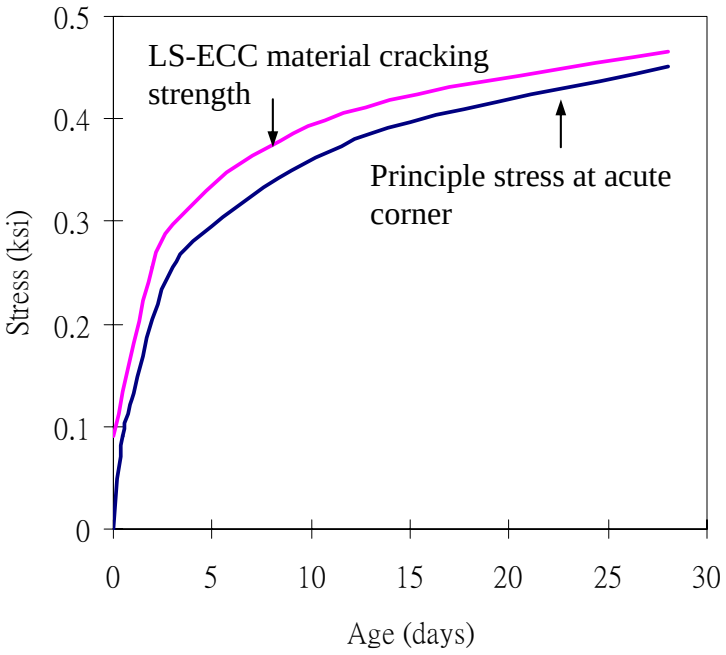

Figure 6.3: Tensile stress and strength development at the acute corner of a 45 degree skewed LS-ECC link slab

6.2 Materials

Compared with ECC M45, new ingredients used in LS-ECC include expansive cement and shrinkage reducing admixtures. Contact information of the suppliers of these two ingredients was added into the new special provision.

6.3 ECC Mix Requirement

In this subsection, mix proportion of ECC M45 in the old version has been replaced by the mix proportion of LS-ECC (**Table 1** in the special provision). Allowable time for submitting adjusted mix design to engineers has been advanced from a minimum of five days to ten working days prior to placement of the ECC link slab. Crack width and free drying shrinkage at different ages (early age, 2 and 3 days, in particular) are added into **Table 2** (special provision) as additional mechanical properties requirements for LS-ECC material.

6.4 Trial Batch

An important point relates to processing is that one should not mix chemical admixtures together before they enter the ECC material. In particular, shrinkage reducing admixture should never mix with high range water reducer first before adding into the ECC mix. In construction of Grove Street Bridge ECC link slab, it was observed that high range water reducer and retarder were mixed before adding into the ECC.

6.5 Preparation, Placement, and Cure of ECC Material

While the large frame restrained shrinkage test on LS-ECC was cast at daytime, nighttime casting is preferred for conservativeness and in accordance with MDOT standard procedures for concrete deck pouring. Nighttime casting is recommended for the next ECC link slab construction. Daytime casting may be recommended in the future as more experience from the field is gained. Seven days of wet curing is necessary for future LS-ECC slab construction and needs to be enforced.

6.6 Quality Assurance

As shown in **Table 2** (special provision), free drying shrinkage and crack width should be monitored at the ages of 2, 3, 7, 14, and 28 days. Therefore, this subsection adds the test method of free drying shrinkage and the geometry of free drying shrinkage specimen.

7. Monitoring of the Grove Street Bridge and ECC Link Slab (Task 6)

Grove Street Bridge and ECC link slab were periodically visited and monitored through out the whole research period. Results are summarized in this section.

7.1 Fourteen-month-visit

Figure 7.1 shows the ECC link slab and the adjacent concrete deck after opening to traffic for 14 months. The deterioration of the concrete surface was found to be much severer than that of the ECC surface. As can be seen from **Figure 7.1(b)**, scaling was observed on the surface of the adjacent concrete deck. In contract, no scaling could be found on the surface of the ECC link slab and the slab remained in a very good shape pretty much similar to the condition when the bridge was just completed. It was also found that the traffic lane line on the ECC link slab remains much more visible than that on the concrete deck (see circled area in **Figure 7.1(a)**). This observation suggests a better wearing and scaling resistance of ECC material when compared to concrete.

(a) (b)

Figure 7.1: (a) 14-month-old ECC link slab on Grove Street Bridge over I-94 and (b) deterioration of adjacent concrete deck enlarged from the area marked with rectangle in (a) (December 7, 2006)

The crack width of the early age cracking was found to remain approximately 0.006” to 0.01”. **Figure 7.2** shows one of the early age cracks on the ECC link slab after exposing to the traffic and environmental loading for 14 months. The cracking pattern was not monitored due to traffic.

Figure 7.2: Crack width of early age cracks within ECC link slab maintains approximately 0.006” to 0.01” (December 7, 2006)

Periodic cracking was found in the concrete railing of the sidewalk. **Figure 7.3** illustrates such a crack with crack width approximately 0.02” to 0.04”.

Figure 7.3: Cracking on the concrete railing with crack width approximately 0.02” to 0.04”

7.2 Twenty-one-month visit

Figure 7.4 shows the ECC link slab and the adjacent concrete deck after opening to traffic for 21 months. As can be seen, the traffic lines have been repainted. The crack pattern and crack width were found to remain the same as observed a few days after placement. **Figure 7.5** shows one of the cracks on the ECC link slab after exposing to the traffic and environmental loading for 21 months.

Figure 7.4: 21-month-old ECC link slab on Grove Street Bridge over I-94 (July 5, 2007)

Figure 7.5: Crack width of early age cracks within ECC link slab maintains approximately 0.006” to 0.01” (July 5, 2007)

Cracking and spalling was observed in the adjacent concrete deck (**Figure 7.6(a)**). **Figure 7.6(b)** shows the spalling of a concrete curb. The crack width is about half inch. Severe cracking (dark color area) was found in the sharp corner of the skewed concrete deck and the crack pattern is shown in **Figure 7.6(c)**. The crack has been repaired and sealed with epoxy-based sealer, and therefore shows a darker color. The crack pattern is consistent with the finite element analysis result on the skew angle effect discussed in **Section 3.1.5**. **Figure 7.6(d)** shows a large crack along the traffic direction. This crack has also been sealed. **Figure 7.6(e)** gives a close look of the crack and the crack width is approximately 0.15”. **Figure 7.6(f)** shows a new crack form along the repaired/sealed

crack. This illustrates the deficiency of current repair technology and result in repeated repair.

(a) (b)

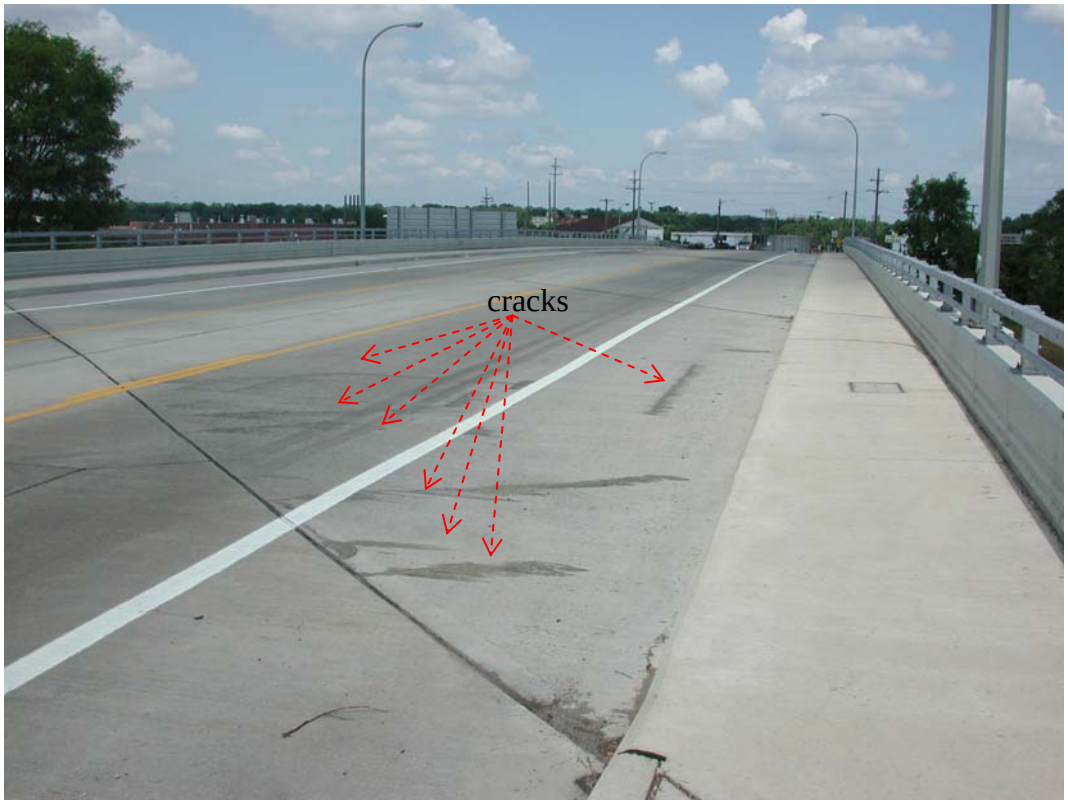

(c)

Figure 7.6: Concrete deck cracks: (a) Cracking in the adjacent concrete deck, (b) spalling in the curb, (c) cracking in the acute corner

(d)

(e) (f)

Figure 7.6: Concrete deck cracks: (d) cracking a long the traffic direction, (e) repaired crack in the acute corner, and (f) new crack along the repaired crack in the acute corner

7.3 Twenty-four-month visit

Figure 7.7 shows the ECC link slab and the adjacent concrete deck after opening to traffic for 24 months. The crack pattern and crack width were found to remain the same as observed a few days after placement. The crack width did not increase and in some cases cracks sealed with blackish color material - perhaps calcite mixed with dirt from traffic. These cracks remain bridged by fibers that maintain load carrying capacity. **Figure 7.8** shows one of the cracks on the ECC link slab after exposing to the traffic and environmental loading for 24 months.

Figure 7.7: 24-month-old ECC link slab on Grove Street Bridge over I-94 (October 16, 2007)

Figure 7.8: Crack width of those early age cracks within ECC link slab maintains approximately 0.006” to 0.01” (October 16, 2007)

7.4 Twenty-seven-month visit

Figure 7.9 shows the 27-month-old ECC link slab. The link slab has now been exposed to three winters of Michigan weather and the crack width remains unchanged. **Figure 7.10** shows one of the cracks on the ECC link slab after exposing to the traffic and environmental loading for 27 months.

Figure 7.9: 27-month-old ECC link slab on Grove Street Bridge over I-94 (January 18, 2008)

Figure 7.10: Crack width of early age cracks within ECC link slab maintains approximately 0.006” to 0.01” (January 18, 2008)

8. Conclusion and Future Activities

This report describes research activities conducted during the last year with the goal of identifying the cause(es) of early age cracking and replicating the cracking behavior observed in Grove Street bridge ECC link slab, developing a new ECC material for the link slab application to provide an additional buffer against the tendency for cracking in high skew bridge decks in general, and to further improves upon the early age cracking found in the Grove Street ECC link slab with a skew angle of 45 degrees.

Small scale restrained shrinkage ring test, small scale restrained prism test, and finite element analysis were used to identify any potential factors (material, processing, curing, and structure) that may cause the early age cracking. It was concluded that low water to cement ratio, low retarder to cement ratio, low SP to cement ratio, use of gravity-based mixer, high curing temperature, low curing relative humidity, wind effect, rebar as stress concentrator, and skew angle all contribute to the early age cracking behavior. From the ring tests, it seems that curing humidity, curing temperature, and water to cement ratio are more dominant than wind effect, use of gravity mixer, retarder to cement ratio, and SP to cement ratio. The presence of rebar as stress concentrator and skew angle are recognized as important factors causing cracking. However, it is hard to say which are more dominant based on current results. A small frame restrained shrinkage test was used to test out the combination of those factors. Similar crack pattern and crack width were observed in the small frame restrained shrinkage test at early age. Based on this study, it can be concluded that the formation of early age cracking in Grove Street bridge ECC link slab was indeed a combination of several factors. Those factors include M45 in nature is a low water to cement ratio mix, use of gravity mixer, wind effect, high ambient temperature in Phase I, low ambient humidity, presence of steel reinforcing bars, excessive restraint, high skew angle, and inadequate soaking water for curing.

High volumes of fly ash, shrinkage reducing agent, and expensive cement were used to reduce the shrinkage deformation of ECC and to control the crack width of ECC at early ages. Shrinkage deformation of the resulting LS-ECC was greatly reduced by about 50%

both at early age and later age. No cracking was found in the LS-ECC restrained shrinkage ring (1 crack with tight crack width of $6x10^{-4}$ inch) was found in high temperature exposures), small frame restrained shrinkage test, and large frame restrained shrinkage test at early ages. In addition, LS-ECC, both the fresh and the harden properties, meets all minimum values set within the revised ECC link slab special provision. It was concluded the resulting LS-ECC can be a potential material solution for future ECC link slab applications.

A revised ECC link slab special provision is provided and can be found in **Appendix B**. Major revisions include limiting the skew angle to no more than 25 degree, replacing ECC M45 with LS-ECC material in future construction of ECC link slab, recommending nighttime casting, enforcing water curing for at least 7 days, and measuring free drying shrinkage and crack width when conducing quality assurance tests.

The crack pattern and crack width in Grove Street bridge ECC link slab were found to remain after being open to traffic for 27 months (3 winters). The crack width did not increase and in some cases cracks sealed with blackish color stuff - perhaps calcite mixed with dirt from traffic. These cracks remain bridged by fibers which maintain load capacity. Cracking and spalling were observed in the adjacent concrete deck. Severe cracking was found in the sharp corner of skewed concrete deck and this can be explained by higher stress state in the sharp corner as analyzed by finite element method. It was also found that new crack form along the repaired crack suggesting that current repair technology is inadequate and result in costly repeated repairs.

9. References

American Association of State Highway and Transportation Officials, AASHTO (U.S. Code Organization)

American Society for Testing and Materials, ASTM (U.S. Code Organization)

Atis, C.D., "High-Volume Fly Ash concrete with High Strength and Low Drying Shrinkage," *Journal of Materials in Civil Engineering*, 2004. **15**(2): p. 153-156.

Aveston, J., Cooper, G., and Kelly, A., "Single and Multiple Fracture," *Properties of Fiber Composites*, Guildford, UK, pp.15-24, 1971

Bilodeau, A., V. Sivasundaram, K.E. Painter, and V.M. Malhotra, "Durability of Concrete Incorporating High Volumes of Fly Ash from Sources in the U.S.," *ACI Materials Journal*, No.91, 1994, pp.3-12

Bisallion, A., Rivest, M., and Malhotra, V.M., "Performance of High-Volume Fly Ash Concrete in Large Experimental Monoliths," *ACI Materials Journal*, 1994. **91**(2): p. 178-187.

Fu, G., J. Feng, J. Dimaria, and Y. Zhuang, "Bridge Deck Corner Cracking on Skewed Structures," *MDOT Report RC-1490*, Sept. 2007

Gilani, A. and Jansson, P., 2004, "Link Slabs for Simply Supported Bridges." *MDOT Report Number MDOT SPR-54181*, Structural Research Unit, Construction and Technology Support Area, Michigan Department of Transportation. Lansing, Michigan.

He, Zhen, X. Zhou, and Z. Li, "New Experimental Method for Studying Early-age Cracking of Cement-based Materials," *ACI Materials Journal*, No.101, 2004, pp.50-56

Kanda, T., "Design of Engineered Cementitious Composites for Ductile Seismic Resistant Elements," *Ph.D. Dissertation*, Department of Civil and Environmental Engineering, University of Michigan, Ann Arbor, 329 pp, 1998

Kanda, T., Kanakubo, T., Nagai, S., and Maruta, M., "Technical Consideration in Producing ECC Pre-cast Structural Element," in *Proceeding of International RILEM Workshop on High Performance Fiber Reinforced Cementitious Composites in Structural Applications*, G. Fischer and V.C. Li Eds., pp.229-242, 2006

Kayali, O., "Effect of High Volume Fly Ash on Mechanical Properties of Fiber Reinforced Concrete," *Materials and Structures*, 2004. **37**(269): p. 318-327

Li, V.C., "Post-Crack Scaling Relations for Fiber-Reinforced Cementitious Composites," *Journal of Materials in Civil Engineering*, vol.4, no.1, pp.41-57, 1992

Li, V.C., and Wu, H.C., "Conditions for Pseudo Strain-Hardening in Fiber Reinforced Brittle Matrix Composites," *J. of Applied Mechanics Review*, vol.45, no.8, pp.390-398, 1992

Li, V.C., and Leung, C.K.Y., "Theory of Steady State and Multiple Cracking of Random Discontinuous Fiber Reinforced Brittle Matrix Composites," *Journal of Engineering Mechanics*, vol.118, no.11, pp.2246-2264, 1992

Li, V.C., M .Lepech, M. Li, "Final Report on Demonstration of Durable Link Slabs for Jointless Bridge Decks Based on Strain-Hardening Cementitious Composites", *MDOT Report*, Dec., 2005.

Li, V.C. and E. Yang, "Self Healing in Concrete Materials," in *Self Healing Material: An Alternative Approach to 20 Centuries of Materials Sciences*, S. van der Zwaag Ed., Springer, Sept. 2007, pp.161-193

Lin, Z., T. Kanda, and V.C. Li, "On Interface Property Characterization and Performance of Fiber-Reinforced Cementitious Composites," *Journal of Concrete Science and Engineering*, no.1, pp.173-184, 1999

Lura, P., and Jensen, O. M., "Measuring Techniques for Autogenous Strain of Cement Paste," *Knud Højgaard Conference on Advanced Cement-Based Materials*, Lyngby, Denmark, June 2005

Marshall, D.B., and Cox, B.N., "A J-Integral Method for Calculating Steady-State Matrix Cracking Stresses in Composites," *Mechanics of Materials*, no.8, pp.127-133, 1988

MDOT Inspector's Report on I-94 Wbd over Gratiot (S10-4 77111), June 2006

Mindess, S., Young, J.F., and Darwin, D., *Concrete*. Second ed. 2002: Prentice Hall.

Redon, C., V.C. Li, C. Wu, H. Hoshiro, T. Saito, and A. Ogawa, "Measuring and Modifying Interface Properties of PVA Fibers in ECC Matrix," *ASCE J. Materials in Civil Engineering*, Vol. 13, No. 6, Nov./Dec., 2001, pp399-406.

Section 706. Structural Concrete Construction.

Wang, S., and Li, V.C., "Polyvinyl Alcohol Fiber Reinforced Engineered Cementitious Composites: Material Design and Performances," *Proceedings of Int'l RILEM workshop on HPFRCC in structural applications*, pp.65-73, 2006

Weather Underground, http://www.wunderground.com/

Wu, H.C., and Li, V.C., "Snubbing and Bundling Effects on Multiple Crack Spacing of Discontinuous Random Fiber-Reinforced Brittle Matrix Composites," *Journal of American Ceramics Society*, vol.75, no.12, pp.3487-3489, 1992

Appendix A: Original ECC Link Slab Special Provision

MICHIGAN
DEPARTMENT OF TRANSPORTATION

SPECIAL PROVISION
FOR
ECC BRIDGE DECK LINK SLAB

a. **Description. –** This work consists of building a link slab of Engineered Cementitious Composite (ECC) within a newly constructed, rehabilitated, or retrofitted bridge. Except as modified by this special provision, all work is to be in accordance with the 2003 Standard Specifications for Construction.

b. **Materials. –** Fine aggregates used for ECC material must be virgin silica sand consisting of a gradation curve with 50% particles finer than 0.04 mil and a maximum grain size of 12 mil. Fine aggregates meeting this requirement are available from US Silica Corporation (701 Boyce Memorial Drive, Ottawa, Illinois 61350 (800) 635-7263) under the trade name "F-110 Foundry Silica Sand". Approved equal will be accepted.

Fibers to be used for ECC material must be manufactured of poly-vinyl-alcohol (PVA) with a fiber diameter of 1.5 mil and a length between 0.3 inch and 0.5 inch. The surface of the fiber must be oiled by the manufacturer with 1.2% (by weight) hydrophobic oiling compound along the length of the fiber. Fiber strength should be 232 kips per square inch with a tensile elastic modulus of 5,800 kips per square inch. Fibers meeting this requirement are available from Kuraray America (101 East 52nd Street, 26th Floor, New York, New York 10022 (212) 986-2230) under the trade name "REC-15". Approved equal will be accepted.

c. **ECC Mix Design Requirements. -** The ECC mixture requirements are shown in Table 1 within this special provision. For the mixture proportions listed, fine aggregate weight is assumed to have a dry bulk density of 2.60. The Contractor will adjust the mix design for aggregate absorption, and for specific gravity if it differs by more than 0.02 from the assumed value. At the site, additional HRWR may be added to the mix to adjust the workability of the mix. Water additions are not allowed at the bridge site or in transit.

The adjusted mix design must be submitted to the Engineer a minimum of five days prior to placement of the ECC link slab. Mechanical properties requirements for ECC material are shown in Table 2 within this special provision.

The ECC material provider must be approved by the Engineer and should be familiar and experienced with batching, mixing, and placement of ECC material.

Table 1

ECC Mix Design Parameter	**Value** (lb/cyd)
Mix Water (net)	544
Portland Cement, Type I	973
Fly Ash, Type F	1167
Fine Aggregate, Dry	778
High Range Water Reducer (HRWR)	14.6
Poly-vinyl-alcohol Fibers	43.8
Retarding Admixture	Optional

Table 2

ECC Material Properties	**7 day**	**14 day**	**28 day**
Minimum Compressive Strength (psi)	3200	4000	4500
Minimum Uniaxial Tensile Strength (psi)	500	500	500
Minimum Tensile Strain Capacity	2% (uniaxial tension)		

d. **Trial Batch.** – The Contractor will appoint a technical representative capable of making adjustments to the batching and mixing of ECC material. This representative should be familiar with the mixing, batching, and placement of ECC material. The technical representative will designate a batching sequence of ECC material to ensure uniform fiber dispersion, and homogeneity of the material. This batching sequence must be approved by the Engineer. The technical representative will be present at the trial batch and at the first placement of ECC material to make recommendations and adjustments.

A three cubic yard trial batch is to be mixed and placed, at the mix plant or on the project as designated by the Engineer, a minimum of seven working days prior to full production. The engineer will be notified of the time of the trial batch mix. Quality assurance specimens will be cast from this trial batch according to section (g) of this special provision and tested to validate early age hardened properties of the ECC mixture. The trial batch will be prepared following the adjusted mix design and with the same materials that will be used in the ECC link slab mixture. For the trial batch to be considered successful, fiber dispersion, flowability, and mixture rheology must meet the approval of the Engineer or their representative. If the trial batch does not meet these requirements, the trial batch will be repeated at no additional cost to the department.

e. **Preparation, Placement, and Cure of ECC Material. –** Trucks delivering ECC material to the project must be fully discharged within one hour of charging at the plant. Preparation of the formwork and concrete surfaces should proceed according to section 706.03 H. One hour prior to placement of the link slab all concrete/ECC interfaces will be wetted with a uniform spray application of water. Water collecting in depressions will be blown out with clean, oil free, compressed air.

Finishing of the surface should follow section 703.06 M. Special care must be taken to ensure that creation of transverse surface grooves does not disturb fiber distribution on the finished surface. Light texturing with a rake can achieve this result. If this is not possible, texturing of the hardened surface must be undertaken to achieve an acceptable riding surface.

Apply a layer of wet burlap to the concrete surface as soon as the surface will support it without deformation. This burlap is to be soaked in water for a minimum of 12 hours prior to application. Maintain a saturated condition within the burlap, and as conditions allow place a system of soaker hoses on the deck surface. For a minimum of two days the burlap must be kept continuously wet. The wet curing system supplied by the Contractor must be capable of maintaining a continuously saturated condition within the burlap and free water on the deck surface. If white polyethylene sheeting or plastic coated burlap is used, the soaker hoses must be placed under the plastic. The wet curing system will not be removed until the Contractor receives approval from the Engineer. The Contractor shall control the water runoff so as not to cause traffic hazard or soil erosion problems. The curing water runoff shall not be discharged into surface water. Compressive strength test results will not be basis for removal of the wet curing system.

Sidewalk, curb, or barrier will not be cast on the deck until the link slab has received its continuous two day cure. Heavy equipment will not be permitted on the link slab until the link slab has reached an age of at least 4 days, and then not until the ECC has attained the 28-day strength listed in Table 2 within this special provision.

f. **Quality Assurance. –** Quality assurance of ECC materials will be consistent with sections 706.04 O, 106, and 605. In addition to standard compressive cylinders, uniaxial tensile test plates will be cast on site at the time of placement at identical intervals to casting of compressive cylinders. Dimensions for uniaxial tensile specimens are shown in Figure 1, and are to be cast by a concrete testing technician approved or designated by the Engineer. Uniaxial tension tests are to be performed by a testing organization or research facility experienced and familiar with conducting uniaxial tension testing of strain hardening cementitious composites. Uniaxial tension tests are to be run on a servohydraulic testing system under displacement control using a test speed of 0.1mil/sec. Testing may be conducted at the Advanced Civil Engineering Materials Research Laboratory at the University of Michigan under the direction of Professor Victor C. Li (2326 George G. Brown Laboratory, 2350 Hayward Street, Ann Arbor, Michigan 48109-2125, (734) 764-3368). Other testing laboratories must be approved by the Engineer prior to testing.

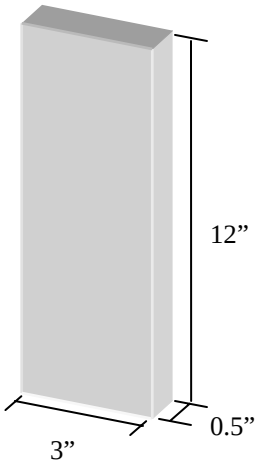

Figure 1

g. Measurement and Payment.

Contract Item (Pay Item)	**Pay Unit**
Bridge Deck Link Slab Construction	square yard
ECC Material	cubic yard

Bridge Deck Link Slab Construction includes removal of old concrete within the link slab area of a retrofitted bridge, formwork necessary for placement of link slab, consolidation (if necessary), finishing, texturing, and curing of the link slab ECC material. This work will be measured and paid for in square yards of surface constructed within the limits shown on the plans, including area of drain castings.

ECC Material includes finishing and placing the ECC material within the prepared link slab limits as shown on the plans. The quantity will be documented, measured, and paid for using batch plant tickets with deductions made for material wasted or rejected. The initial trial batch quantity will be included in this quantity. Any additional trial batches necessary to adjust the mix will be prepared at no additional cost to the Department.

Appendix B: Revised ECC Link Slab Special Provision

MICHIGAN
DEPARTMENT OF TRANSPORTATION

SPECIAL PROVISION
FOR
ECC BRIDGE DECK LINK SLAB
(Revised, Jan., 2008)

a. **Description. –** This work consists of building a link slab of Engineered Cementitious Composite (ECC) within a newly constructed, rehabilitated, or retrofitted bridge. Except as modified by this special provision, all work is to be in accordance with the 2003 Standard Specifications for Construction.

b. **Skewed Bridge.** – ECC link slab can be used in skewed bridge. However, the skew of the bridge should be limited to no more than 25 degrees.

c. **Materials. –** Cement used for ECC material must be Type I Portland cement, which is a finely ground Ordinary Portland Cement (OPC) with Blaine surface area of 1806 ft^2/lb. Type I Portland cement is available from Holcim (1100 Victors Way, Suite 50, Ann Arbor, MI 48108, (800) 854-4656). Approved equal will be accepted.

Fly ash used for ECC material is a ASTM C618 class F fly ash with particle size of 0.4-0.8 mils. Class F fly ash is available from Boral Material Technologies (45 NE Loop 410, Suite 700, San Antonio, Texas 78216, (210) 349-4069). Approved equal will be accepted.

Fine aggregates used for ECC material must be virgin silica sand consisting of a gradation curve with 50% particles finer than 0.04 mil and a maximum grain size of 12 mil. Fine aggregates meeting this requirement are available from US Silica Corporation (701 Boyce Memorial Drive, Ottawa, Illinois 61350 (800) 635-7263) under the trade name “F-110 Foundry Silica Sand”. Approved equal will be accepted.

Fibers to be used for ECC material must be manufactured of poly-vinyl-alcohol (PVA) with a fiber diameter of 1.5 mil and a length between 0.3 inch and 0.5 inch. The surface of the fiber must be oiled by the manufacturer with 1.2% (by weight) hydrophobic oiling compound along the length of the fiber. Fiber strength should be 232 kips per square inch with a tensile elastic modulus of 5,800 kips per square inch. Fibers meeting this requirement are available from Kuraray America (101 East 52nd Street, 26th Floor, New York, New York 10022 (212) 986-2230) under the trade name “REC-15”. Approved equal will be accepted.

Water reducing, high range admixture (superplasticizer) complying with ASTM C 494, Type F or G, ASTM C 1017, Type 1 or 2. In addition, the selected water reducing, high range admixture should be comprised of a polycarboxylate chemical composition. Water reducing, high range admixtures meeting this requirement are available from W.R. Grace (62 Whittemore Avenue, Cambridge, Massachusetts 02140, (617) 876-1400) under the trade name "ADVACast ® 530". Approved equal will be accepted.

Shrinkage compensate mineral admixture used for ECC material is a type of expansive cement. Expansive cement is available from CTS cement (11065 Knott Avenue, Suite A, Cypress, CA 90630, (800) 929-3030) under the trade name "CTS Komponent". Approved equal will be accepted.

Shrinkage reducing admixture used for ECC material is a type of chemical additive which can reduce water surface tension. Shrinkage reducing admixture is available from W.R. Grace (62 Whittemore Avenue, Cambridge, Massachusetts 02140, (617) 876-1400) under the trade name "Eclipse Plus". Approved equal will be accepted.

d. **ECC Mix Design Requirements. -** The ECC mixture requirements are shown in Table 1 within this special provision. For the mixture proportions listed, fine aggregate weight is assumed to have a dry bulk density of 2.60. The Contractor will adjust the mix design for aggregate absorption, and for specific gravity if it differs by more than 0.02 from the assumed value. At the site, additional HRWR may be added to the mix to adjust the workability of the mix. Water additions are not allowed at the bridge site or in transit.

The adjusted mix design must be submitted to the Engineer a minimum of ten working days prior to placement of the ECC link slab. Mechanical properties requirements for ECC material are shown in Table 2 within this special provision.

The ECC material provider must be approved by the Engineer and should be familiar and experienced with batching, mixing, and placement of ECC material.

Table 1

ECC Mix Design Parameter	**Value (lb/cyd)**
Mix Water (net)	531
Portland Cement, Type I	595
Fly Ash, Type F	1399
Fine Aggregate, Dry	770
High Range Water Reducer (HRWR)	9.1
Expansive Cement	105
Shrinkage Reducing Admixture	8.4
Poly-vinyl-alcohol Fibers	43.7
Retarding Admixture	Optional

Table 2

ECC Material Properties	2 day	3 day	7 day	14 day	28 day
Minimum Compressive Strength (psi)			3200	4000	4500
Minimum Uniaxial Tensile Strength (psi)			500	500	500
Minimum Tensile Strain Capacity	2% (uniaxial tension)				
Maximum Free Drying Shrinkage (με)	200	500	800	1000	1100
Maximum Average Crack Width (inch)	0.004				

e. **Trial Batch.** – The Contractor will appoint a technical representative capable of making adjustments to the batching and mixing of ECC material. This representative should be familiar with the mixing, batching, and placement of ECC material. The technical representative will designate a batching sequence of ECC material to ensure uniform fiber dispersion, and homogeneity of the material. This batching sequence must be approved by the Engineer. Precaution should be taken to avoid mixing chemical admixtures together before they enter the ECC material. The technical representative will be present at the trial batch and at the first placement of ECC material to make recommendations and adjustments.

A three cubic yard trial batch is to be mixed and placed, at the mix plant or on the project as designated by the Engineer, a minimum of seven working days prior to full production. The engineer will be notified of the time of the trial batch mix. Quality assurance specimens will be cast from this trial batch according to section (g) of this special provision and tested to validate early age hardened properties of the ECC mixture. The trial batch will be prepared following the adjusted mix design and with the same materials that will be used in the ECC link slab mixture. For the trial batch to be considered successful, fiber dispersion, flowability, and mixture rheology must meet the approval of the Engineer or their representative. If the trial batch does not meet these requirements, the trial batch will be repeated at no additional cost to the department.

f. **Preparation, Placement, and Cure of ECC Material. –** Trucks delivering ECC material to the project must be fully discharged within one hour of charging at the plant. Preparation of the formwork and concrete surfaces should proceed according to Structural Concrete Construction section 706.03 H. One hour prior to placement of the link slab all concrete/ECC interfaces will be wetted with a uniform spray application of water. Water collecting in depressions will be blown out with clean, oil free, compressed air.

Placement of ECC link slab during summer should be executed at night when the air temperature is higher than 50^{o}F. Nighttime casting should follow Structural Concrete

Construction section 703.06 I. During winter when the air temperature is below 50°F, placement of ECC link slab should be conducted at daytime. Cold weather precautions should follow Structural Concrete Construction section 703.06 J.

Finishing of the surface should follow Structural Concrete Construction section 703.06 M. Special care must be taken to ensure that creation of transverse surface grooves does not disturb fiber distribution on the finished surface. Light texturing with a rake can achieve this result. If this is not possible, texturing of the hardened surface must be undertaken to achieve an acceptable riding surface.

Curing of ECC link slab should follow Structural Concrete Construction section 703.06 N. Upon finishing of the surface, the curing compound should be applied by spraying uniformly on the ECC link slab surface. A layer of wet burlap should be applied to the concrete surface as soon as the surface will support it without deformation. This burlap is to be soaked in water for a minimum of 12 hours prior to application. Maintain a saturated condition within the burlap, by placing a system of soaker hoses on the deck surface. For a minimum of seven days the burlap must be kept continuously wet. The wet curing system supplied by the Contractor must be capable of maintaining a continuously saturated condition within the burlap and free water on the deck surface. If white polyethylene sheeting or plastic coated burlap is used, the soaker hoses must be placed under the plastic. The wet curing system will not be removed until the Contractor receives approval from the Engineer. The Contractor shall control the water runoff so as not to cause traffic hazard or soil erosion problems. The curing water runoff shall not be discharged into surface water. Compressive strength test results will not be basis for removal of the wet curing system.

Sidewalk, curb, or barrier will not be cast on the deck until the link slab has received its continuous seven day cure. Heavy equipment will not be permitted on the link slab until the link slab has reached an age of at least 10 days, and then not until the ECC has attained the 28-day strength listed in Table 2 within this special provision.

g. **Quality Assurance. –** Quality assurance of ECC materials will be consistent with sections 706.04 O, 106, and 605. In addition to standard compressive cylinders, uniaxial tensile test plates and free drying shrinkage test prism bars will be cast on site at the time of placement at identical intervals to casting of compressive cylinders. Dimensions for uniaxial tensile and free drying shrinkage specimens are shown in Figure 1, and are to be cast by a concrete testing technician approved or designated by the Engineer. Uniaxial tension tests are to be performed by a testing organization or research facility experienced and familiar with conducting uniaxial tension testing of strain hardening cementitious composites. Uniaxial tension tests are to be run on a servohydraulic testing system under displacement control using a test speed of 0.1mil/sec. Free drying shrinkage tests are to be conducted according to ASTM C157/C157M-99 and C596-01 standards, except that the storing of the specimens before test is modified. The specimens should be demolded after one day. Upon demolding, the specimens are moved to a room maintained at a relative humidity of 50±4 % while the specimens are at a temperature of 73±3°F and the

measurement starts. Take comparator readings of specimen at the age of 2, 3, 7, 14, and 28 days. Testing may be conducted at the Advanced Civil Engineering Materials Research Laboratory at the University of Michigan under the direction of Professor Victor C. Li (2326 George G. Brown Laboratory, 2350 Hayward Street, Ann Arbor, Michigan 48109-2125, (734) 764-3368). Other testing laboratories must be approved by the Engineer prior to testing.

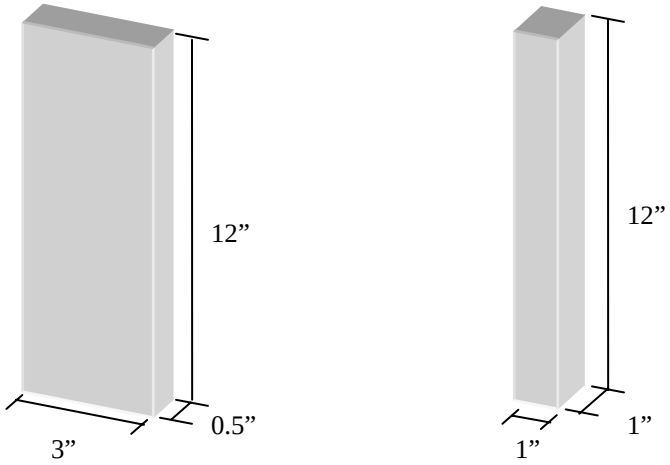

Uniaxial Tensile Specimen Free Drying Shrinkage Specimen

Figure 1

h. **Measurement and Payment.**

Contract Item (Pay Item)	**Pay Unit**
Bridge Deck Link Slab Construction	square yard
ECC Material	cubic yard

Bridge Deck Link Slab Construction includes removal of old concrete within the link slab area of a retrofitted bridge, formwork necessary for placement of link slab, consolidation (if necessary), finishing, texturing, and curing of the link slab ECC material. This work will be measured and paid for in square yards of surface constructed within the limits shown on the plans, including area of drain castings.

ECC Material includes finishing and placing the ECC material within the prepared link slab limits as shown on the plans. The quantity will be documented, measured, and paid for using batch plant tickets with deductions made for material wasted or rejected. The initial trial batch quantity will be included in this quantity. Any additional trial batches necessary to adjust the mix will be prepared at no additional cost to the Department.